HOST SPECIES-SPECIFIC INTERACTIONS OF PROTEIN KINASE R AND POXVIRUS PSEUDOSUBSTRATE INHIBITORS

by

CHEN PENG

B.E., Shenyang Pharmaceutical University, 2010

AN ABSTRACT OF A DISSERTATION

submitted in partial fulfillment of the requirements for the degree

DOCTOR OF PHILOSOPHY

Division of Biology
College of Arts and Sciences

KANSAS STATE UNIVERSITY
Manhattan, Kansas

2016

Abstract

Poxviruses are large double-stranded DNA viruses that collectively exhibit a broad host range. Whereas many members of the poxvirus family are capable of infecting various host species, others are restricted to only one or a very limited numbers of species, such as variola virus, which is the causative agent of smallpox and is restricted to humans. Since the entry of poxviruses is not dependent upon any specific receptors, the cell tropism is therefore fully determined by the virus' ability to manipulate the cellular signaling networks that are responsible for antagonizing viral infections. Double-stranded RNA (dsRNA)-dependent protein kinase (PKR) is a unique antiviral protein found in most vertebrates, which serves both as a virus sensor by detecting the presence of dsRNA and an antiviral effector by suppressing cap-dependent translation during virus infection. Many viruses, including poxviruses, have therefore evolved genes that encode for PKR inhibitors, such as vaccinia virus K3L, which shows sequence homology to the N-terminal region of the eukaryotic translation initiation factor 2α (eIF2α), the substrate of PKR. K3L is able to inhibit PKR-mediated eIF2α phosphorylation *in vitro* and *in vivo*. Because K3L was shown to be indispensable for virus replication in Syrian hamster cells but not in human cells, it was categorized as a host range factor. However, the molecular basis for K3L's host range function is not fully understood. We examined the interactions of poxvirus K3L orthologs, especially vaccinia virus K3L and M156R, the K3L ortholog in the rabbit-specific myxoma virus, and PKR from a variety of host species in multiple assays, and found that K3L and M156R inhibit PKR in a species-specific manner, which likely contributes to the cell tropism and host range for both viruses. Inactivation of M156R or K3L led to virus attenuation in cells, which could be rescued by ectopic expression of viral PKR inhibitors. We also identified the helix αG region as the main molecular determinant for PKR's sensitivity to inhibition by

K3L orthologs. In conclusion, the research summarized here indicates that the interactions of PKR and poxvirus pseudosubstrate inhibitors play important roles in virus host range and virulence.

HOST SPECIES-SPECIFIC INTERACTIONS OF PROTEIN KINASE R AND POXVIRUS PSEUDOSUBSTRATE INHIBITORS

by

CHEN PENG

B.E., Shenyang Pharmaceutical University, 2010

A DISSERTATION

submitted in partial fulfillment of the requirements for the degree

DOCTOR OF PHILOSOPHY

Division of Biology
College of Arts and Sciences

KANSAS STATE UNIVERSITY
Manhattan, Kansas

2016

Approved by:

Major Professor:
Dr. Stefan Rothenburg

Copyright

Abstract

Poxviruses are large double-stranded DNA viruses that collectively exhibit a broad host range. Whereas many members of the poxvirus family are capable of infecting various host species, others are restricted to only one or a very limited numbers of species, such as variola virus, which is the causative agent of smallpox and is restricted to humans. Since the entry of poxviruses is not dependent upon any specific receptors, the cell tropism is therefore fully determined by the virus' ability to manipulate the cellular signaling networks that are responsible for antagonizing viral infections. Double-stranded RNA (dsRNA)-dependent protein kinase (PKR) is a unique antiviral protein found in most vertebrates, which serves both as a virus sensor by detecting the presence of dsRNA and an antiviral effector by suppressing cap-dependent translation during virus infection. Many viruses, including poxviruses, have therefore evolved genes that encode for PKR inhibitors, such as vaccinia virus K3L, which shows sequence homology to the N-terminal region of the eukaryotic translation initiation factor 2α (eIF2α), the substrate of PKR. K3L is able to inhibit PKR-mediated eIF2α phosphorylation *in vitro* and *in vivo*. Because K3L was shown to be indispensable for virus replication in Syrian hamster cells but not in human cells, it was categorized as a host range factor. However, the molecular basis for K3L's host range function is not fully understood. We examined the interactions of poxvirus K3L orthologs, especially vaccinia virus K3L and M156R, the K3L ortholog in the rabbit-specific myxoma virus, and PKR from a variety of host species in multiple assays, and found that K3L and M156R inhibit PKR in a species-specific manner, which likely contributes to the cell tropism and host range for both viruses. Inactivation of M156R or K3L led to virus attenuation in cells, which could be rescued by ectopic expression of viral PKR inhibitors. We also identified the helix αG region as the main molecular determinant for PKR's sensitivity to inhibition by

K3L orthologs. In conclusion, the research summarized here indicates that the interactions of PKR and poxvirus pseudosubstrate inhibitors play important roles in virus host range and virulence.

Table of Contents

List of Figures

List of Tables

Acknowledgements

To my wife Yijing: Nothing listed in this dissertation could have been accomplished without your unconditional love and support. You have been and will always be my source of motivation. Thank you for all what you have done to give me a sweet home.

To my parents Lanxia, Ruiming and my son Suyu: I want to thank you for your love and support.

To my advisor Stefan: I want to thank you for offering me a position when I most needed it and thank you for all the help and care you gave me throughout my Ph.D. study. I could not have achieved what I have today without your guidance and support. Thank you.

My sincere thanks also goes to my supervisory committee members: Dr. Jeroen Roelofs, Dr. Loubna Tazi and Dr. Raymond R. R. Rowland as well as my outside chair Dr. Randall Phebus for their encouragement, insightful comments and invaluable advice during my Ph.D. study. I want to especially thank Dr. Loubna Tazi for proofreading my dissertation again and again to make it better.

To my fantastic lab mates and friends Sherry and Julhasur: Thank you for all the things you have taught me. Thank you Sherry for your incredible patience for helping me to proofread everything I wrote. I have learned so much from the both of you, thank you.

Dedication

This work is dedicated to my wife Yijing Li and my son Suyu Peng, they have proved to be my incredible source of joy and laughter.

Chapter 1 - Introduction

Poxviruses

Phylogeny

Poxviruses are large double-stranded DNA viruses whose replication is restricted to the cytoplasm of host cells (1). Poxviruses as a family, can infect almost all vertebrate species and many invertebrates (1). Poxviruses can be classified into two subfamilies: *Chordopoxvirinae*, whose members mainly infect vertebrate hosts, and *Entomopoxvirinae*, which includes poxviruses that are restricted to insect hosts. The subfamily *Chordopoxvirinae* is currently grouped in to ten genera: orthopoxviruses, yatapoxviruses, leporipoxviruses, capripoxviruses, cervidpoxviruses, suipoxviruses, parapoxviruses, molluscipoxviruses, crocodylipoxviruses and avipoxviruses (Figure 1.1). Among these ten genera, yatapoxviruses, leporipoxviruses, capripoxviruses, cervidpoxviruses and suipoxviruses can be classified as "clade II poxviruses due to the fact that they form a sister-clade to orthopoxviruses in phylogenetic trees (Fig. 1.1) (1-3).

Two of the best known members of all poxviruses are variola virus, the causative agent of smallpox, which caused more human fatalities than all other infectious diseases combined, and vaccinia virus, which is often considered the prototypic poxvirus. The studies presented in this dissertation will be focused on vaccinia virus and myxoma virus, a member of the leporipoxvirus genus.

Vaccinia virus

Vaccinia virus is the most extensively studied poxvirus. Historically, vaccinia virus was the first animal virus observed microscopically, replicated and titered successfully in tissue culture, physically purified and biochemically characterized. Vaccinia virus was used in the vaccination campaign against smallpox led by the World Health Organization, which eventually led to the eradication of smallpox in 1977 (4, 5). The study of vaccinia virus also contributed largely to the advancement of many aspects of biological research. For example, the discovery of RNA polymerase in purified vaccinia virus virions revised an once universal perception that virus particles are simply packets of nucleic acids without any protein products (6). Vaccinia virus has also been extensively used as an expression vector for various purposes such as vaccine development and cancer treatment due to the relative ease of generating and isolating recombinant viruses, and due to its genetic capacity for taking large amounts of foreign DNA (7).

The precise origin and the natural host(s) of vaccinia virus is/are unknown. The current strains of vaccinia virus have been repeatedly passaged in cultured cells and animals for many decades (1). Experimentally, vaccinia virus displays a broad host range. Many vaccinia virus strains are able to establish infections experimentally in primates, rodents, lagomorphs and ungulates (1). Some variants of vaccinia virus have also been identified such as buffalopox, which probably represent a vaccinia virus strain that escaped during the vaccination campaign (1). Vaccinia virus usually causes mild infections in humans. But the virus can cause serious illness, even death, in immunocompromised individuals. In addition, vaccinia virus that is maternally passed to the fetus can cause lethal infections (1).

Like all poxviruses, vaccinia virus encodes a large pool of proteins aimed to modulate the host's antiviral immune responses to benefit the survival and replication of the virus. These genes are collectively termed immunomodulatory genes. The protein products of these genes often interact with one or multiple host factors that are involved in antiviral immune responses. Protein products of the vaccinia virus immunomodulatory genes function by modulating different aspects of the antiviral responses of the host. Examples of targets include the complement regulatory proteins, interferon-binding proteins, interleukin-18-binding proteins, soluble tumor necrosis factor-binding proteins, NF-κB-binding proteins, inhibitors of apoptosis, etc (reviewed in (8)). Some vaccinia virus genes were found to be indispensable for virus replication in cell lines derived from certain species, but not in the others, such as E3L and K3L, and are hence termed host range genes (1). Vaccinia virus E3L and K3L are both inhibitors of the host's antiviral protein kinase R (PKR). The detailed mechanism of PKR inhibition by K3L and E3L will be discussed later in this chapter.

Myxoma virus

Myxomatosis

Myxoma virus is a member of the genus leporipoxvirus. Infections that are caused by myxoma virus and rabbit fibroma virus, two members of this genus, are strictly restricted to animals of the leporidae family, which include rabbit and hare species. Myxoma virus infection was first documented in Uruguay, in 1896, where an outbreak of a novel lethal disease in laboratory-raised European rabbits, later termed myxomatosis, was observed (9). In 1898, the disease was suggested to be caused by a viral pathogen, which made myxomatosis one of the earliest described animal diseases to be associated with a virus. Thirty years after the initial documentation of the virus in South America, myxomatosis was observed for the first time in North America (9, 10).

Myxoma virus is extremely virulent in European rabbits, causing a mortality rate close to 100% (reviewed in (11)). Clinical signs of myxomatosis, including conjunctivitis, elevated temperature and raised cutaneous lesions can be observed as early as 4 days post infection. At 8-10 days after infection, animals usually begin to develop more severe symptoms such as swollen head, drooping ears, closed eyelids and mucopurulent rhinitis. In male animals, extreme swelling of the scrotum and testes can also be observed at this stage. Death caused by myxomatosis often occurs 8 to 12 days post infection (11, 12). The virus found in secretions and in skin lesions can be transmitted by direct contacts or by biting arthropod vectors such as mosquitos and fleas to naïve animals (13, 14).

The natural hosts of myxoma virus are *Sylvilagus* leporids including the South American tapeti rabbit (*Sylvilagus brasiliensis*) and the North American brush rabbit (*Sylvilagus bachmani*) (15). Interestingly, in contrast to the lethal disease myxomatosis caused by myxoma virus in

European rabbits, the virus only causes mild symptoms in its natural hosts, including innocuous cutaneous fibromas, which are often restricted to the site of inoculation. Death is often not observed unless in very young rabbits (9, 15).

Immune responses to myxoma virus infection

Rabbits infected with myxoma virus can develop IgG and IgM antibodies in serum to levels that are quantifiable by ELISA or neutralization assays as early as six days post infection (12, 16). Antibodies produced in serum remain detectable for as long as two years in wild rabbits that were naturally infected (17). These IgG antibodies can also cross the placenta, and can be found in kittens until 6 weeks after birth (18). However, it remains inconclusive whether maternal antibodies provide sufficient protection from natural infection (19). Besides antibody mediated immunity, cell mediated immunity also plays an important role in clearing the poxvirus infection and preventing reinfection. During myxoma virus infection, cell mediated immunity constitutes dendritic cell activation and the production of appropriate cytokines to activate Th1 skewed CD4+ T cells (20, 21). In experimental settings, rabbits that have recovered from myxomatosis naturally do not develop myxomatosis even with high doses of virus challenge, but they do initiate a localized immune reaction at the site of inoculation, indicating the involvement of cell mediated immunity in response to reinfection of myxoma virus (19, 22).

Genome structure of myxoma virus

Like all poxviruses, the myxoma virus genome is composed of linear double-stranded DNA. The genes in the myxoma virus genome are tightly compact and efficiently organized (23). The Lausanne (Lu) strain, which is often considered to be the reference myxoma virus strain, contains 161,774 base pairs (bp) with a A/T content of 56.4% (23). A total of 171 complete open reading frames have been annotated in the genome. The myxoma virus Lu

genome, like other poxvirus genomes, contains terminal inverted repeats (TIR) that are 11.5 kb in length. The boundaries between TIRs and the central core sequences lie between the M008.1L/R and the M009L/M156R genes. The central core of the genome, which is relatively conserved across all poxviruses, constitutes of genes that are essential for virus replication such as those that encode for transcriptional machinery or structural components of the virion. The immunomodulatory genes and/or host range factors, on the other hand, are more often localized toward the ends of the genome, especially in the TIR regions (23).

Myxoma virus promoters, like all poxvirus promoters, are classified into three categories: Early, intermediate and late. All promoter sequences found in myxoma virus contain core elements that are found in other leporipoxviruses and are also conserved among all orthopoxviruses (23).

In addition to the Lu strain, the genome of a myxoma virus MSW strain, which naturally infects brush rabbits (*Sylvilagus bachmani*) was also fully sequenced and published (24). The MSW genome is slightly larger than that of the Lu strain of MYXV, containing 164,600 bp of dsDNA, due to an expanded TIR. Five complete genes, including M156R, M154L, M153R, M152R, and M151R as well as part of M150R are duplicated in the TIR. Compared to the genome of the Lu strain, no novel genes were found, but five genes were found to be disrupted due to mutations, insertions or deletions. The MSW strain exhibits higher virulence than the Lu strain in European rabbits, indicated by their ability to kill infected European rabbits more rapidly (25). European rabbits infected with the MSW strain of MYXV usually die within 10 days without showing clinical signs of myxomatosis. Importantly, in contrast to the Lu strain, the MSW strain of MYXV caused 100% mortality in wild rabbits that are genetically resistant to the

Lu strain of MYXV. Unfortunately, it is not immediately clear which gene(s) are responsible for the difference in virulence between the Lu strain and the MSW strain (25).

Replication cycle

All poxviruses replicate exclusively in the cytoplasm of infected cells (reviewed in (26)). Two types of mature virions are generated during a replication cycle and can initiate new infections; the intracellular mature virus and the extracellular enveloped virus (27). The entry of myxoma virus does not require any specific receptors on the surface of the host cell (6, 28). Myxoma virus particles can attach to target cells by membrane fusion, or by the process of endocytosis (29). A permissive infection is defined by the completion of three stages of viral transcriptions and translations, known as early, intermediate and late stages (26). The initiation of intermediate and late transcription requires the completion of the early and intermediate protein synthesis, respectively (26). The newly packaged virus particle is transported through microtubules and is wrapped with membranes derived from the Golgi to form the intracellular enveloped virus, which can either stay in the infected cells as an intracellular mature virus or be released to form the extracellular enveloped virus. Extracellular mature viruses are free virus particles that can initiate new infections by attaching to naïve uninfected cells, while the release of intracellular mature virus requires cell lysis (6, 30, 31).

Myxoma virus immunomodulatory proteins

Like many large DNA viruses, myxoma virus encodes a large number of genes, whose protein products are specialized to manipulate or evade the host antiviral immune responses in order to establish successful replication. These proteins target different pathways of the host immune responses to favor virus replication, and are therefore collectively termed viral immunomodulatory factors (reviewed in (32-34)). Based on their subcellular localization during

an infection, myxoma virus immunomodulatory factors can be categorized into two groups. "Viromimetics" are those that are usually secreted or cell surface-bound, which mainly mimic the host immune factors to disrupt their functions (35). Members of the other group, named "virostealth", however, remain intracellular to prevent infected cells from entering apoptosis or keep the virus from being recognized by the immune system (35). The viral immunomodulatory proteins can also be grouped based on their mode of action. Viroreceptors mimic cytokine receptors to disrupt the action of cytokines. For example, myxoma virus M-T7, a homolog of the interferon-γ receptor, is secreted during virus infection to sequester free interferon-γ (36, 37). Viromitigators are those that stay intracellularly and disturb specific signal transduction cascades that are critical for the regulation of antiviral activities (35). A well-studied example of viromitigators is the myxoma virus M-T5, an ankyrin-repeat protein that interrupts pathways mediated by Akt and cullin-1 through direct binding (38). Moreover, myxoma virus also possesses genes that encode proteins aimed to terminate the cascade of apoptosis such as SERP-2, M11L, M-T2, M-T4 and M-T5 (38-42). In addition, many myxoma virus immunomodulatory proteins are multifunctional. For example, M-T7 was shown to be able to inhibit interferon-γ and to interact with heparin binding proteins such as chemokines (43). Recently, another dual function immunomodulatory protein, M029, was identified, which was able to both inhibit the antiviral kinase protein kinase, PKR and conscript RHA/DHX9 to promote viral replication and expand the host tropism (44).

Myxoma virus host range factors

As a family, poxviruses can infect a variety of animal species, including insects, birds and mammals. However, the host range of each individual poxvirus varies tremendously even between very closely related strains. For instance, variola virus, the causative agent of smallpox

evolved as a human-specific pathogen. Others, such as cowpox virus, in contrast, an orthopoxvirus closely related orthopoxvirus to variola virus, is known to infect more than three hundred different species (6). The difference in host range sizes among poxviruses is believed to be caused by viral proteins that influence virus host ranges, termed host range factors. Myxoma virus infection is restricted to rabbits and hares, making it a great model organism to study viral host range factors and their interactions with the host's antiviral proteins. However, the molecular mechanisms by which myxoma virus displays such a narrow host range remain unknown. Recently, several host range proteins have been identified and characterized in myxoma virus. A myxoma virus lacking M062R was shown to cause abortive replication in rabbit cells and asymptomatic infections in European rabbits (45). In addition, a binding partner of M062, named sterile alpha motif domain 9 (SAMD9), was identified in human cells, and was convincingly shown to be responsible for the blockage of M062R-deficient myxoma virus in human cells (45). However, the rabbit homologue of SAMD9 was not characterized and it is therefore unknown if M062R functions in a species-specific manner (46). Moreover, a mutant strain deficient for M063R was able to replicate to similar levels as the wild type virus in monkey BGMK cells but failed to replicate in rabbit RK13 cells and was not able to cause myxomatosis in European rabbits (47). In addition, myxoma virus M064R is another gene closely related to M062R and M063R, however, in contrast to the latter two, M064R functions solely as a virulence factor and lacks the host range functional properties of M062R and M063R (48). Another interesting example of a myxoma virus host range factor is M-T2, which is a dual function inhibitor of the host tumor necrosis factor alpha. M-T2 has two activities; 1) the secreted protein binds and inhibits extracellular tumor necrosis factor alpha, and 2) the same protein also localizes to the cell surface where it binds and inhibits cellular tumor necrosis factor

receptor alpha receptor. The first activity is rabbit-specific while the second one is not (41, 49-51).

Importantly, all myxoma virus immunomodulatory proteins and host range factors evolved in the natural hosts of myxoma virus: *Sylvilagus* rabbits, such as the brush rabbit or tapeti rabbit. However, studies on their functions were performed mostly in laboratory rabbits, which are derived from European rabbits (*Oryctolagus cuniculus*). Therefore, it is possible that some host species-specific interactions are neglected and some identified functions might be the consequences of off-target interactions between myxoma virus proteins and the host antiviral factors from *Oryctolagus* rabbits.

Evolution of myxoma virus in Australia and Europe

Myxoma virus naturally infects North American brush (*Sylvilagus bachmani*) and South American tapeti (*Sylvilagus brasiliensis*) rabbits. In 1950, myxoma virus was introduced into Australia as a biological control of invasive feral European rabbits, which caused tremendous economic and ecological havoc. Because European rabbits had never naturally encountered the virus before its deliberate release, the evolution of myxoma virus in Australia became one of the best examples to study how a virus evolves to adapt to a new host species and how the host co-evolves simultaneously. The virus initially released in Australia was termed the standard laboratory strain (SLS), which was isolated from a European rabbit in Brazil and passaged many times in laboratory European rabbits (52).

Based on the fatality rate and the clinical symptoms it causes, myxoma virus can be categorized into 5 levels of virulence. The SLS strain is of grade 1 virulence, causing a case fatality rate of 99.8% in laboratory European rabbits (22). After its initial release, the virus began to become attenuated and soon, viruses of grade 3 and 4 virulence with 70-95% case fatality rate

started to dominate the field despite the regular and repeated release of grade 1 viruses into the field (12, 53). The grade 1 virus could be isolated in the field only within 6 months of the release in a given area, indicating the extremely fast pace of virus evolution (54).

In addition to the attenuation of the virus, wild rabbits also became more resistant to myxoma virus infection. The quick emergence of more attenuated myxoma virus strains provided opportunities for rabbits with certain levels of genetic resistance to survive. In one study, rabbit kittens from the area around Lake Urana captured in the field were housed and raised in laboratory settings and challenged with a grade 3 strain (KM13) of virus to monitor their responses. The percentage that died from myxomatosis dropped from above 80% in 1953 to around 30% in 1958, suggesting that quick selection of resistant animals in this area occurred (55-57).

A similar trajectory of virus-host coevolution was observed in Europe. Two years after the release of MYXV in Australia, the virus was illegally introduced into Maillebois, a commune 70 km west of Paris. The released virus was a more virulent strain than the SLS, and was derived from a laboratory in Lausanne, Switzerland, hence it was named the Lausanne strain. The virus soon spread throughout Europe and Britain, causing ecological problems and economical loss in the rabbit farming industry until it was controlled by mass vaccination and an enforced quarantine (58). It was estimated that the rabbit population in France dropped by 90-98% due to the spread of myxoma virus (14). The evolution of myxoma virus in Europe was very similar to that in Australia. Grade 3 and 4 viruses were isolated from the field in France three years after the initial release, and grade 3 viruses became the predominant isolates in both Britain and France (12, 59). The common evolutionary trajectory of myxoma virus in Australia and Europe

suggests a possibility that common mechanisms were involved in virus evolution on two continents, especially the evolution of virus attenuation.

Type I interferon-mediated antiviral responses

Interferons

Interferons are a group of cytokines found in jawed vertebrates that mediate potent antiviral and anti-proliferative effects (60). Interferons are one of the earliest lines of protection for the host in response to virus infection. The finding that all vertebrates characterized to date have genes encoding members of the interferon family and the high conservation of interferons suggests their importance for the immune response against pathogens. Interferons are named after their ability to interfere with viral infection. In addition to its involvement in antiviral immunity, interferons also play roles in activating natural killer cells and macrophages, up-regulating antigen presentation and are responsible for inducing infection-related symptoms in organisms such as fever and muscle pain (61).

The interferon family can be grouped into two major categories: Type I and type II interferons. Type I interferons share considerable structural homology and can be further classified into two major groups: Interferon α and interferon β. Type II interferon includes only one member, interferon γ, which differs dramatically from type I interferons in mode of action, aspects of the receptors and structure and will not be discussed in depth in this dissertation.

Type I interferon-mediated antiviral signaling pathways

Human interferon α can be divided into thirteen subtypes, including interferon α1, α2, α4, α5, α6, α7, α8, α10, α13, α14, α16, α17, α21 (61). The genes encoding type I interferons are all localized and clustered on chromosome nine in humans (62). Both interferon α and β bind to common receptors localized on the surface of most cells called type I interferon receptors (reviewed in (63)). The binding of interferons to their receptors can trigger a series of antiviral

immune reactions by inducing the expression of hundred of genes that act to antagonize virus infections (64).

Production of interferons can be triggered by the activation of two major types of viral sensors: Toll-like receptors which are localized on the cell surface or in endosomes; and intracellular cytosolic nucleic acid receptors, which together are collectively termed pattern recognition receptors (65, 66). These pattern recognition receptors work as sentinels in cells to detect the presence of foreign nucleic acids including DNA and RNA and subsequently initiate immune responses upon activation. Toll-like receptors are primarily expressed in immune cells such as dendritic cells and macrophages, while cytosolic receptors are found in almost all cell types (67).

When a host cell is invaded by a virus, cytosolic receptors such as RIG-I (retinoic acid-inducible gene 1) and MDA-5 (melanoma Differentiation-Associated protein 5) are activated, which subsequently activate interferon-regulatory factors (IRFs) and NF-κB (68). The latter two function as transcription factors and translocate into the nucleus to induce the expression of type I interferons, which are then secreted and induce an interferon-mediated immune response in a paracrine or autocrine manner. This induces the expression and activation of interferon stimulated genes in the infected cell and in surrounding cells to fight viral infections (Fig. 1.2) (68).

The double-stranded RNA-dependent protein kinase

The genes that are up-regulated by type I interferons are called interferon stimulated genes (ISGs) (64). Among them, the double-stranded RNA-dependent protein kinase (PKR) is unique, because it functions as both a pattern recognition receptor that senses viral invasion and an interferon-induced antiviral effector that suppresses viral replication. PKR is found in bony

fish, amphibians, reptiles and mammals, suggesting an important role in the defense against viral infections over the course of vertebrate evolution. The following entails a detailed descriptions of PKR's enzymatic activity and its role in antiviral immune responses.

Activation and activity

PKR is a protein found in vertebrates and is known as an antiviral protein kinase. PKR is composed of two N-terminal double-stranded RNA binding domains that bind double-stranded (ds) RNA, a linker region and a C-terminal kinase domain that categorizes it as a member of the family eukaryotic translation initiation factor 2 α (eIF2α) kinase family. In unstimulated cells, PKR is expressed at intermediatel levels and remains in a latent monomeric form (69, 70). Traditional activation of PKR requires the presence of dsRNA produced during viral replication. Binding of dsRNA to the dsRNA binding domains of PKR triggers conformational rearrangements of the molecule, which bring two monomers into close proximity to form dimers (71). Activation of PKR needs a minimum of 30 base pairs of dsRNA and the optimal activation requires double-stranded RNA that is longer than 80 base pairs (72, 73). The activation is sequence-independent, allowing PKR to be activated by RNA of a variety sources (73). In addition to double-stranded RNA, a human protein named PACT (PKR activating protein), and its mouse homolog RAX (PKR associated protein X) have also been identified as internal PKR activators in response to cellular stress such as serum starvation, peroxide or arsenite treatment (74-77).

Upon activation, PKR molecules dimerize and the concomitant autophosphorylation occurs on the threonine residue 446 in human PKR (78, 79). The active dimer subsequently phosphorylates the residue serine 51 in eIF2α (80). Phosphorylated eIF2α then competitively inhibits the recycling of the GDP-bound form of eIF2 to the GTP-bound form by eIF2B, which is

a guanine exchange factor for eIF2α that is present only in limited amounts. Cap-dependent translation then halts because eIF2α can no longer be recycled for re-initiation of translation (reviewed in (81)). Because cap-dependent viruses rely on the host translational machineries for the translation of viral proteins, replications of these viruses are therefore repressed when the host translation is blocked by phosphorylation of eIF2α by active PKR (82).

Inhibition of PKR by viruses

PKR activation is an important process in the antiviral immune response due to its special role as both a virus sensor and an antiviral effector. Therefore, many viruses have evolved genes, whose protein products aim to directly target PKR, or to sequester dsRNA, to subvert the antiviral immune responses mediated by PKR (83). The mode of action of viral PKR inhibitors varies dramatically from virus to virus but almost every single step of PKR activation and activity has been targeted by at least one viral antagonist (83). For example, vaccinia virus E3, influenza virus NS1 and herpes virus US11 inhibit PKR by binding dsRNA and thereby preventing PKR dimerization (84-86). Vaccinia virus K3L and human immunodeficiency virus tat compete with eIF2α for PKR binding (87, 88). Apart from directly inhibiting PKR, some other viral products such as herpes virus γ34.5 can alleviate PKR-mediated translational suppression by inducing dephosphorylation of eIF2α, the substrate of PKR (89, 90). Overall, the PKR-mediated antiviral response constitutes one of the earliest obstacles that viruses have to overcome in order to establish successful replication in vertebrates.

Fast evolution of PKR

In addition to PKR, four other eIF2α kinases have been recognized in higher eukaryotes that can regulate translation (reviewed in 81) (Fig. 1.3). Members of the eIF2α kinase family all

contain homologous kinase domains, but possess different regulatory domains, which can detect and be activated by different stress signals (91). PKR differs from other eIF2α kinases due to its unique evolutionary trajectory. Specifically, PKR faces the challenges to not only maintain its ability to bind and phosphorylate eIF2α, a highly conserved protein, but also simultaneously evade inhibition by viral eIF2α homologues such as vaccinia virus K3L. A recent study of our lab examined the evolutionary pattern of the kinase domain of PKR and found that PKR has evolved much faster than the other eIF2α kinases PERK (PKR-like endoplasmic reticulum kinase), HRI (heme-regulated inhibitor kinase) and GCN2 (general control nonderepressible 2). Moreover, 35 sites in the kinase domain were identified to have been under positive selection, and the mutation of more than half of these residues altered the sensitivity of human PKR to vaccinia virus K3L (92). A related study published at the same time focused on primate PKRs revealed a similar pattern supporting the rapid evolution of PKR (93). In addition to PKR, this study also showed that residues in vaccinia virus K3L are also under strong positive selection as a result of the counteracting adaptive changes in the kinase domain of PKR. In contrast to PKR, eIF2α is highly conserved across species and over the course of evolution. All these studies suggest that the molecular arms-race between PKR and its viral antagonists likely drive the fast evolution of both.

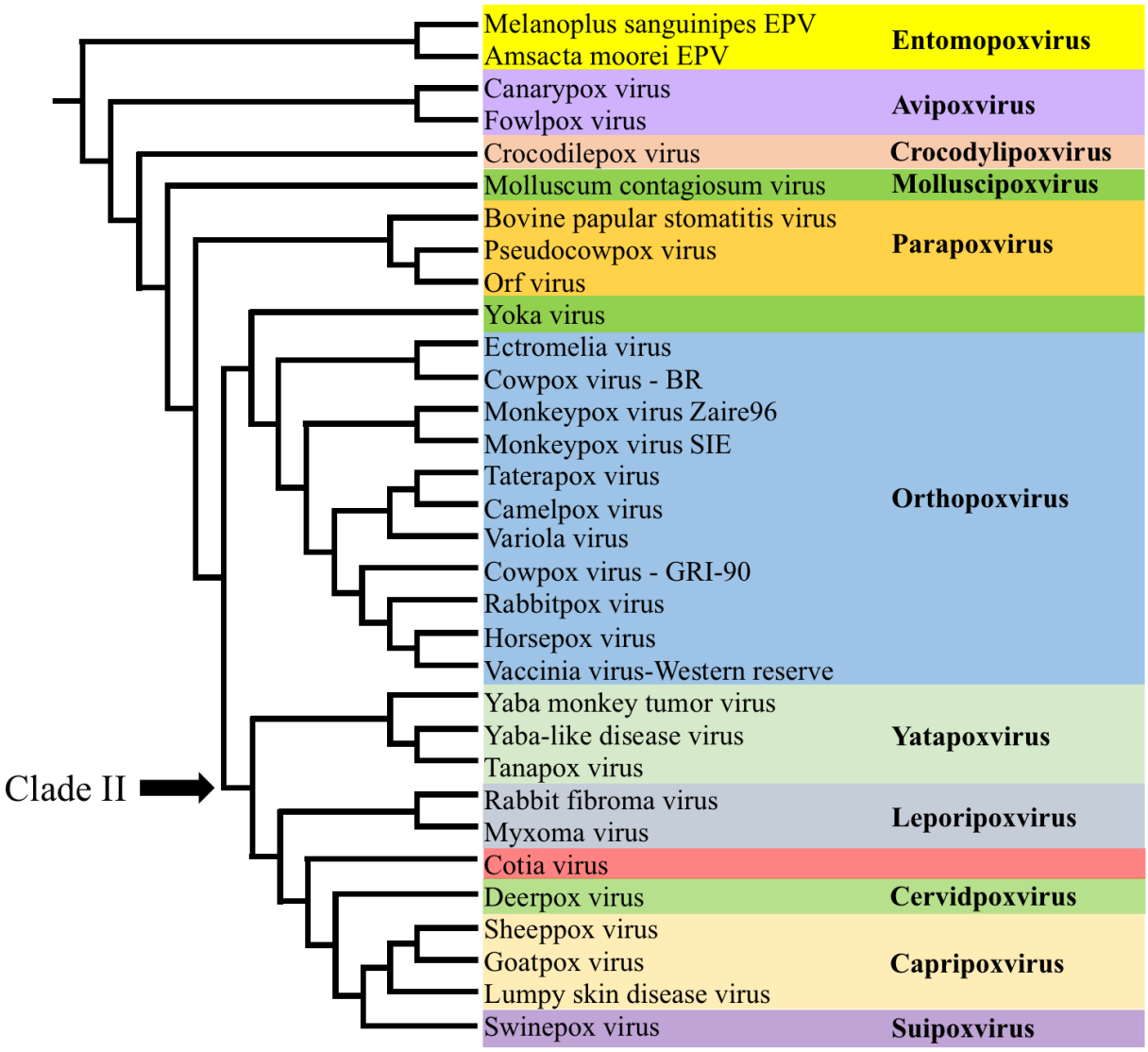

Figure 1.1 Phylogeny of poxviruses

Phylogenetic tree of fully sequenced poxviruses adapted from Haller *et al*. (1).

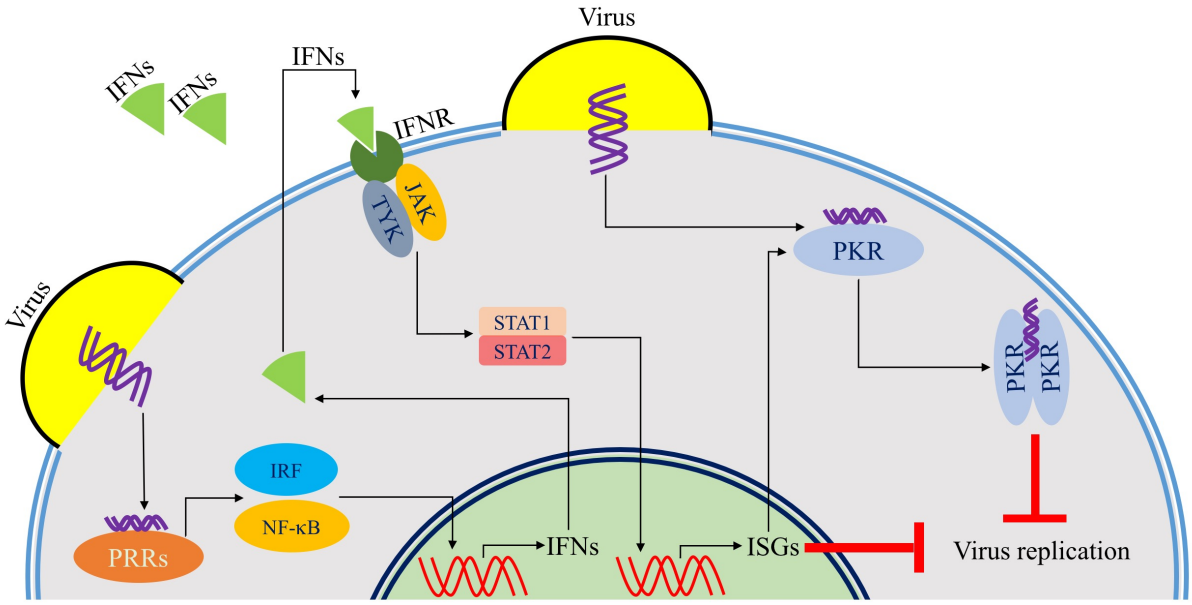

Figure 1.2 Type I interferon-mediated antiviral pathways

Upon virus infection, double-stranded RNA (purple) is detected by pattern recognition receptors, which subsequently upregulate type I interferons (IFNs, light green). IFNs are secreted and trigger upregulation of interferon stimulated genes (ISGs) including PKR by binding to IFN receptors (IFNR, dark green), which activates the JAK-STAT pathway, to fight against viral infection. Double-stranded RNA can be directly detected by PKR, which is required for PKR dimerization and activation.

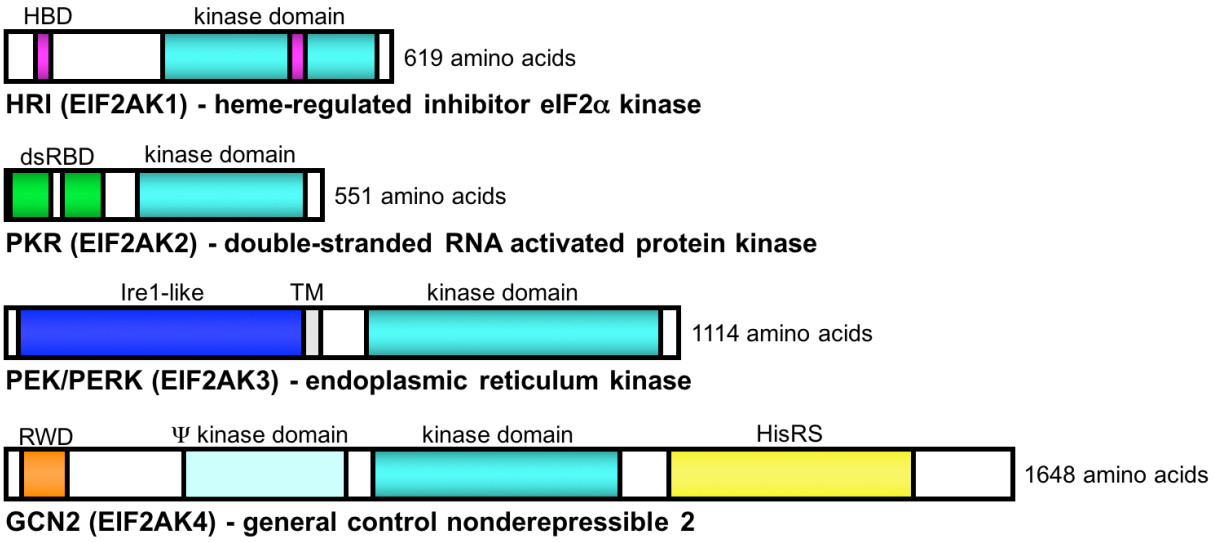

Figure 1.3 Domain organization of eIF2α kinases

Abbreviations: HBD: heme binding domain; dsRBD: double-stranded RNA binding domain; TM: transmembrane; RWD: RING finger-containing proteins, WD-repeat-containing proteins; HisRS; Histidyl-tRNA synthetase; ZBD: Z-DNA binding domain

References

1. Haller SL, Peng C, McFadden G, Rothenburg S (2014) Poxviruses and the evolution of host range and virulence. *Infection, Genetics and Evolution* 21:15–40.

2. Bratke KA, McLysaght A (2008) Identification of multiple independent horizontal gene transfers into poxviruses using a comparative genomics approach. *BMC Evolutionary Biology* 8(1):67.

3. Hughes AL, Friedman R (2005) Poxvirus genome evolution by gene gain and loss. *Molecular Phylogenetics and Evolution* 35(1):186–195.

4. Moss B (2011) Smallpox vaccines: targets of protective immunity. *Immunology Review* 239(1):8–26.

5. McFadden G (2005) Poxvirus tropism. *Nature Reviews of Microbiology* 3(3):201–213.

6. Broyles SS, Moss B (1987) Sedimentation of an RNA polymerase complex from vaccinia virus that specifically initiates and terminates transcription. *Molecular and Cellular Biology* 7(1):7–14.

7. Moss B (1991) Vaccinia virus: a tool for research and vaccine development. *Science* 252(5013):1662–1667.

8. Smith GL, et al. (2013) Vaccinia virus immune evasion: mechanisms, virulence and immunogenicity. *Journal of General Virology* 94(Pt 11):2367–2392.

9. Fenner F, Ratcliffe FN (1965) Myxomatosis. *Myxomatosis*.

10. Kessel JF, Prouty CC, Meyer JW (1931) Occurrence of Infectious Myxomatosis in Southern California. *Experimental Biology and Medicine* 28(4):413–414.

11. Kerr PJ (2012) Myxomatosis in Australia and Europe: a model for emerging infectious diseases. *Antiviral Research* 93(3):387–415.

12. Best SM, Collins SV, Kerr PJ (2000) Coevolution of host and virus: cellular localization of virus in myxoma virus infection of resistant and susceptible European rabbits. *Virology* 277(1):76–91.

13. Fenner F, Ross J, Thompson HV, King CM (1994) *Myxomatosis.* (Oxford University Press).

14. Kerr PJ, Merchant JC, Silvers L, Hood GM, Robinson AJ (2003) Monitoring the spread of myxoma virus in rabbit Oryctolagus cuniculus populations on the southern tablelands of New South Wales, Australia. II. Selection of a strain of virus for release. *Epidemiology and Infeciont* 130(1):123–133.

15. Kerr PJ, Best SM (1998) Myxoma virus in rabbits. *Revue scientifique et technique* -

International Office of Epizootics 17(1):256–268.

16. Jeklova E, et al. (2008) Characterisation of immunosuppression in rabbits after infection with myxoma virus. *Veterinary Microbiology* 129(1-2):117–130.

17. Kerr P, McFadden G (2002) Immune responses to myxoma virus. *Viral Immunology* 15(2):229–246.

18. Fenner F, Marshall ID (1954) Passive immunity in myxomatosis of the european rabbit (Oryctolagus cuniculus): the protection conferred on kittens born by immune does. *Journal of Hygiene* 52(03):321–336.

19. Kerr PJ (1997) An ELISA for epidemiological studies of myxomatosis: persistence of antibodies to myxoma virus in European rabbits (Oryctolagus cuniculus). *Wildlife Research* 24(1):53–65.

20. Cameron CM, Barrett JW, Liu L, Lucas AR, McFadden G (2005) Myxoma virus M141R expresses a viral CD200 (vOX-2) that is responsible for down-regulation of macrophage and T-cell activation in vivo. *Journal of Virology* 79(10):6052–6067.

21. Cameron CM, Barrett JW, Mann M, Lucas A, McFadden G (2005) Myxoma virus M128L is expressed as a cell surface CD47-like virulence factor that contributes to the downregulation of macrophage activation in vivo. *Virology* 337(1):55–67.

22. Fenner F, Woodroofe GM (1953) The pathogenesis of infectious myxomatosis; the mechanism of infection and the immunological response in the European rabbit (Oryctolagus cuniculus). *British Journal of Experimental Pathology* 34(4):400–411.

23. Cameron C, et al. (1999) The complete DNA sequence of myxoma virus. *Virology* 264(2):298–318.

24. Kerr PJ, et al. (2013) Comparative analysis of the complete genome sequence of the California MSW strain of myxoma virus reveals potential host adaptations. *Journal of Virology* 87(22):12080–12089.

25. Silvers L, et al. (2006) Virulence and pathogenesis of the MSW and MSD strains of Californian myxoma virus in European rabbits with genetic resistance to myxomatosis compared to rabbits with no genetic resistance. *Virology* 348(1):72–83.

26. Traktman P (1996) Poxvirus DNA replication. *DNA replication in eukaryotic cells. Cold Spring Harbor Laboratory Press, Cold Spring Harbor, NY, 775-798*

27. Smith GL, Vanderplasschen A, Law M (2002) The formation and function of extracellular enveloped vaccinia virus. *Journal of General Virology* 83(12):2915–2931.

28. Bengali Z, Townsley AC, Moss B (2009) Vaccinia virus strain differences in cell attachment and entry. *Virology* 389(1-2):132–140.

29. Townsley AC, Weisberg AS, Wagenaar TR, Moss B (2006) Vaccinia virus entry into cells via a low-pH-dependent endosomal pathway. *Journal of Virology* 80(18):8899–8908.

30. Locker JK, et al. (2000) Entry of the two infectious forms of vaccinia virus at the plasma membane is signaling-dependent for the IMV but not the EEV. *Molecular Biology of the Cell* 11(7):2497–2511.

31. Vanderplasschen A, Hollinshead M, Smith GL (1998) Intracellular and extracellular vaccinia virions enter cells by different mechanisms. *Journal of General Virology* 79(4):877–887.

32. Nash P, et al. (1999) Immunomodulation by viruses: the myxoma virus story. *Immunology Review* 168:103–120.

33. Barrett JW, Cao JX, Hota-Mitchell S, McFadden G (2001) Immunomodulatory proteins of myxoma virus. *Seminar in Immunology* 13(1):73–84.

34. Johnston JB, McFadden G (2003) Poxvirus immunomodulatory strategies: current perspectives. *Journal of Virology* 77(11):6093–6100.

35. Nash P, Barrett J, Cao JX, Mitchell SH (1999) Immunomodulation by viruses: the myxoma virus story. *Immunological reviews 168.1:103-120*

36. Upton C, Mossman K, McFadden G (1992) Encoding of a homolog of the IFN-gamma receptor by myxoma virus. *Science* 258(5086):1369–1372.

37. Mossman K, Upton C, McFadden G (1995) The Myxoma Virus-soluble Interferon-Receptor Homolog, M-T7, Inhibits Interferon- in a Species-specific Manner. *Journal of Biological Chemistry*.

38. Werden SJ, Barrett JW, Wang G, Stanford MM, McFadden G (2007) M-T5, the ankyrin repeat, host range protein of myxoma virus, activates Akt and can be functionally replaced by cellular PIKE-A. *Journal of Virology* 81(5):2340–2348.

39. Turner PC, et al. (1999) Myxoma virus Serp2 is a weak inhibitor of granzyme B and interleukin-1beta-converting enzyme in vitro and unlike CrmA cannot block apoptosis in cowpox virus-infected cells. *Journal of Virology* 73(8):6394–6404.

40. Wang G, et al. (2004) Myxoma virus M11L prevents apoptosis through constitutive interaction with Bak. *Journal of Virology* 78(13):7097–7111.

41. Schreiber M, Rajarathnam K, McFadden G (1996) Myxoma virus T2 protein, a tumor necrosis factor (TNF) receptor homolog, is secreted as a monomer and dimer that each bind rabbit TNFalpha, but the dimer is a more potent TNF inhibitor. *Journal of Biological Chemistry* 271(23):13333–13341.

42. Hnatiuk S, et al. (1999) Role of the C-Terminal RDEL Motif of the Myxoma Virus M-T4 Protein in Terms of Apoptosis Regulation and Viral Pathogenesis. *Virology* 263(2):290–306.

43. Lalani AS, et al. (1997) The purified myxoma virus gamma interferon receptor homolog M-T7 interacts with the heparin-binding domains of chemokines. *Journal of Virology* 71(6):4356–4363.

44. Rahman MM, Liu J, Chan WM, Rothenburg S, McFadden G (2013) Myxoma virus protein M029 is a dual function immunomodulator that inhibits PKR and also conscripts RHA/DHX9 to promote expanded host tropism and viral replication. *PLoS Pathogens* 9(7):e1003465.

45. Liu J, Wennier S, Zhang L, McFadden G (2011) M062 Is a Host Range Factor Essential for Myxoma Virus Pathogenesis and Functions as an Antagonist of Host SAMD9 in Human Cells. *Journal of Virology* 85(7): 3270-3282

46. Liu J, Wennier S, Zhang L, McFadden G (2011) M062 is a host range factor essential for myxoma virus pathogenesis and functions as an antagonist of host SAMD9 in human cells. *Journal of Virology* 85(7):3270–3282.

47. Barrett JW, et al. (2007) Myxoma virus M063R is a host range gene essential for virus replication in rabbit cells. *Virology* 361(1):123–132.

48. Liu J, et al. (2012) Myxoma virus M064 is a novel member of the poxvirus C7L superfamily of host range factors that controls the kinetics of myxomatosis in European rabbits. *Journal of Virology* 86(9):5371–5375.

49. Schreiber M, Sedger L, McFadden G (1997) Distinct domains of M-T2, the myxoma virus tumor necrosis factor (TNF) receptor homolog, mediate extracellular TNF binding and intracellular apoptosis inhibition. *Journal of Virology* 71(3):2171–2181.

50. Sedger L, McFadden G (1996) M-T2: a poxvirus TNF receptor homologue with dual activities. *Immunology and Cell Biology* 74(6):538–545.

51. Schreiber M, McFadden G (1996) Mutational analysis of the ligand-binding domain of M-T2 protein, the tumor necrosis factor receptor homologue of myxoma virus. *Journal of Immunology* 157(10):4486–4495.

52. Kerr PJ, et al. (2012) Evolutionary history and attenuation of myxoma virus on two continents. *PLoS Pathogens* 8(10):e1002950.

53. Parer I, Conolly D, Sobey WR (1985) Myxomatosis: the effects of annual introductions of an immunizing strain and a highly virulent strain of myxoma virus into rabbit populations at Urana, N.S.W. *Wildlife Research* 12(3):407–423.

54. Fenner F, Marshall ID (1957) A comparison of the virulence for European rabbits (Oryctolagus cuniculus) of strains of myxoma virus recovered in the field in Australia, Europe and America. *Journal of Hygiene* 55(02):149–191.

55. Marshall ID, Fenner F (1958) Studies in the epidemiology of infectious myxomatosis of rabbits: V. Changes in the innate resistance of Australian Wild rabbits exposed to myxomatosis. *Journal of Hygiene* 56(02):288–302.

56. Marshall ID, Douglas GW (1961) Studies in the epidemiology of infectious myxomatosis of rabbits: VIII. Further observations on changes in the innate resistance of Australian wild rabbits exposed to myxomatosis. *Journal of Hygiene* 59(01):117–122.

57. Sobey WR (1969) Selection for resistance to myxomatosis in domestic rabbits (Oryctolagus cuniculus). *Journal of Hygiene* 67(04):743–754.

58. Alda F, Gaitero T, Suárez M, Doadrio I (2009) Molecular characterisation and recent evolution of myxoma virus in Spain. *Archive in Virology* 154(10):1659–1670.

59. Ross J, Sanders MF (1987) Changes in the virulence of myxoma virus strains in Britain. *Journal of Hygiene* 98(01):113–117.

60. Stetson DB, Medzhitov R (2006) Type I Interferons in Host Defense. *Immunity* 25(3):373–381.

61. Samuel CE (2001) Antiviral Actions of Interferons. *Clinical Microbiology Reviews*.

62. Pestka S (1997) The human interferon-alpha species and hybrid proteins. *Seminar in Oncology* 24(3 Suppl 9):S9–4–S9–17.

63. de Weerd NA, Samarajiwa SA, Hertzog PJ (2007) Type I interferon receptors: biochemistry and biological functions. *Journal of Biological Chemistry*. 282(28): 20053-20057

64. Borden EC, Williams BR (2011) Interferon-stimulated genes and their protein products: what and how? *Journal of Interferon & Cytokine Research* 31(1): 1-4

65. Ng CS, Kato H, Fujita T (2012) Recognition of viruses in the cytoplasm by RLRs and other helicases--how conformational changes, mitochondrial dynamics and ubiquitination control innate immune responses. *International Immunology* 24(12):739–749.

66. Kawai T, Akira S (2010) The role of pattern-recognition receptors in innate immunity: update on Toll-like receptors. *Nature Immunology* 11(5):373–384.

67. Goubau D, Deddouche S, Reis e Sousa C (2013) Cytosolic sensing of viruses. *Immunity* 38(5):855–869.

68. Honda K, Taniguchi T (2006) IRFs: master regulators of signalling by Toll-like receptors and cytosolic pattern-recognition receptors. *Nature Reviews of Immunology* 6(9):644–658.

69. Das S, Ward SV, Tacke RS, Suske G, Samuel CE (2006) Activation of the RNA-dependent protein kinase PKR promoter in the absence of interferon is dependent upon Sp proteins. *Journal of Biological Chemistry* 281(6):3244–3253.

70. Dauber B, Wolff T (2009) Activation of the Antiviral Kinase PKR and Viral Countermeasures. *Viruses* 1(3):523–544.

71. COLE J (2007) Activation of PKR: an open and shut case? *Trends in Biochemical Sciences* 32(2):57–62.

72. Lemaire PA, Anderson E, Lary J, Cole JL (2008) Mechanism of PKR Activation by dsRNA. *Journal of Molecular Biology* 381(2):351–360.

73. García MA, et al. (2006) Impact of protein kinase PKR in cell biology: from antiviral to antiproliferative action. *Microbiology and Molecular Biology Review* 70(4):1032–1060.

74. Patel RC, Sen GC (1998) PACT, a protein activator of the interferon-induced protein kinase, PKR. *The EMBO Journal* 17(15):4379–4390.

75. Ito T, Yang M, May WS (1999) RAX, a cellular activator for double-stranded RNA-dependent protein kinase during stress signaling. *Journal of Biological Chemistry* 274(22):15427–15432.

76. Patel CV, Handy I, Goldsmith T, Patel RC (2000) PACT, a stress-modulated cellular activator of interferon-induced double-stranded RNA-activated protein kinase, PKR. *Journal of Biological Chemistry* 275(48):37993–37998.

77. Ruvolo PP, Gao F, Blalock WL, Deng X, May WS (2001) Ceramide regulates protein synthesis by a novel mechanism involving the cellular PKR activator RAX. *Journal of Biological Chemistry* 276(15):11754–11758.

78. Galabru J, Hovanessian A (1987) Autophosphorylation of the protein kinase dependent on double-stranded RNA. *Journal of Biological Chemistry* 262(32):15538–15544.

79. Dey M, et al. (2005) Mechanistic link between PKR dimerization, autophosphorylation, and eIF2alpha substrate recognition. *Cell* 122(6):901–913.

80. Pathak VK, Schindler D, Hershey JW (1988) Generation of a mutant form of protein synthesis initiation factor eIF-2 lacking the site of phosphorylation by eIF-2 kinases. *Molecular and Cellular Biology* 8(2):993–995.

81. CLEMENS MJ (1996) 5 Protein Kinases That Phosphorylate eIF2 and eIF2B, and Their Role in Eukaryotic Cell Translational Control. *Cold Spring Harbor Monograph Archive* 30(0):139–172.

82. CLEMENS MJ, ELIA A (1997) The Double-Stranded RNA-Dependent Protein Kinase PKR: Structure and Function. *Journal of Interferon Cytokine Research* 17(9):503–524.

83. Langland JO, Cameron JM, Heck MC, Jancovich JK, Jacobs BL (2006) Inhibition of PKR by RNA and DNA viruses. *Virus Research* 119(1):100–110.

84. Romano PR, et al. (1998) Autophosphorylation in the Activation Loop Is Required for Full Kinase Activity In Vivo of Human and Yeast Eukaryotic Initiation Factor. *Molecular and Cellular Biology* 18(4): 2282-2297

85. Min J-Y, Li S, Sen GC, Krug RM (2007) A site on the influenza A virus NS1 protein mediates both inhibition of PKR activation and temporal regulation of viral RNA synthesis. *Virology* 363(1):236–243.

86. Poppers J, Mulvey M, Khoo D, Mohr I (2000) Inhibition of PKR activation by the proline-rich RNA binding domain of the herpes simplex virus type 1 Us11 protein. *Journal of Virology* 74(23):11215–11221.

87. Carroll K, Elroy-Stein O, Moss B, Jagus R (1993) Recombinant vaccinia virus K3L gene product prevents activation of double-stranded RNA-dependent, initiation factor 2 alpha-specific protein kinase. *Journal of Biological Chemistry* 268(17):12837–12842.

88. Brand SR, Kobayashi R, Mathews MB (1997) The Tat protein of human immunodeficiency virus type 1 is a substrate and inhibitor of the interferon-induced, virally activated protein kinase, PKR. *Journal of Biological Chemistry* 272(13):8388–8395.

89. Chou J, Chen JJ, Gross M, Roizman B (1995) Association of a M(r) 90,000 phosphoprotein with protein kinase PKR in cells exhibiting enhanced phosphorylation of translation initiation factor eIF-2 alpha and premature shutoff of protein synthesis after infection with gamma 134.5- mutants of herpes simplex virus 1. *Proceedings of the National Academy of Sciences of USA* 92(23):10516–10520.

90. Rajan P, et al. (1995) A novel translational regulation function for the simian virus 40 large-T antigen gene. *Journal of Virology* 69(2):785–795.

91. Donnelly N, Gorman AM, Gupta S, Samali A (2013) The eIF2α kinases: their structures and functions. *Cellular and Molecular Life Sciences* 70(19):3493–3511.

92. Rothenburg S, Seo EJ, Gibbs JS, Dever TE, Dittmar K (2009) Rapid evolution of protein kinase PKR alters sensitivity to viral inhibitors. *Nature Structural and Molecular Biology* 16(1):63–70.

93. Elde NC, Child SJ, Geballe AP, Malik HS (2009) Protein kinase R reveals an evolutionary model for defeating viral mimicry. *Nature* 457(7228):485–489.

Chapter 2 - Characterization of the host range function of K3L and selected K3L orthologs

Abstract

Poxviruses exhibit wide variation in host range. For example, vaccinia virus (VACV), which was used for the vaccination against smallpox, has a very broad host range and is able to infect many different species. In contrast, others such as swinepox virus, which only infects pigs, display a very narrow host range. However, the molecular mechanisms controlling the differences in poxvirus host range are unknown. Since the entry of poxviruses into a host cell is species-independent, the host range of any given poxvirus is determined by its ability to subvert the host's antiviral immune responses, in which an important step constitutes the inhibition of the antiviral factor protein kinase R (PKR). PKR suppresses general translation during virus infection and has evolved rapidly in vertebrates, which was likely caused by the selective pressure exerted by several viral inhibitors. VACV encodes the two PKR inhibitors E3L and K3L, both of which are host range genes for the virus. Whereas K3L was shown to be necessary for VACV replication in Syrian hamster BHK21 cells, E3L was essential for replication in cells from other species such as human HeLa cells. To determine the molecular basis for this host range function of K3L and E3L, we used a luciferase reporter transfection assay in PKR-deficient HeLa cells to measure interactions between these inhibitors and PKR from a variety of mammalian species. Our results show a surprising variation in the sensitivity of PKR to VACV inhibitors, especially K3L, and its orthologs from sixteen other poxviruses. We found that the sensitivity of each species' PKR to E3L or K3L correlated with virus replication and the phosphorylation of eIF2α in cell lines derived from the respective species after infection with VACV mutants that lack E3L, K3L or both. Our results show that the host range function of K3L can be explained by species-specific differences in the sensitivity of PKR to these VACV inhibitors. We also found that a K3L ortholog from swinepox virus inhibited only swine PKR but

not PKR from other species tested, which might contribute to the species-specificity of swinepox virus.

Introduction

VACV is a prototypic poxvirus that belongs to the genus orthopoxvirus. VACV is the most intensively studied poxvirus and is well-known for its use as a vaccine strain in the global campaign to eradicate smallpox (reviewed in (1)). Due to its large genetic encoding capacity and the feasibility of genetic manipulation, VACV has also been widely used as a vector for vaccine development (reviewed in (2, 3)). The current strains of VACV used in laboratories have undergone untraceable propagations in animals and cell lines for decades. The origin, and most importantly, the natural host of VACV, is therefore unknown. In experimental settings, VACV displays a broad host range in animals, productively infecting humans, rodents, lagomorphs and ungulates (reviewed in (4, 5)). In addition, VACV can infect cell lines derived from a variety of species (4). However, the molecular mechanisms for the cellular tropism and host specificity of VACV remain unclear. Some poxvirus genes are found to be dispensable for virus replication in cell lines derived from certain species, but are important in others. These genes are therefore termed host range genes. These host range genes directly influence the host range and potentially virulence of poxviruses, because the entry of poxviruses is species-independent, the host range of a particular virus is dependent on its ability to subvert the host innate immune response (4). The protein products of host range genes often target one or multiple pathways associated with the host's antiviral immune response.

One most important group of poxvirus host range genes comprise PKR inhibitors. VACV possesses the PKR inhibitors E3L and K3L, which antagonize the PKR-mediated antiviral response at different steps (6). E3L and K3L gene orthologs are found in many poxviruses, indicating the importance of PKR inhibition for poxvirus replication (7). VACV E3L contains an N-terminal Z-DNA binding domain and a C-terminal dsRNA binding domain. Whereas only the

dsRNA binding domain is required for virus replication in cells, both domains are indispensable for VACV pathogenesis in mice (8, 9). It is generally acknowledged that E3L inhibits PKR by binding dsRNA molecules produced during virus infection, and thereby prevents PKR activation. However, a recent study challenged this perception by showing that the biological function of E3L does not fully rely on its capability to bind double-stranded RNA (10). The study also showed evidence that E3L was able to be co-immunoprecipated with PKR during infection, suggesting E3L may exert its host range function through mechanisms other than double-stranded RNA sequestration (10). However, the extent to which the PKR-E3L interaction contributes to the biological function of E3L remains unknown.

VACV K3L, on the other hand, is a homologue of eIF2α, the substrate of PKR, and functions as a pseudosubstrate inhibitor by binding to eIF2α binding site on the kinase domain of PKR and therefore excluding eIF2α (11-14). Interestingly, deletion of K3L diminished the replication of VACV in Syrian hamster BHK21 and murine L929 cells but not in human HeLa cells, which categorized K3L as a host range gene of VACV (6). Orthologs of VACV K3L are found in most orthopoxviruses and all clade II poxviruses (7). Their sequences, however, are highly divergent compared to that of other poxvirus genes. In fact, K3L orthologs from different poxviruses can display as low as 25% sequence identity with each other (7). One explanation for this is that since K3L orthologs from different poxviruses evolved in different animal reservoirs, the evolutionary pressure exerted by the host's antiviral immune response may have driven the K3L orthologs to evolve to optimize their activity in the natural host of each virus. Interestingly, Elde *et al.* found that under an experimentally induced selective pressure, in which E3L is deleted from VACV, the remaining PKR inhibitor K3L could quickly evolve to evade the antiviral effects imposed by PKR through an accordion-like expansion of the K3L gene locus.

The quick amplification of K3L copy number allows for more efficient accumulation of mutations, which facilitated the selection of mutations that have improved PKR inhibitory capability (15). The result of this experimentally accelerated virus evolution can possibly explain how K3L and its orthologs evolved in different animal hosts, which ultimately causing their divergence.

As a result of the selective pressure exerted by highly divergent K3L orthologs, PKR from different species also exhibit high levels of variation (16). Notably, we and others showed that the high degree of diversity in the kinase domain of PKR resulted in varied levels of sensitivity displayed by different species' PKR to VACV K3L. For example, whereas human PKR was largely resistant to K3L inhibition, mouse PKR was very sensitive (16). Moreover, PKR from hominoid primates were more resistant to K3L inhibition than those from old or new world monkeys (17). The species-specific inhibition of PKR by K3L was observed in a variety of assay systems, however, the extent to which it contributes directly to the host range function of K3L and how it influences the host range of VACV have not been studied.

In this chapter, we thoroughly examined the inhibitory effect of VACV K3L and its poxvirus orthologs from 16 different poxviruses on PKR from various mammalian species using a previously described transfection assay (16). We also investigated how the inhibition of host PKR by K3L contributes to the cellular tropism of VACV and the PKR-mediated antiviral response in cell lines derived from different species. In addition to VACV K3L, we also analyzed a K3L ortholog from swinepox virus named C8L, and found that it evolved to specifically inhibit swine PKR with the highest efficiency. The host species-specific inhibition of swine PKR by C8L may therefore contribute to the limited host range displayed by the swinepox virus.

Materials and Methods

Plasmids, cell lines and viruses

PKR and viral genes were cloned into the pSG5 vector (Stratagene) for transient expression in mammalian cells. Cloning of European rabbit PKR, brush rabbit PKR, Eastern cottontail PKR, Sheep PKR, rat PKR, Syrian hamster PKR, Chinese hamster PKR and Guinea pig PKR was described in detail in Chapter 3. Cloning of knock-down resistant human PKR and mouse PKR was described previously (16). Chimpanzee PKR, orangutan PKR, gibbon PKR, macaque PKR and tamarin PKR were kindly provided by Nels Elde. Turkish hamster PKR was cloned from cDNA generated from testicular total RNA from a Turkish hamster. Armenian hamster PKR was cloned from the total RNA collected from AHL-1 cells. Cat PKR was cloned from CRFK cells (ATCC-CCL94) and was identical to XP_003984379.1. Dog PKR was cloned from MDCK cells (ATCC-CCL34). Three identical cDNA clones contained the same amino-acid difference from NP_001041600.1. Horse PKR was cloned from horse cells (efc cells, kindly provided by Udeni Balasuriva and Ying Fang) and was identical to XP_008514381.1. Cow PKR was cloned from cow cells MDBK cells (ATCC-CRL6071) and was identical to NP_835210.2. Camel PKR was cloned from camel Dubca cells (ATCC-CRL2276) and was identical to XP_006192853.1. Pig PKR was cloned from swine PK-15 cells. VACV K3L (Copenhagen strain) and swinepox virus C8L were cloned into pSG5. All open reading frames were sequenced to confirm correct sequences.

PKR^{kd} HeLa cells and control HeLa cells were kindly provided by Charles Samuel (19). RK13 and PK-15 cells were kindly provided by Bernard Moss. Generation of RK13 cells with ectopic expression of E3 and K3 was described (20). CRFK cells, MDBK cells, PK-15 cells and rat-1 cells were obtained from ATCC. All cell lines were maintained in DMEM (Gibco)

supplemented with 5% FBS and 50µg/ml gentamycin at 37˚C with 5% CO_2. For transfection assays, plasmids were prepared using the NucleoBond Xtra Midi Endotoxin Free plasmid preparation kit (Macherey-Nagel).

The Copenhagen VC-2 and vp872 (K3L-deficient) VACV strains were kindly provided by Bernard Moss. The construction of VC-R1 (E3L-deficient), vp872 (K3L-deficient) and VC-R2 (E3L-deficient, K3L-deficient) was described previously in (18). All virus strains used were amplified in PKR^{kd} HeLa cells and purified by sucrose-gradient ultracentrifugation with the protocol described in (21).

Luciferase assay

5 x10^4 HeLa-PKR^{kd} cells were seeded in 24-well plates one day before transfection. For each transfection, firefly luciferase (pGL3promoter, 50 ng, Promega), and pSG5 plasmids encoding PKR (200 ng), VACV K3L, VACV E3L or swinepox virus C8L (400 ng) were transfected using GenJet-HeLa. For controls, empty pSG5 vector was transfected using the same amount. Each transfection was conducted in triplicate. After 48 hours, cell lysates were harvested using mammalian lysis buffer (Goldbio) and luciferase activity was determined using luciferase detection reagents (Promega) in a luminometer (Berthold). Each experiment was performed at least three times and representative experiments are shown in the results. Error bars represent the standard deviations of three replicate transfections.

Western blot analyses and Infection assays

Different cell lines indicated in the figures were infected with VC-2, vp872, VC-R1 and VC-R2 at an MOI of 5 for 1 hour. Total protein was collected 6 hours after infection with 1%-SDS in PBS. Protein samples were separated on 10% SDS-PAGE gels and transferred to PVDF membranes (GE Healthcare) using a methanol-based wet transfer apparatus (BioRad).

Membranes were blocked with 5% non-fat milk or 5% BSA when detecting eIF2α-P in TBST buffer (20mM Tris, 150mM NaCl and 0.1% Tween-20 pH7.6) for 3 hours at 4˚C with agitation and then incubated overnight with the rabbit anti-serum raised against eIF2α-P (Biosource International) at 4˚C with rocking, and then stripped and re-probed with antibody against total eIF2α (SantaCruz). After washing, membranes were incubated with goat-anti-rabbit or goat-anti-mouse secondary antibodies (1:30,000) in TBST containing 5% non-fat milk for 1 hour at room temperature with agitation followed by TBST washing 4 times at 20 minutes each. Proteins were detected with Proto-Glo ECL (National Diagnostics) and images were taken with a Kodak image system.

To determine virus titers, cell lines were infected with VC-2, VC-R1, vp872 and VC-R2 at an MOI of 0.01. Viruses were collected 48 hours after infection by repeated freeze-thaw cycles and tittered on monolayers of RK13+E3L+K3L cells (20). Infections were performed in duplicates. Error bars indicate standard deviation.

To examine the expression of K3L and K3L orthologs, human HeLa-PKR^{kd} cells were transfected transiently with FLAG-tagged K3L orthologs. Protein lysates were collected 48 hours after transfection with 1%SDS-PBS. Total protein was collected 6 hours after infection with 1%-SDS in PBS. Protein samples were separated on 12% SDS-PAGE gels and transferred to PVDF membranes (GE Healthcare) using a methanol-based wet transfer apparatus (BioRad). Membranes were blocked with 5% non-fat milk in TBST for 3 hours at 4˚C with agitation and then incubated overnight with the rabbit anti-FLAG antibody at 4˚C with rocking, and then stripped and re-probed with antibody against β-actin. After washing, membranes were incubated with goat-anti-mouse secondary antibodies (1:30,000) in TBST containing 5% non-fat milk for 1 hour at room temperature with agitation followed by TBST washing 4 times at 20 minutes each.

Proteins were detected with Proto-Glo ECL (National Diagnostics) and images were taken with a Kodak image system.

Results

K3L inhibits PKR in a species-specific manner

To directly assess the inhibitory capability of K3L on PKR from different species, we utilized a previously described transfection-based luciferase assay, in which we co-transfected plasmids encoding PKR, K3L and firefly luciferase into a line of PKR-deficient HeLa cells (described in Chapter 3). We cloned PKR from the following 23 mammalian species: human (*Homo sapiens*), chimpanzee (*Pan troglodytes*), orangutan (*Pongo borneo*), gibbon (*Hylobates leucogenys*), Rhesus macaque (*Macaca mulatta*), tamarin (*Saguinus labiatus*), mouse (*Mus musculus*), brown rat (*Rattus norvegicus*), Guinea pig (*Cavia porcellus*), Syrian hamster (*Mesocricetus auratus*), Armenian hamster (*Cricetulus migratorius*), Turkish hamster (*Mesocricetus brandti*), Chinese hamster (*Cricetulus griseus*), brush rabbit (*Sylvilagus bachmani*), European rabbit (*Oryctolagus cuniculus*), Eastern cottontails (*Sylvilagus floridanus*), cat (*Felis catus*), dog (*Canis lupus*), pig (*Sus scrofa*), horse (*Equus caballus*), cow (*Bos Taurus*), camel (*Camelus dromedaries*) and sheep (*Ovis aries*). The protein sequences identities between these PKRs are shown in Table 2.1. We examined their sensitivities to VACV K3L. First, we observed that transfection of PKR alone significantly reduced the expression of luciferase to comparable levels among different species, suggesting PKR from different species are expressed comparably and are catalytically competent in human HeLa-PKR^{kd} cells (Fig. 2.1). Co-transfection of K3L with all the PKRs resulted in varied levels of luciferase expression, suggesting the inhibition of PKR by K3L is species-specific (Fig. 2.2). Particularly, co-transfection of K3L resulted in at least a three-fold increase of luciferase activities in cells co-transfected with PKR from rhesus macaque, tamarin, mouse, Syrian hamster, Turkish hamster, Chinese hamster, brush rabbit, European rabbit, Eastern cotton tail, cat, dog, horse, cow and

camel, indicating PKR from these species were sensitive to VACV K3L inhibition. In contrast, co-transfection of K3L with PKR from human, chimpanzee, rat, Guinea pig, Armenian hamster, pig and sheep resulted in none or a slight increase (less than 2 fold) of luciferase activity, suggesting PKR from those species are largely resistant, or completely resistant to K3L inhibition. PKR from the orangutan or gibbon were only moderately sensitive to K3L inhibition, resulting in a 2-3 fold increase of luciferase activity. The results from the transfection assay indicate that PKR from different species differ in their sensitivities to inhibition by VACV K3L. Interestingly, even some closely related species exhibited very drastic differences in PKR sensitivities to K3L inhibition. For instance, whereas mouse PKR was sensitive to K3L, rat PKR was completely resistant. A similar phenomenon was also observed between Syrian hamster PKR, which was very sensitive to K3L, and Armenian hamster PKR, which was completely resistant. In the group of ungulate species tested, PKR from pig and sheep were completely resistant to K3L inhibition while PKR from horse, cow and camel species were sensitive.

In addition to K3L, VACV also contains a second PKR inhibitor, E3L, which is composed of a double-stranded RNA binding domain and a Z-DNA binding domain. We assessed the inhibitory ability of E3L on PKR from the aforementioned species in the same assay and found that E3L was able to increase the reduction of luciferase activity by PKR from most of these species with the exceptions of Syrian hamster and Turkish hamster, both of which are *Mesocricetus* hamsters closely related to each other (Fig. 2.3). Interestingly, both Syrian hamster and Turkish hamster PKR were very sensitive to K3L inhibition.

Overall, our data indicate that inhibition of PKR by VACV K3L and E3L is species-specific. The species-specific inhibition of PKR by VACV K3L follows a random pattern and

could not have been predicted with our current knowledge. Meanwhile, VACV E3L displays a very low level of species-specificity.

Variola virus (VARV) is the causative agent of smallpox, which is a deadly infectious disease restricted to humans. To examine the inhibitory effect of the VARV K3L ortholog on PKR from different species, especially human PKR, we cloned the VARV K3L ortholog, C3L, as well as the K3L orthologs from TATP (taterapox virus) and CMLV (camelpox virus), which are the closest known relatives of VARV. The TATP and CMLV M96-K3L orthologs display 93.2% and 92.0% protein sequence identities with VARV C3L, respectively, and 99% identity between each other (Fig. 2.4). In the luciferase assay, we found that VARV C3L inhibited PKR from gibbon, mouse, brush rabbits, European rabbits, Eastern cottontails, cat, dog, horse, camel and sheep with high efficiency (larger than 3-fold increase of luciferase activity) (Fig. 2.5). However, in contrast to K3L, VARV C3L failed to inhibit PKR from Syrian, Turkish and Chinese hamster species, but instead showed high levels of inhibition of sheep PKR, which was resistant to VACV K3L inhibition (Fig. 2.5). Remarkably, human PKR was largely resistant to VARV C3L inhibition, showing less than two-fold increase of luciferase activity (Fig. 2.5).

On the other hand, the TATP K3L ortholog 037 only failed to inhibit PKR from Guinea pig and pig, but in contrast to VACV K3L, TATP 037 inhibited PKR from primates, rat, Armenian hamster and sheep, which were resistant to VACV K3L (Fig. 2.6). The CMLV K3L ortholog V032 from the M96 strain exhibited a very similar pattern of species-specific PKR inhibition compared to TATP 037 (Fig. 2.7). The only difference observed between TATP 037 and CMLV M96-V032 was that Armenian hamster PKR was sensitive to TATP 037, but was resistant to CMPV V032 (Fig. 2.6 and 2.7). We also tested the CMLV V032 from the CMS strain and found that it was a loss-of-function variant (Fig. 2.8). The PKR sensitivities to

poxvirus K3L orthologs from VACV, VARV, TATP and CMLV were summarized in Table 4.2. Our results showed that the K3L orthologs from VARV, TATP and CMLV exhibited species-specific inhibition of PKR. However, the sensitivity of any given PKR to different K3L orthologs may vary. For example, human PKR was largely resistant to the inhibitions of VACV and VARV K3L orthologs, but was intermediately sensitive to that of the K3L orthologs from TATP and CMLV.

A possible explanation for why human PKR was insensitive to VARV C3L inhibition is that human PKR might have evolved to evade inhibition from VARV C3L. This might have come with the price that human PKR could have become sensitive to other poxvirus inhibitors by chance. To further examine this, we cloned K3L orthologs from 16 poxviruses including VACV, VARV, CPXV (cowpox virus), TATP, SPPV (sheeppox virus), DPV (deerpox virus), MYXV (myxoma virus), RFV (rabbit fibroma virus), SWPV (swinepox virus), TPV (tanapox virus), YMTV (yaba monkey tumor virus), YKV (yoka poxvirus), COTV (cotia virus), RCPV (raccoonpox virus), SKPV (skunkpox virus) and VPV (volepox virus). These K3L orthologs are highly diverse and can display as low as 22.7% sequence identity with one another (Table 2.3). We tested the inhibitory capabilities of these K3L orthologs on human PKR in the luciferase assay and found that human PKR exhibited differential sensitivities to different K3L orthologs (Fig. 2.9). In consistent with what we observed previously, human PKR was largely resistant to VACV K3L and VARV C3L (Fig. 2.9). In addition, we found that human PKR was completely resistant to inhibition of MYXV and RFV K3L orthologs, and was largely resistant to the K3L orthologs from YKV (Fig. 2.7). Interestingly, the K3L orthologs from SPPV, DPV, TPV, COTV, RCPV and SKPV showed strong inhibition on human PKR (Fig. 2.9). As a control, we performed the similar test on mouse PKR, which was sensitive to VACV K3L inhibition (Fig.

2.9). The results showed that in contrast to human PKR, mouse PKR was resistant to K3L orthologs from SPPV, DPV and TPV, which suggest that the reason why human PKR was sensitive to these three K3L orthologs was not due to their enhanced expression compared to VACV K3L (Fig. 2.10).

Inhibition of PKR is indispensable for VACV replication

We next determined if the species-specific inhibition of PKR constitutes K3L's function in VACV cell tropism. We infected selected cell lines originated from different species with the Copenhagen strain of VACV termed VC-2, or VC-2-derived recombinant viruses including vp872 (K3L-knock out), VC-R1 (E3L-knock out), or VC-R2 (E3L, K3L-double knock out) at a low MOI (0.01) and monitored replication 48 hours after infection by titering each infection in a line of RK13 cells stably expressing K3L and E3L, which is permissive for all viruses (18). In addition, we measured phosphorylation of eIF2α six hours after infection with a high MOI (MOI=5) as a readout for PKR's catalytic activity. A previous study from our lab indicated that the VC-R2 strain, which lacks both PKR inhibitors K3L and E3L failed to replicate in RK13 cells, but was able to replicate to slightly lower levels than VC-2, VC-R1 and vp872 in RK13 cells that stably express PKR inhibitors K3L and E3L, indicating that PKR is the major obstacle that VACV has to overcome in order to successfully replicate in these cells (18). Here we show that VC-R2, VC-R1 and vp872 were all able to replicate to comparable titers as the wild type virus VC-2 in HeLa-PKR^{kd} cells (Fig. 2.11 A). In addition, increased phosphorylation of eIF2α was not observed in HeLa-PKR^{kd} cells infected with any strains of VACV (Fig. 2.11 B). These results suggest that PKR was the only factor that prevented VACV lacking PKR inhibitors from replicating in HeLa cells, and that VACV replication did not lead to the activation of any other eIF2α kinases other than PKR.

Next, we focused on PKR-competent cell lines derived from four different species. We first infected Dubca cells and MDCK cells, which were derived from a camel and a dog, respectively. The wild type VC-2 strain and the K3L-deficient vp872 strain were able to replicate in both Dubca (Fig. 2.12 A) and MDCK (Fig. 2.12 B) cells to comparable titers after 48 hours,

suggesting K3L was not required for virus replication in these cell lines. The E3L-deficient VC-R1 strain was also able to replicate to some extent in both Dubca (Fig. 2.12 A) and MDCK (Fig. 2.12 B) cells, but not as well as VC-2 and vp872. In addition, the VC-R2 strain failed to replicate in either cell line (Fig. 2.12 A, 2.12 B). We also measured eIF2α phosphorylation six hours after infection and found that infection with VC-2, vp872 and VC-R1 did not result in increased eIF2α phosphorylation compared to mock-infected cells, which correlated with their ability to replicate in both cell lines (Fig. 2.13 A, 2.13 B). In contrast, infection with the VC-R2 strain, which lacks any PKR inhibitors and was not able to replicate in either cell line, resulted in a strong induction of eIF2α phosphorylation in Dubca (Fig. 2.13 A) and MDCK (Fig. 2.13 B) cells. All these data suggest that K3L or E3L alone were able to inhibit PKR-induced phosphorylation of eIF2α, and to rescue the PKR-mediated suppression of virus replication. These findings correlated well with our previous observations that camel and dog PKR were sensitive to both K3L and E3L inhibition in the luciferase assay.

We next infected rat rat-1 cells, derived from a brown rat, and swine PK-15 cells, PKR from these corresponding species were sensitive to E3L but completely resistant to K3L inhibition. Similar to what we have observed in MDCK and Dubca cells, both VC-2 and vp872 were able to replicate to comparable levels in rat-1 cells (Fig. 2.14 A) and PK-15 cells (Fig. 2.14 B). However, we found that VC-R1 and VC-R2, which both lack E3L, failed to replicate in either cell line (Fig. 2.14 A, 2.14 B). We also determined eIF2α phosphorylation following virus infections and found that infection with VC-2 and vp872 did not induce any eIF2α phosphorylation, whereas both VC-R1 and VC-R2 infections led to comparable levels of eIF2α phosphorylation in both cell lines (Fig. 2.15 A, 2.15 B). These results suggested that K3L alone was not able to inhibit the PKR-mediated phosphorylation of eIF2α and also failed to rescue

virus replication, which correlates with our previous observations that rat and swine PKR were resistant to K3L inhibition in the luciferase assay. We also tested cat CRFK cells and cow MDBK cells, but these cells were non-permissive for VACV and none of the viruses were able to replicate in them.

Overall, our data confirm that successful replication of VACV correlates with effective inhibition of PKR during virus infection, and indicates that the species-specific inhibition of PKR exhibited by K3L indeed contributes to its host range function for VACV.

Host species-specific inhibition of swine PKR by swinepox virus C8L

Swinepox virus is a poxvirus that exhibits an extremely narrow host range, infecting only pigs. We examined the PKR inhibitory ability of C8L, the K3L ortholog from swinepox virus, which displays 44% sequence identity with K3L at the protein level. As shown in Fig. 2.16, co-transfection of C8L and PKR from mouse, human, Syrian hamster, Armenian hamster, Chinese hamster, Guinea pig, rat, European rabbit and chicken resulted in no increase or only small increase of luciferase activity, indicating PKR from these species were largely resistant to C8L inhibition. In contrast, co-transfection of C8L and swine PKR resulted in a dramatic increase of luciferase activity. This observation suggests that swinepox virus C8L may have evolved to inhibit swine PKR, but not PKR from other species. This constitutes an example of host species-specific inhibition of PKR by poxvirus pseudosubstrate inhibitors, and may contribute to the mechanism by which swinepox virus infection is restricted in pigs.

Discussion

K3L was previously shown to be indispensable for VACV replication in Syrian hamster BHK21 cells, but not in human HeLa cells, suggesting that K3L is a host range factor (7). However, the molecular mechanisms by which K3L exerts its host range function are not fully understood. The most commonly used method to study the host range function of a virus gene is to examine virus replication in cells derived from various species after deleting or inserting the gene in the virus genome. However, this does not yield insights into the interactions between the host range proteins and their host interacting/binding partners. We established a cell culture-based luciferase assay, in which the interaction of PKR and its viral antagonists can be measured and represented by relative luciferase activity, allowing us to assess the sensitivity of PKR to poxvirus inhibitors (16). Using this assay, we discovered that Syrian hamster PKR is highly sensitive to K3L inhibition, while human PKR is largely resistant, which may explains why K3L is required for VACV replication only in Syrian hamster BHK21 cells but not in Human HeLa cells for VACV replication.

From the results we obtained from 23 different species, we would have not been able to predict PKR's sensitivity to K3L based on its species origin, such as that all rodent PKR would be sensitive. In fact, PKR from even closely related species, e.g. mouse and rat or Syrian hamster and Armenian hamster, displayed drastically different sensitivities to K3L inhibition. We previously showed that the helix αG region, which contains residues that directly contact eIF2α, on the kinase domain of PKR was mainly responsible for its sensitivity to K3L (16). A multiple sequence alignment within the helix αG region from 23 PKRs revealed that this region is highly diverse with only three residues being conserved across all species compared (Fig. 2.17). This finding is striking because eIF2α, the binding substrate of PKR, is highly conserved. How such

diverse regions in PKR maintains their interactions with the highly conserved binding partner, eIF2α, is still an evolutionary conundrum.

We divided the 23 PKRs into two groups according to their sensitivities to K3L, being either sensitive or resistant using a 3-fold increase of luciferase activity as cut-off between them. We then plotted the frequency of amino acids that appearing at each position of the helix αG region for each group using WebLogo (22, 23). Unfortunately, we could not immediately identify any particular residues or residue combinations that could directly explain the sensitivity or resistance of PKR to K3L inhibition. However, we noticed that residues 2, 3, 6, 10, 11, 14 (indicated by red arrows) were highly diverse across species (Fig. 2.18). We projected these residues onto the crystal structure of the kinase domain of human PKR, and found that these 6 residues are all located at the interacting interface (facing outside) between PKR and eIF2α (Fig. 2.19, 2.20). This finding suggests that the intermolecular interactions between pseudosubstrate inhibitors, such as K3L, and PKR may have driven the divergence of the helix αG region of PKR. Interestingly, in the helix αG region, multiple residues (including A488, F489, T491, S492, K493, T496 and D500 numbered according to human PKR) were found to be under strong positive selection in rodents (personal communication with Sherry Haller), mammals (16) and primates (16). This observation further supports the hypothesis that the positive selective pressure exerted by virus inhibitors has driven the rapid evolution of the helix αG region on PKR. Because we were not able to readily identify signatures between sensitive and resistant PKR, it seems that the sensitivity to K3L inhibition is determined by multiple amino acid combinations and/or that residues outside of helix αG might contribute to the differences, for example, by the spatial orientation of helix αG.

Our results showed remarkably that human PKR was largely resistant to the inhibition of the VARV K3L ortholog C3L. It is possible that human PKR evolved to evade inhibition from C3L as a result of virus-host co-evolution. However, this evasion may come at a price by making human PKR more susceptible to K3L orthologs from other poxviruses, such as SPPV, TATP, DPV, TPV, COTV, RCPV and SKPV as determined in our luciferase assay.

The sensitivities of PKR to K3L and E3L inhibition play important roles in determining VACV host ranges as determined by our infection analyses. We observed that deletion of E3L from VACV did not affect the virus' ability to suppress eIF2α phosphorylation in cell lines in which the PKR was sensitive to K3L inhibition, such as camel Dubca and dog MDCK cells. However, in cell lines where the endogenous PKR was resistant to K3L inhibition, such as swine PK-15 and brown rat rat-1 cells, the presence of K3L alone failed to prevent PKR-mediated eIF2α phosphorylation or rescue virus replication. All these data demonstrate that the host range function of K3L is mainly due to its varied ability to inhibit different species' PKR.

Swinepox virus is the causative agent of swinepox, a disease strictly restricted to pigs (24). Piglets younger than 4-months old are very susceptible to swinepox and can develop an acute disease. Adult animals infected with swinepox virus usually develop a mild disease that is non-lethal (24). The high host specificity and low virulence of swinepox virus have stimulated interest in developing swinepox virus as pig-specific vaccine vector for other infectious diseases in pigs (25). However, the molecular mechanism by which swinepox infection is restricted in swine is unknown. We showed that the swinepox virus K3L ortholog C8L specifically inhibited swine PKR with the highest efficiency. This host species-specific inhibition of PKR may contribute to the restriction of swinepox virus to pigs.

In conclusion, we studied the inhibitory effect of K3L and its poxvirus ortholog and found that inhibition of PKR by K3L orthologs is species-specific, and this finding may contribute to the molecular mechanism by which K3L and its poxvirus orthologs exert their host range functions.

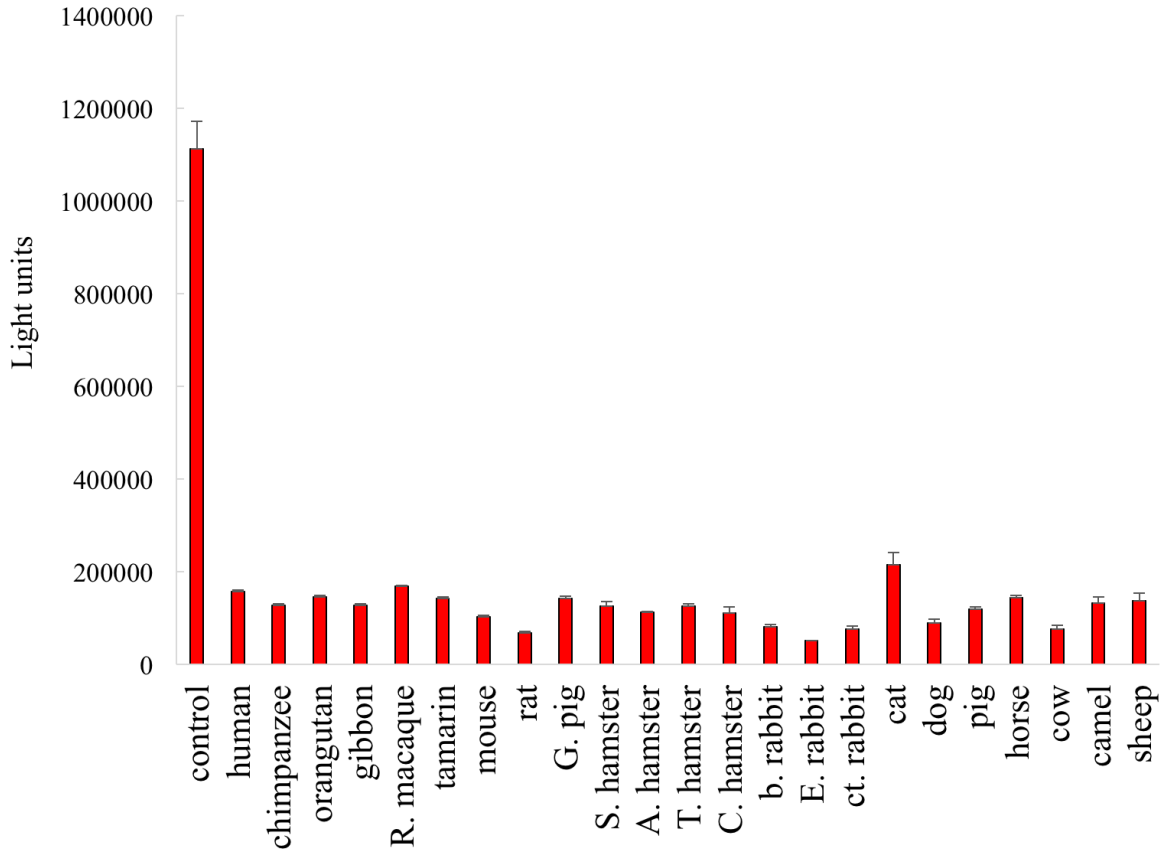

Figure 2.1 Reduction of luciferase translation by PKR

Human HeLa-PKR^{kd} cells were transfected with expression vectors for firefly luciferase (0.05µg), PKR from the indicated species (0.2µg) and empty vector pSG5 (0.4µg). Luciferase activity was measured 48 hours after transfection. Experiments were performed in triplicate and the results are representative of three independent experiments. Error bars indicate standard deviations. Abbreviations used: R=Rhesus; G=Guinea; S=Syrian; A=Armenian; T=Turkish, C=Chinese; b=brush; E=European; ct=cottontail.

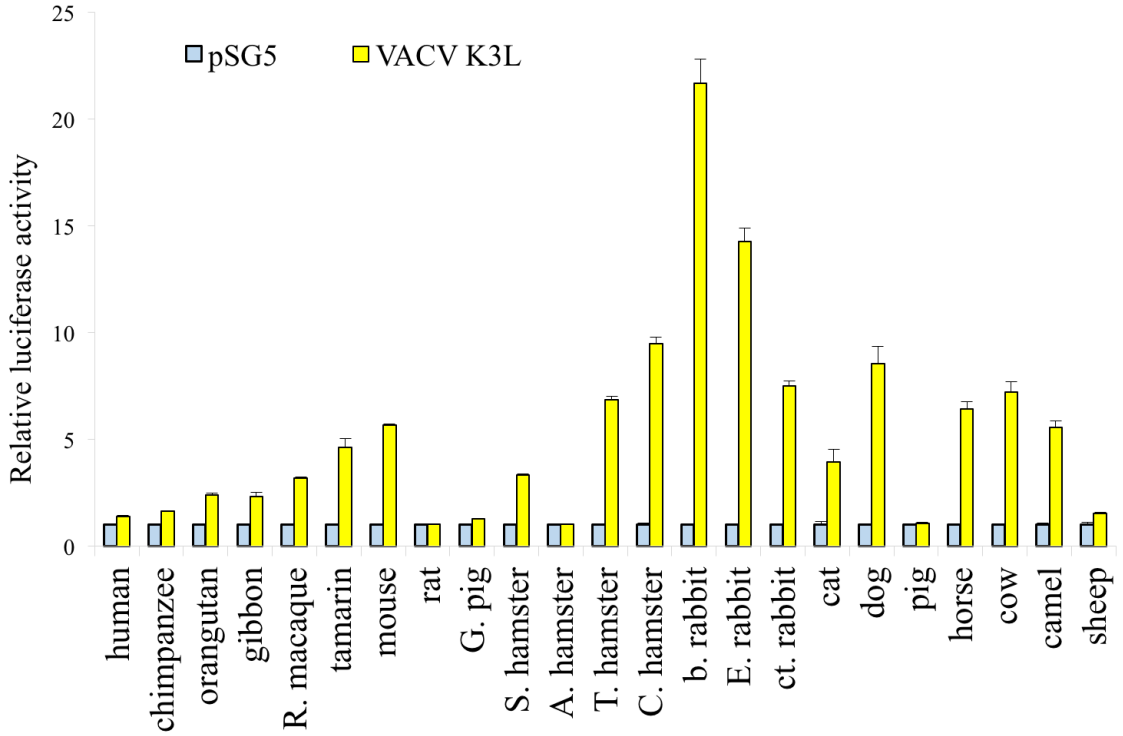

Figure 2.2 Inhibition of PKR by VACV K3L

Human HeLa-PKR^{kd} cells were transfected with expression vectors for firefly luciferase (0.05µg), PKR from the indicated species (0.2µg) and VACV K3L (0.4µg). Luciferase activity was measured 48 hours after transfection and the acquired light units were normalized to PKR-only transfected cells to obtain relative luciferase activities. Experiments were performed in triplicate and the results are representative of three independent experiments. Error bars indicate standard deviations. Abbreviations used: R=Rhesus; G=Guinea; S=Syrian; A=Armenian; T=Turkish, C=Chinese; b=brush; E=European; ct=cottontail.

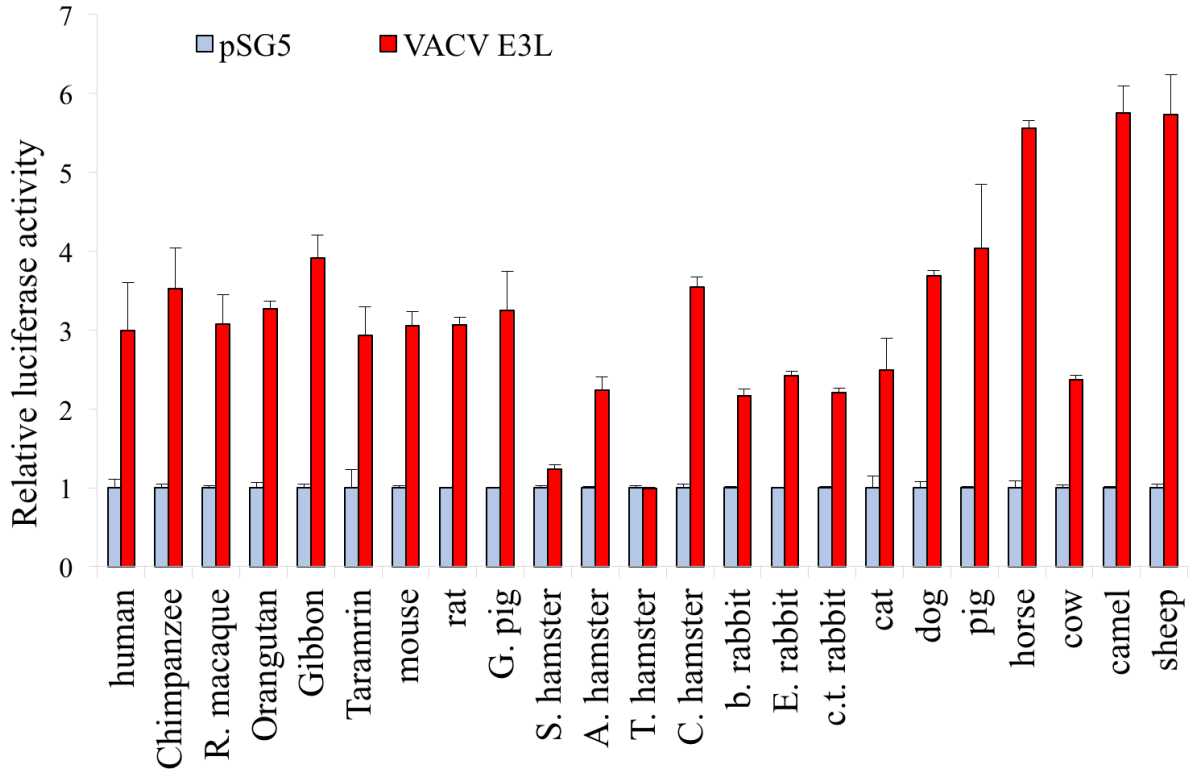

Figure 2.3 Inhibition of PKR by VACV E3L

Human HeLa-PKR^{kd} cells were transfected with expression vectors for firefly luciferase (0.05µg), PKR from the indicated species (0.2µg) and VACV E3L (0.4µg). Luciferase activity was measured 48 hours after transfection and the acquired light units were normalized to PKR-only transfected cells to obtain relative luciferase activities. Experiments were performed in triplicate and the results are representative of three independent experiments. Error bars indicate standard deviations. Abbreviations used: R=Rhesus; G=Guinea; S=Syrian; A=Armenian; T=Turkish, C=Chinese; b=brush; E=European; ct=cottontail.

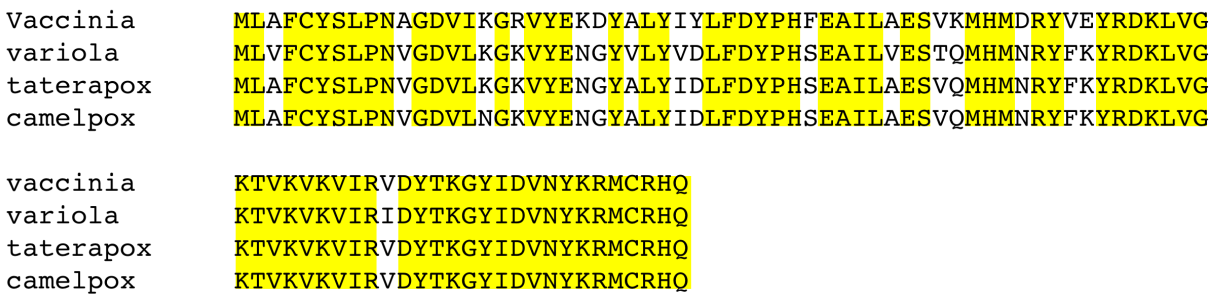

Figure 2.4 Comparison of poxvirus K3L orthologs

Sequences alignment was performed using the program MUSCLE (url: http://www.ebi.ac.uk/Tools/msa/muscle). Conserved residues (100% identical) are highlighted in yellow.

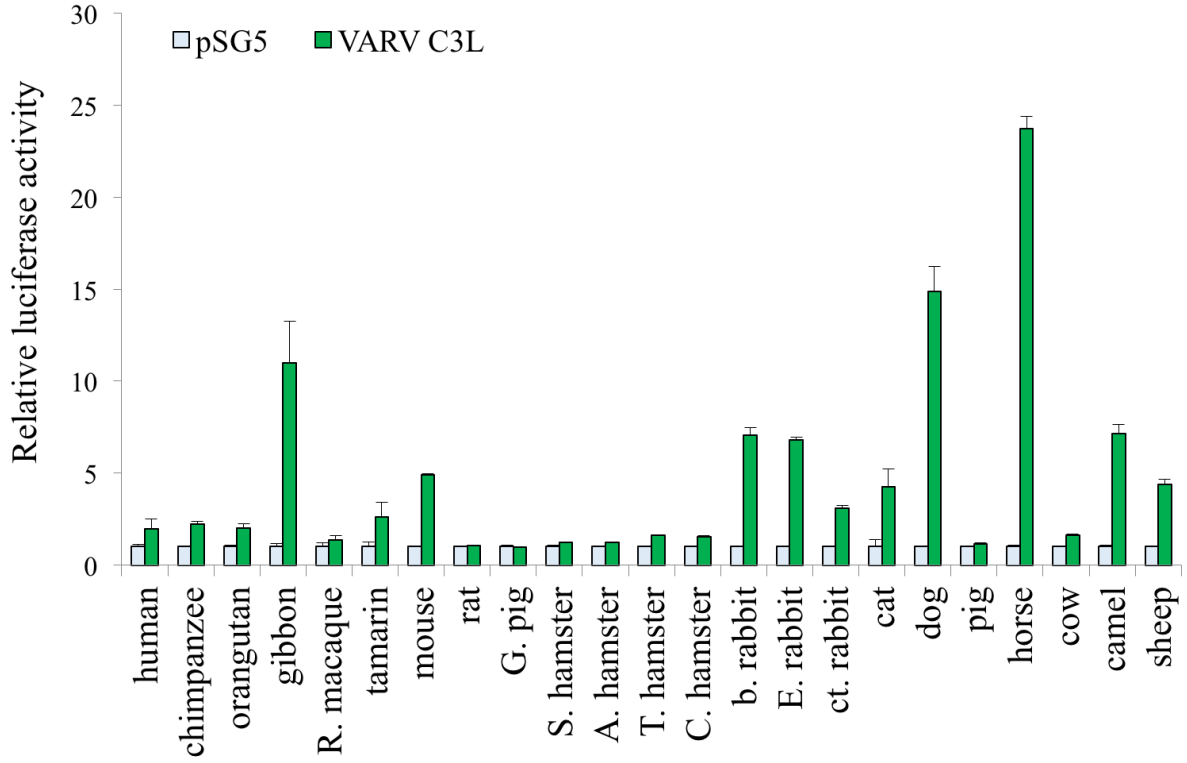

Figure 2.5 Inhibition of PKR by VARV C3L

Human HeLa-PKR^{kd} cells were transfected with expression vectors for firefly luciferase (0.05µg), PKR from the indicated species (0.2µg) and VARV C3L (0.4µg). Luciferase activity was measured 48 hours after transfection and the acquired light units were normalized to PKR-only transfected cells to obtain relative luciferase activities. Experiments were performed in triplicate and the results are representative of three independent experiments. Error bars indicate standard deviations. Abbreviations used: R=Rhesus; G=Guinea; S=Syrian; A=Armenian; T=Turkish, C=Chinese; b=brush; E=European; ct=cottontail.

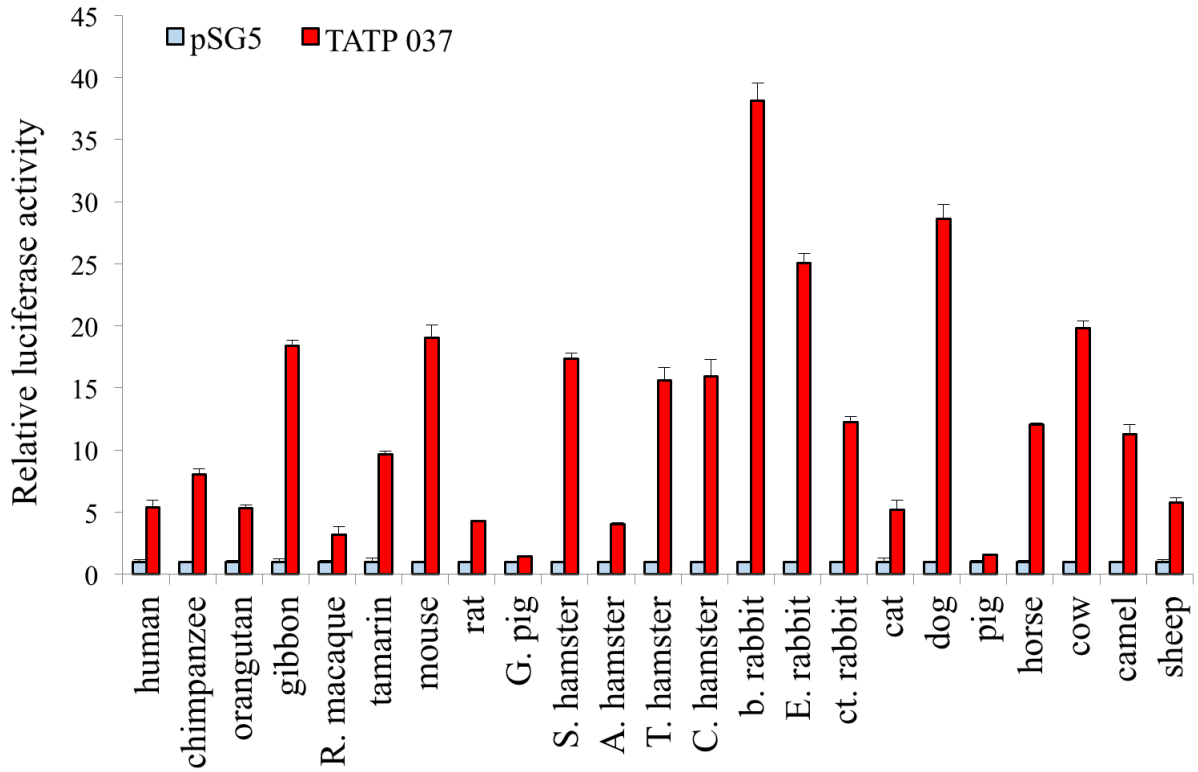

Figure 2.6 Inhibition of PKR by TATP 037

Human HeLa-PKR^{kd} cells were transfected with expression vectors for firefly luciferase (0.05µg), PKR from the indicated species (0.2µg) and TATP 037 (0.4µg). Luciferase activity was measured 48 hours after transfection and the acquired light units were normalized to PKR-only transfected cells to obtain relative luciferase activities. Experiments were performed in triplicate and the results are representative of three independent experiments. Error bars indicate standard deviations. Abbreviations used: R=Rhesus; G=Guinea; S=Syrian; A=Armenian; T=Turkish, C=Chinese; b=brush; E=European; ct=cottontail.

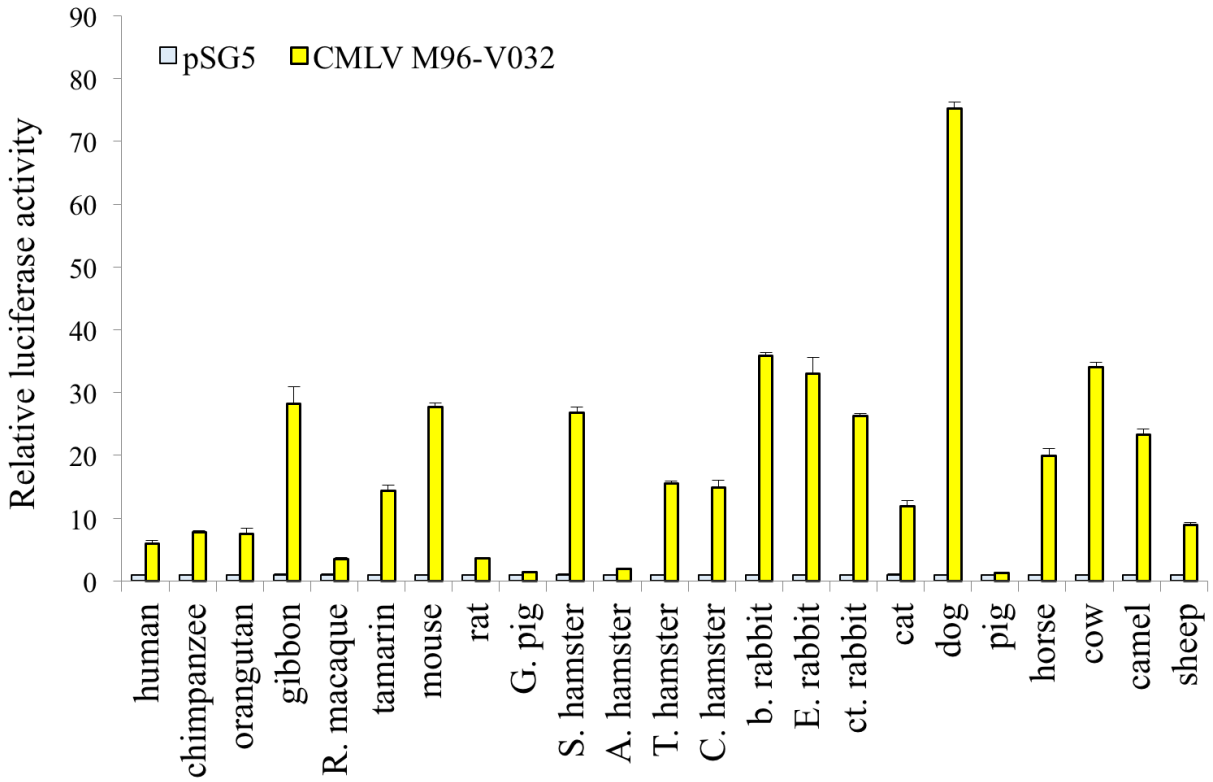

Figure 2.7 Inhibition of PKR by CMLV M96-V032

Human HeLa-PKR^{kd} cells were transfected with expression vectors for firefly luciferase (0.05µg), PKR from the indicated species (0.2µg) and CMLV V032 (0.4µg). Luciferase activity was measured 48 hours after transfection and the acquired light units were normalized to PKR-only transfected cells to obtain relative luciferase activities. Experiments were performed in triplicate and the results are representative of three independent experiments. Error bars indicate standard deviations. Abbreviations used: R=Rhesus; G=Guinea; S=Syrian; A=Armenian; T=Turkish, C=Chinese; b=brush; E=European; ct=cottontail.

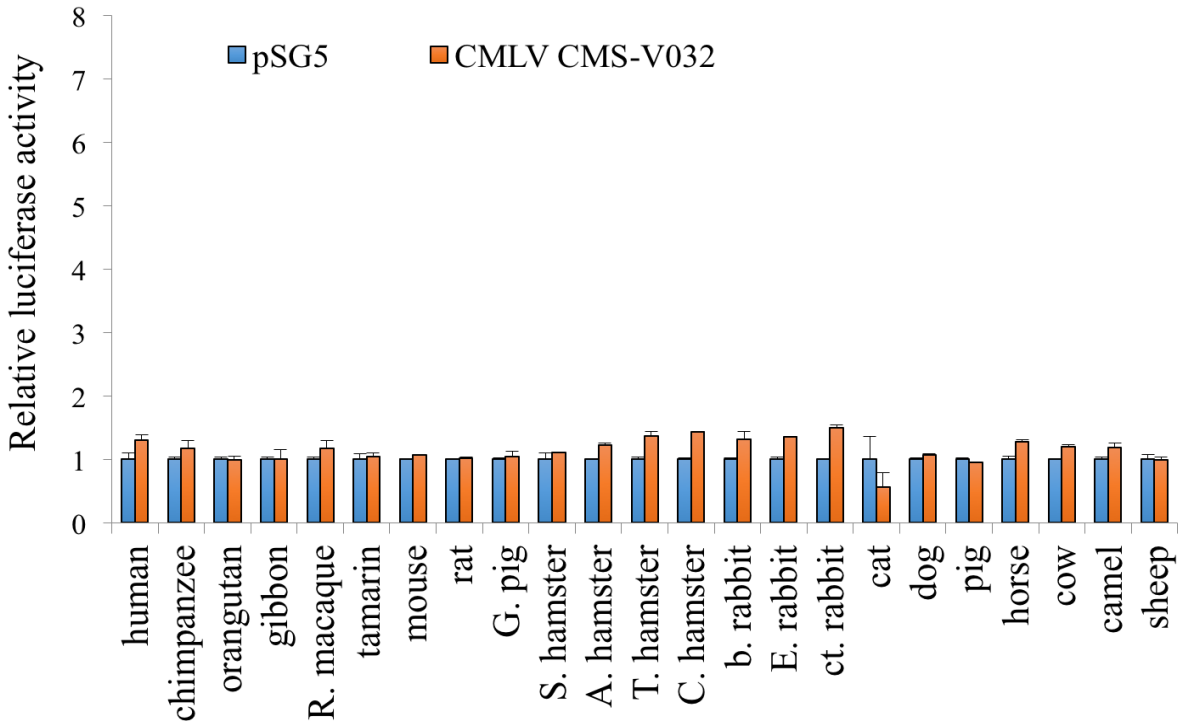

Figure 2.8 Inhibition of PKR by CMLV CMS-V032

Human HeLa-PKR^{kd} cells were transfected with expression vectors for firefly luciferase (0.05µg), PKR from the indicated species (0.2µg) and CMLV CMS-V032 (0.4µg). Luciferase activity was measured 48 hours after transfection and the acquired light units were normalized to PKR-only transfected cells to obtain relative luciferase activities. Experiments were performed in triplicate and the results are representative of three independent experiments. Error bars indicate standard deviations. Abbreviations used: R=Rhesus; G=Guinea; S=Syrian; A=Armenian; T=Turkish, C=Chinese; b=brush; E=European; ct=cottontail.

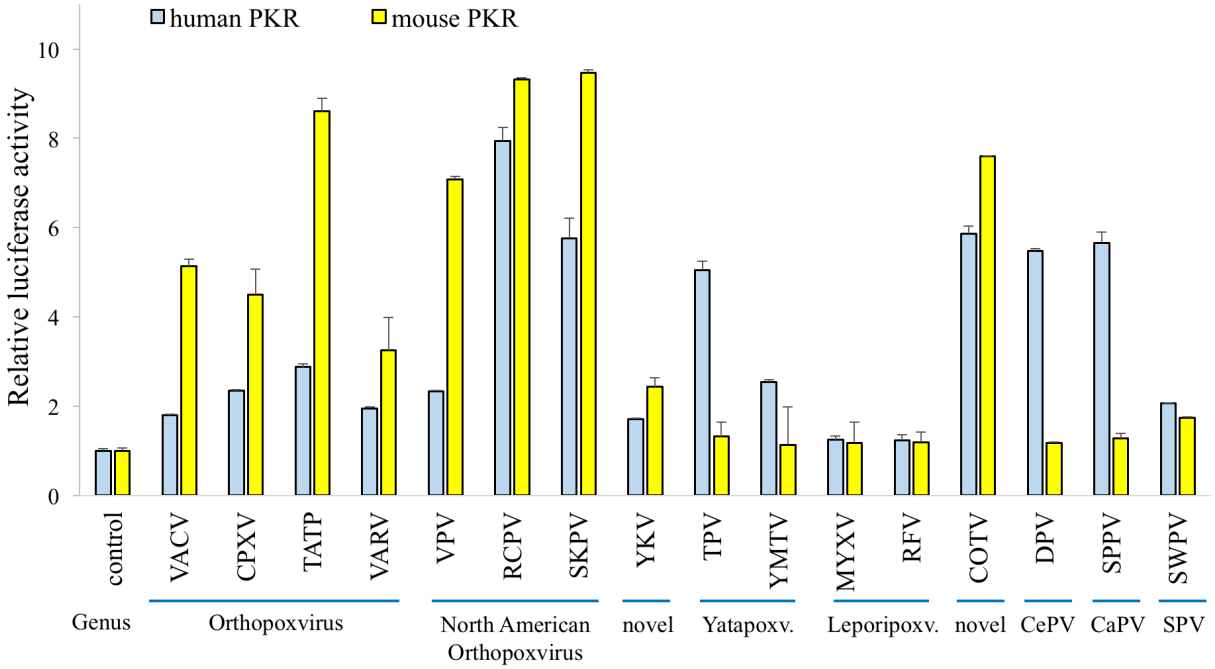

Figure 2.9 Inhibition of human and mouse PKR by poxvirus K3L orthologs

Human HeLa-PKR^{kd} cells were transfected with expression vectors for firefly luciferase (0.05µg), human or mouse PKR (0.2µg) K3L orthologs from the indicated poxviruses (0.8µg). Luciferase activity was measured 48 hours after transfection and the acquired light units were normalized to human PKR-only transfected cells to obtain relative luciferase activities. Experiments were performed in triplicate and the results are representative of three independent experiments. Error bars indicate standard deviations. Poxvirus species are shown above the lines, genera are indicated below the blue lines. Abbreviations: VACV=vaccinia virus; VARV=variola virus; CPXV=cowpox virus; TATP=taterapox virus; SPPV=sheeppox virus; DPV=deerpox virus; MYXV=myxoma virus; RFV=rabbit fibroma virus; SWPV=swinepox virus; TPV=tanapox virus; YMTV=yaba monkey tumor virus; YKV=yoka poxvirus; COTV=cotia virus; RCPV=racoonpox virus; SKPV=skunkpox virus; VPV=volepox virus; CePV=Cervidpoxvirus; CaPV=Capripoxvirus; SPV=Suipoxvirus.

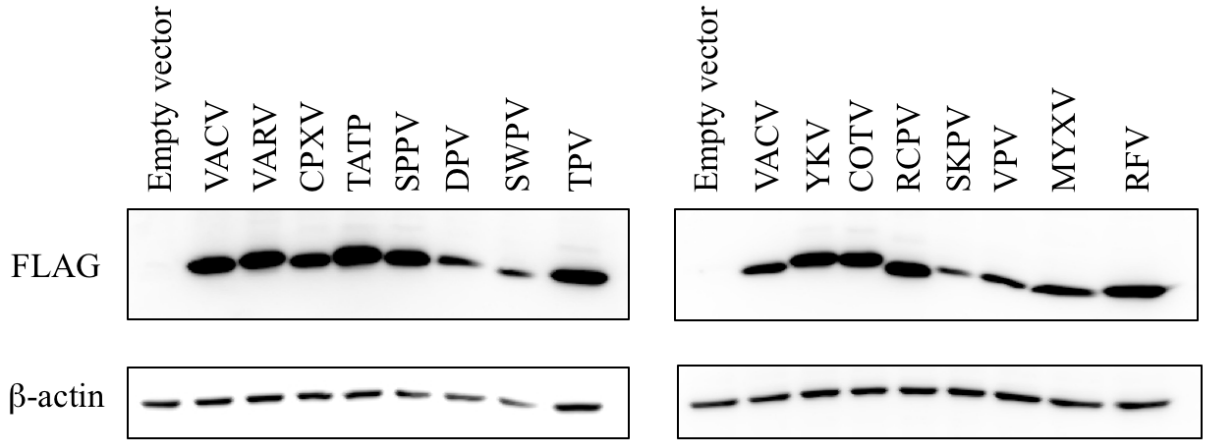

Figure 2.10 Expression of K3L orthologs

Monolayers of HeLa-PKR^{kd} cells in 6-well plates were transfected with FLAG-tagged poxvirus K3L orthologs (3μg/well). Protein lysates were collected 48 hours later and were subjected to Western blot analyses. PVDF membranes were probed with anti-FLAG antibodies followed by anti-β-actin antibodies. Abbreviations: VACV=vaccinia virus; VARV=variola virus; CPXV=cowpox virus; TATP=taterapox virus; SPPV=sheeppox virus; DPV=deerpox virus; MYXV=myxoma virus; RFV=rabbit fibroma virus; SWPV=swinepox virus; TPV=tanapox virus; YMTV=yaba monkey tumor virus; YKV=yoka poxvirus; COTV=cotia virus; RCPV=racoonpox virus; SKPV=skunkpox virus; VPV=volepox virus;

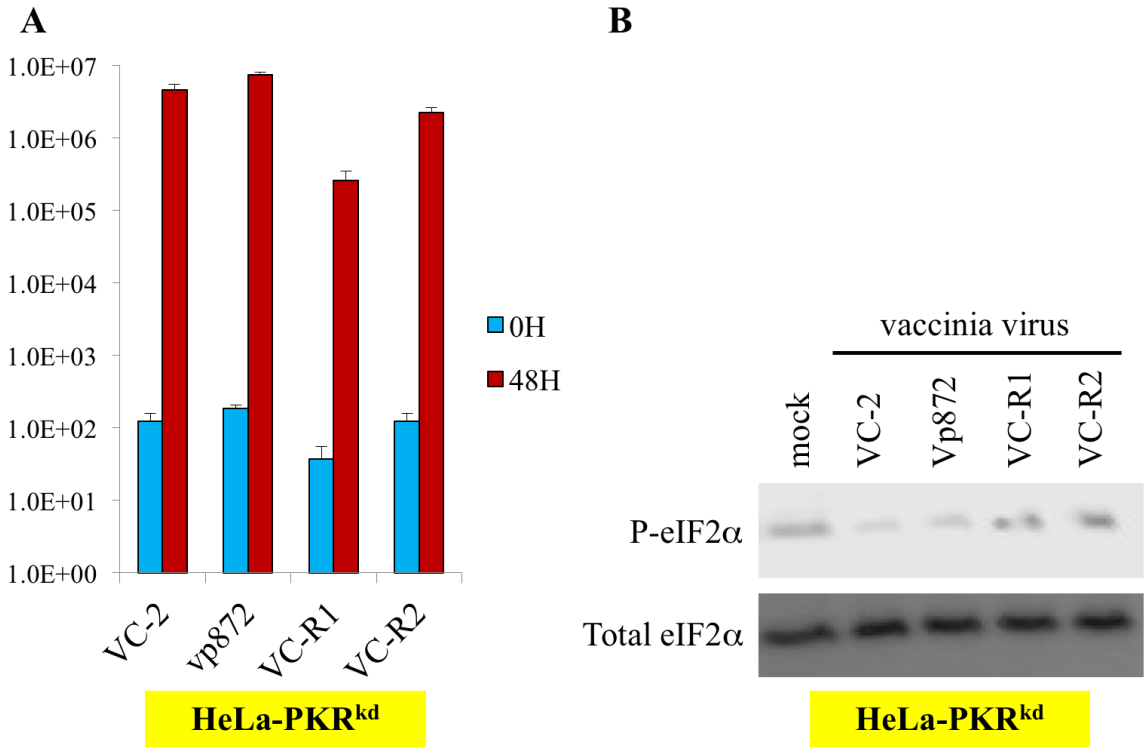

Figure 2.11 VACV infection in HeLa cells

(A) Confluent monolayers of HeLa-PKR^{kd} cells in 6-well plates were infected with VC-2 (Copenhagen wild type), VC-R1 (E3L-deficient), vp872 (K3L-deficient) and VC-R2 (K3L-deficient/E3L-deficient) at an MOI of 0.01. Viruses were collected 0 and 48 hours post infections and titered on RK13 cells that stably express VACV E3L and K3L. (B) Confluent monolayers of HeLa-PKR^{kd} cells in 6-well plates were infected with the indicated virus strains at an MOI of 5. Total protein lysates were collected 6 hours post infection and separated on SDS-PAGE gels followed by Western blot analyses. The blocked membranes were first incubated with anti-phospho-51 eIF2α antibody, then stripped and reprobed with antibody against total eIF2α.

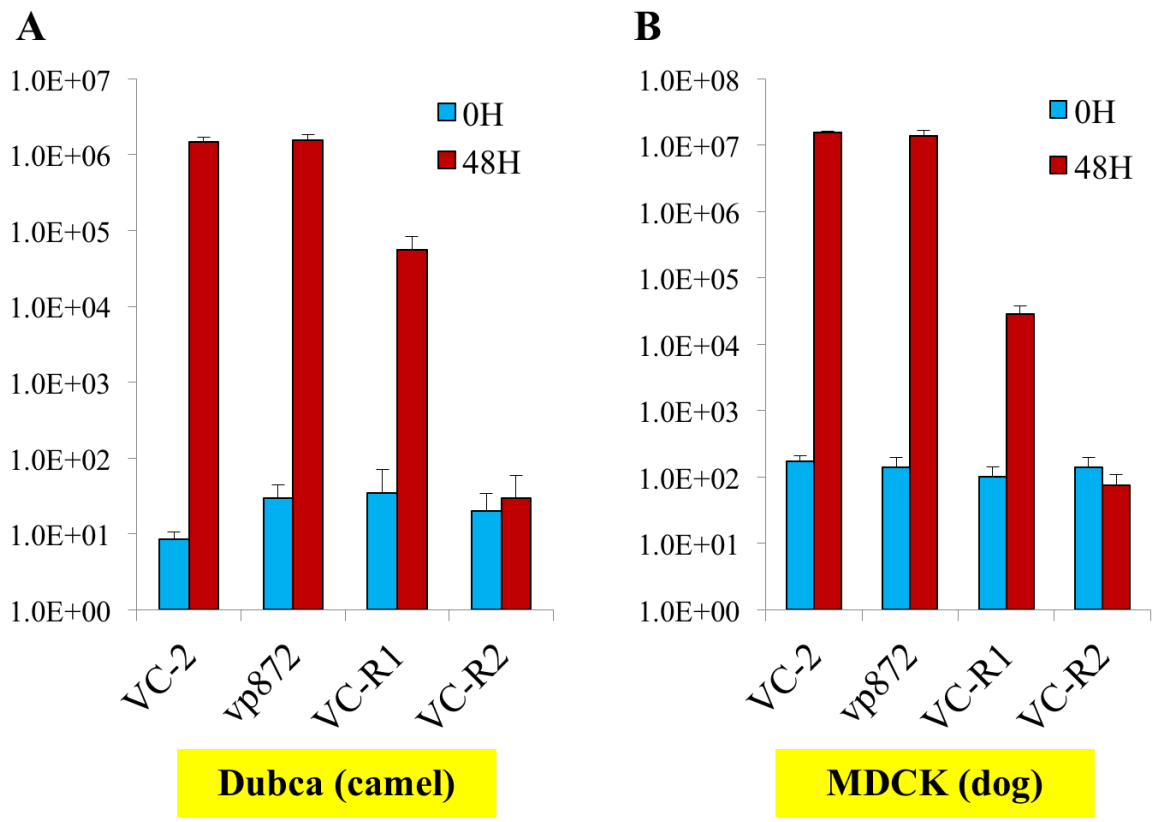

Figure 2.12 Replication of VACV in Dubca and MDCK cells

Confluent monolayers of camel Dubca cells (A) or canine MDCK cells (B) in 6-well plates were infected with VC-2 (Copenhagen wild type), VC-R1 (E3L-deficient), vp872 (K3L-deficient) and VC-R2 (K3L-deficient/E3L-deficient) at an MOI of 0.01. Viruses were collected 0 and 48 hours post infections and tittered on RK13 cells that stably express VACV E3L and K3L. Infections were performed in duplicate and error bars indicate standard deviation.

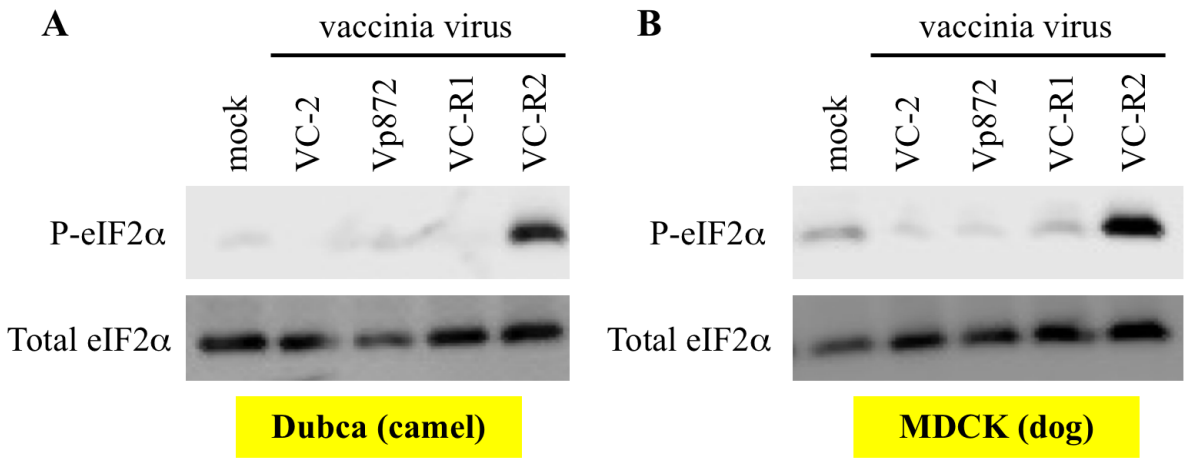

Figure 2.13 Phosphorylation of eIF2α in VACV-infected Dubca and MDCK cells

Confluent monolayers of camel Dubca cells (A) or canine MDCK cells (B) in 6-well plates were infected with VC-2 (Copenhagen wild type), VC-R1 (E3L-deficient), vp872 (K3L-deficient) and VC-R2 (K3L-deficient/E3L-deficient) at an MOI of 5. Total protein lysates were collected 6 hours post infection and separated on SDS-PAGE gels followed by Western blot analyses. The blocked membranes were first incubated with anti-phospho-51 eIF2α antibody, then stripped and re-probed with antibody against total eIF2α.

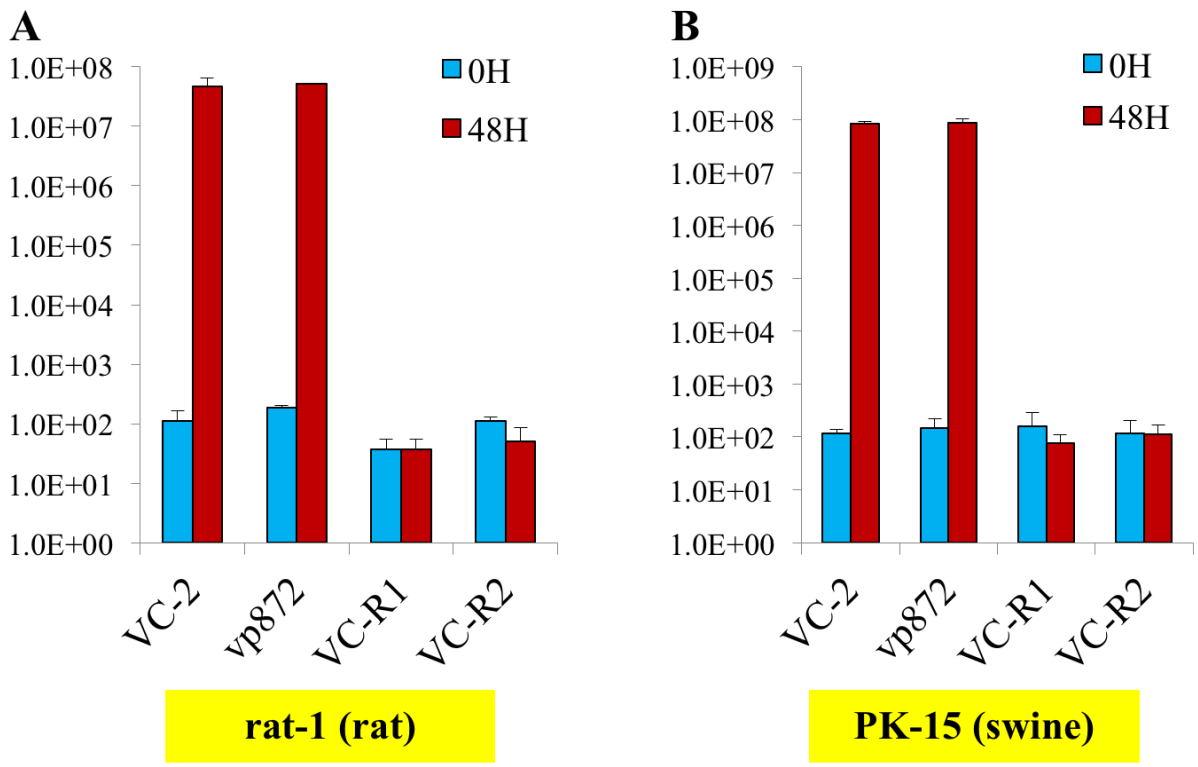

Figure 2.14 Replication of VACV in rat-1 and PK-15 cells

Confluent monolayers of brown rat rat-1 cells (A) and swine PK-15 cells (B) in 6-well plates were infected with VC-2 (Copenhagen wild type), VC-R1 (E3L-deficient), vp872 (K3L-deficient) and VC-R2 (K3L-deficient/E3L-deficient) at an MOI of 0.01. Viruses were collected 0 and 48 hours post infection and tittered on RK13 cells that stably express VACV E3L and K3L. Infections were performed in duplicate and error bars indicate standard deviation.

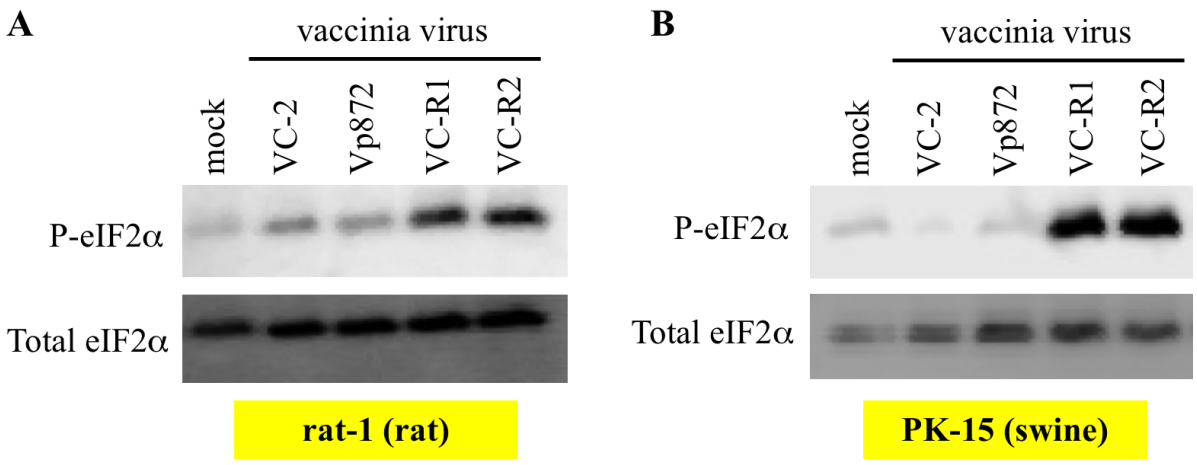

Figure 2.15 Phosphorylation of eIF2α in VACV-infected rat-1 and PK-15 cells

Confluent monolayers of brown rat rat-1 cells (A) and swine PK-15 cells (B) in 6-well plates were infected with VC-2 (Copenhagen wild type), VC-R1 (E3L-deficient), vp872 (K3L-deficient) and VC-R2 (K3L-deficient/E3L-deficient) at an MOI of 5. Total protein lysates were collected 6 hours post infection and separated on SDS-PAGE gels followed by Western blot analyses. The blocked membranes were first incubated with anti-phospho-51 eIF2α antibody, then stripped and re-probed with antibody against total eIF2α.

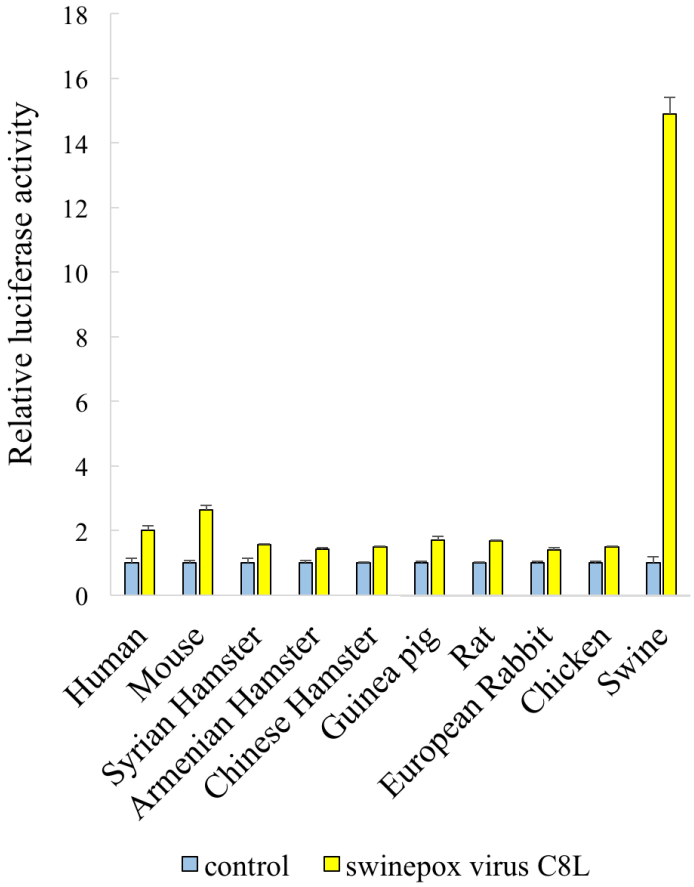

Figure 2.16 Host species-specific inhibition of swine PKR by swinepox virus C8L

Human HeLa-PKR^{kd} cells were transfected with expression vectors for firefly luciferase (0.05μg), PKR from the indicated species (0.2μg) and the swinepox virus C8L (0.4μg). Luciferase activity was measured 48 hours after transfection and the acquired light units were normalized to PKR-only transfected cells to obtain relative luciferase activities. Experiments were performed in triplicate and the results are representative of three independent experiments. Error bars indicate standard deviations.

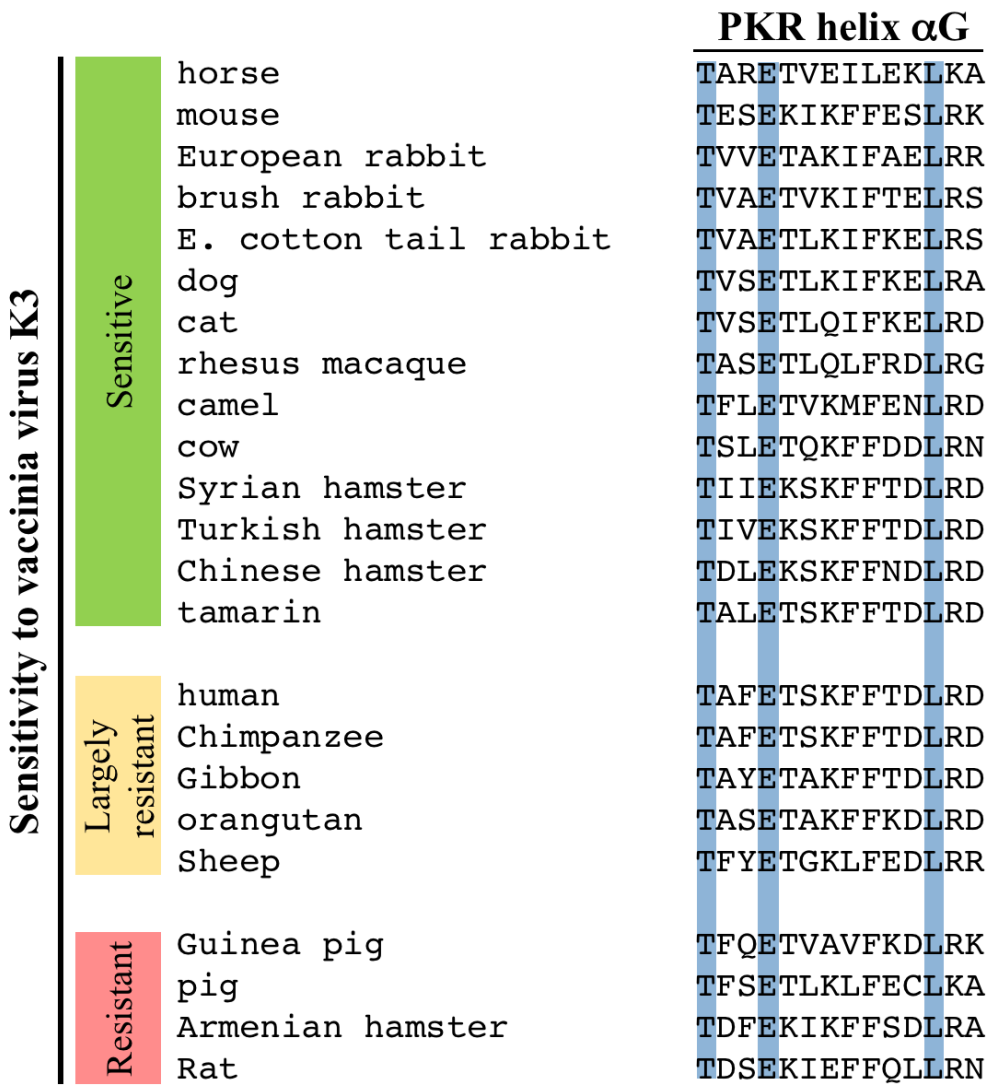

Figure 2.17 Sequences alignment of the helix αG region on PKR

PKR from the indicated species were classified into three groups: Sensitive, largely resistant and resistant according to their sensitivities to VACV K3L as determined in the luciferase assay. The protein sequences of the helix αG regions from each PKR were aligned and conserved amino acids (100% conservation) are highlighted in blue.

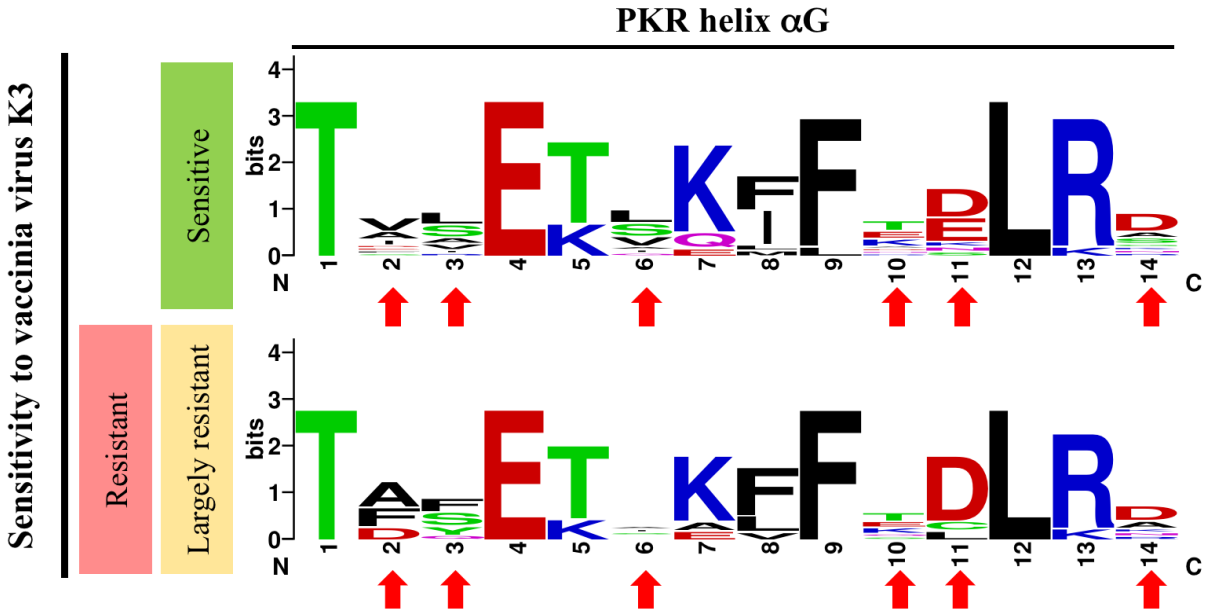

Figure 2.18 The helix αG region of PKR is highly divergent

Sequences were generated using the tool WebLogo (Version 2.8.2 2005-09-08, url: http://weblogo.berkeley.edu) (22-23) based on the multiple sequence alignment shown in Fig 4.10. Red arrows indicate highly divergent residues.

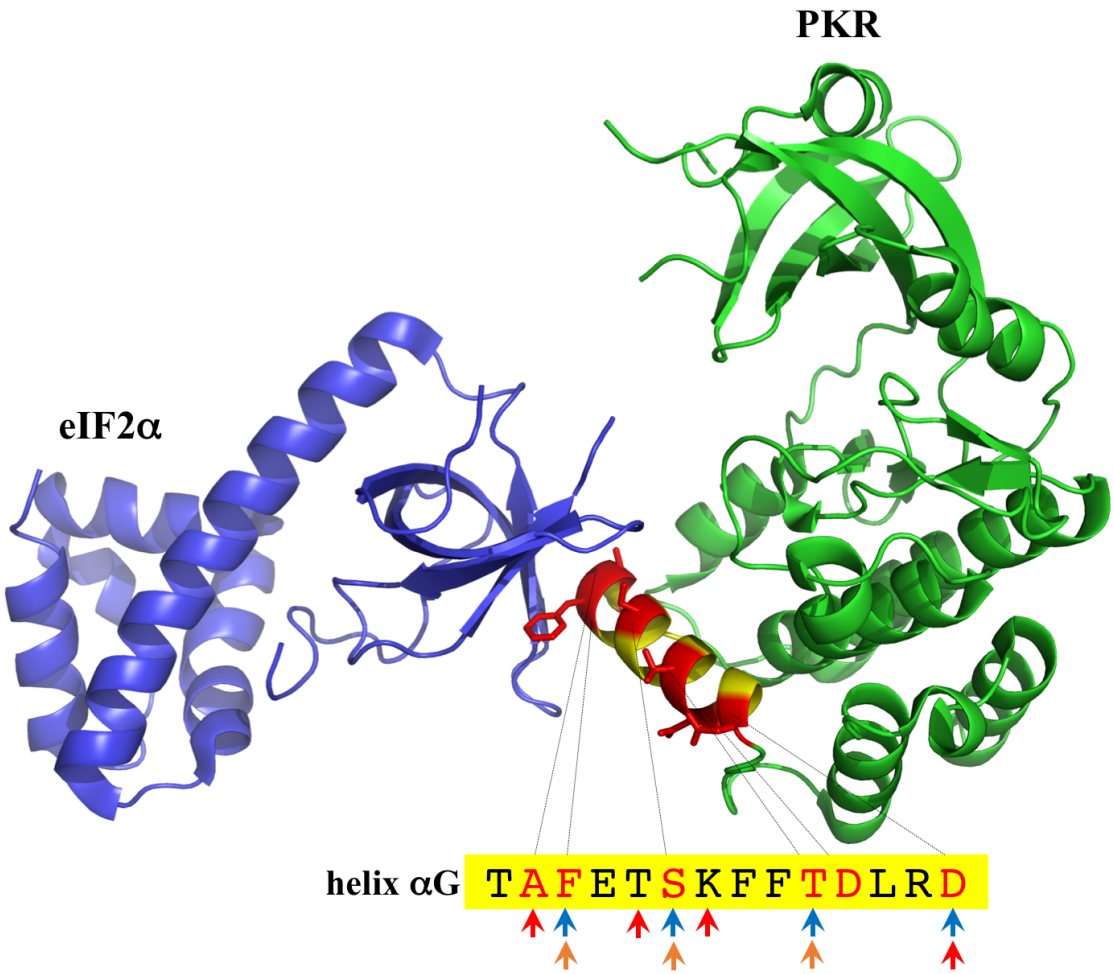

Figure 2.19 Structure of the PKR-eIF2α complex

Structure of the PKR-eIF2α complex was adapted from RCSB PDB 2A1A (17). The residues comprising the helix αG were colored in yellow on the PKR structure. Residues that are highly divergent are colored in red. Arrows indicate residues under positive selection. Color-coded arrows indicate residues identified as being under positive selection. Different colors of arrows indicate different sources of positive selection analyses: blue: personal communication with Sherry Haller; red: Rothenburg et al (16); Orange: Elde et al. (17).

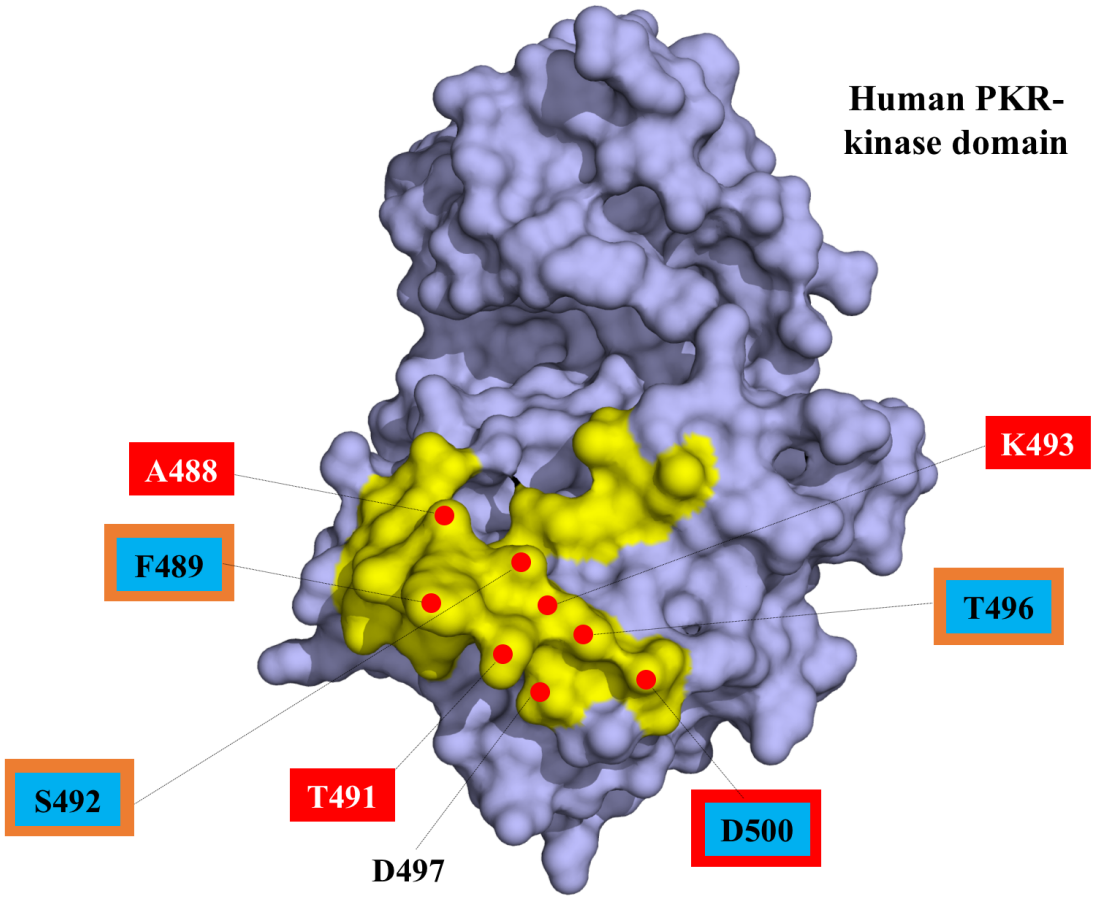

Figure 2.20 Structure of the kinase domain of PKR

The structure of the kinase domain of PKR was adapted from PDB 2A1A (17). The residues directly interacting with eIF2α are colored in yellow and residues that are highly divergent are indicated by red circles. Residues in boxes are those being under positive selective pressure. Boxes are color coded based on the source of the positive selection analyses: Blue: personal communication with Sherry Haller. Red: Rothenburg et al. (16). Orange: Elde et al. (17).

% Identity	1	2	3	4	5	6	7	8	9	10	11	12	13	14	15	16	17	18	19	20	21	22	23
1. human	\	98.7	92.2	91.5	80.9	85.3	60.5	60.8	55.7	62.0	60.8	60.9	61.2	68.1	68.0	68.0	65.5	64.4	63.5	64.0	64.3	66.6	62.3
2. chimpanzee	\	\	92.6	92.2	80.9	85.7	60.0	60.3	56.1	61.5	60.3	60.4	60.7	68.3	68.0	68.0	65.3	64.4	63.5	64.2	64.1	66.6	62.3
3. orangutan	\	\	\	91.8	81.6	84.0	60.5	60.0	55.3	62.0	60.8	60.9	61.2	67.5	67.2	67.2	65.3	63.9	62.7	63.5	63.6	65.7	61.5
4. gibbon	\	\	\	\	81.2	83.8	60.5	60.0	55.5	61.3	60.8	60.1	60.4	68.1	68.1	67.6	64.9	63.9	62.9	64.2	63.9	67.0	62.5
5. r. macaque	\	\	\	\	\	78.5	58.2	58.1	53.3	58.7	57.6	58.3	58.3	63.3	62.8	63.0	62.8	61.1	60.6	60.8	60.1	62.2	58.8
6. tamarin	\	\	\	\	\	\	60.7	60.4	56.1	62.2	61.3	61.5	61.7	67.7	67.4	68.0	64.4	65.2	62.5	65.3	64.1	65.8	61.9
7. mouse	\	\	\	\	\	\	\	77.4	52.0	70.5	71.0	69.5	71.6	59.1	58.2	59.5	54.7	55.9	57.7	55.9	56.2	58.3	55.3
8. rat	\	\	\	\	\	\	\	\	55.9	69.0	71.4	68.0	71.2	57.8	57.3	58.5	56.0	56.7	57.7	57.3	56.2	57.9	54.1
9. G. pig	\	\	\	\	\	\	\	\	\	51.0	52.2	50.6	51.8	56.8	56.8	56.6	52.5	52.7	54.9	52.2	54.5	55.4	52.4
10. S. hamster	\	\	\	\	\	\	\	\	\	\	82.1	97.3	83.0	58.3	58.2	58.2	56.0	55.9	56.6	55.3	55.3	56.3	54.3
11. A. hamster	\	\	\	\	\	\	\	\	\	\	\	80.6	89.9	56.7	56.8	57.0	54.6	55.8	56.2	57.1	54.5	56.2	53.7
12. T. hamster	\	\	\	\	\	\	\	\	\	\	\	\	81.7	57.6	57.9	57.5	55.1	55.0	55.7	54.4	54.3	55.5	53.2
13. C. hamster	\	\	\	\	\	\	\	\	\	\	\	\	\	56.3	56.8	56.4	54.4	55.4	55.4	56.6	54.1	56.4	53.2
14. brush rabbit	\	\	\	\	\	\	\	\	\	\	\	\	\	\	93.2	95.8	63.9	65.1	64.0	63.7	63.5	65.4	61.1
15. E. rabbit	\	\	\	\	\	\	\	\	\	\	\	\	\	\	\	92.9	64.3	65.2	63.7	63.6	63.6	64.5	60.4
16. ct. rabbit	\	\	\	\	\	\	\	\	\	\	\	\	\	\	\	\	64.5	65.9	63.5	63.8	62.6	65.7	60.4
17. cat	\	\	\	\	\	\	\	\	\	\	\	\	\	\	\	\	\	76.7	64.4	63.3	63.9	68.2	62.0
18. dog	\	\	\	\	\	\	\	\	\	\	\	\	\	\	\	\	\	\	64.4	65.5	60.9	65.4	60.2
19. pig	\	\	\	\	\	\	\	\	\	\	\	\	\	\	\	\	\	\	\	63.8	73.6	74.9	71.4
20. horse	\	\	\	\	\	\	\	\	\	\	\	\	\	\	\	\	\	\	\	\	59.9	64.5	59.4
21. cow	\	\	\	\	\	\	\	\	\	\	\	\	\	\	\	\	\	\	\	\	\	75.9	88.2
22. camel	\	\	\	\	\	\	\	\	\	\	\	\	\	\	\	\	\	\	\	\	\	\	74.6
23. sheep	\	\	\	\	\	\	\	\	\	\	\	\	\	\	\	\	\	\	\	\	\	\	\

Table 2.1 PKR sequence identity

Species	VACV K3L	VARV C3L	TATP 037	CMLV M96 V032	CMLV CMS V032
1. human	**1.4**±0.07	**2.0**±0.55	**5.4**±0.58	**6.0**±0.55	**1.3**±0.09
2. chimpanzee	**1.6**±0.03	**2.2**±0.16	**8.0**±0.43	**7.8**±0.17	**1.2**±0.13
3. orangutan	**2.4**±0.08	**2.0**±0.22	**5.3**±0.25	**7.6**±0.83	**1.0**±0.05
4. gibbon	**2.3**±0.19	**11.0**±2.25	**18.3**±0.46 *	**28.3**±2.72 *	**1.0**±0.14
5. r. macaque	**3.2**±0.06	**1.4**±0.22	**3.2**±0.62	**3.5**±0.21	**1.2**±0.12
6. tamarin	**4.6**±0.42	**2.6**±0.81	**9.6**±0.24	**14.4**±0.89	**1.0**±0.06
7. mouse	**5.7**±0.06	**4.9**±0.08	**19.1**±0.99	**27.7**±0.72	**1.1**±0.01
8. rat	**1.0**±0.01	**1.0**±0.02	**4.2**±0.09	**3.6**±0.03	**1.0**±0.02
9. G. pig	**1.3**±0.01	**1.0**±0.03	**1.4**±0.05	**1.4**±0.04	**1.0**±0.08
10. S. hamster	**3.3**±0.06	**1.2**±0.05	**17.3**±0.46	**26.8**±0.93	**1.1**±0.01
11. A. hamster	**1.0**±0.00	**1.2**±0.03	**4.0**±0.16	**2.0**±0.04	**1.2**±0.02
12. T. hamster	**6.9**±0.17	**1.6**±0.03	**15.6**±0.98	**15.5**±0.38	**1.4**±0.07
13. C. hamster	**9.5**±0.31	**1.6**±0.04	**16.0**±1.34	**14.9**±1.16	**1.4**±0.01
14. brush rabbit	**21.7**±1.14 *	**7.1**±0.38	**38.2**±1.41 *	**35.9**±0.50	**1.3**±0.12
15. E. rabbit	**14.2**±0.65	**6.8**±0.15	**25.0**±0.81	**33.0**±2.62	**1.4**±0.01
16. ct. rabbit	**7.5**±0.26	**3.1**±0.13	**12.3**±0.46	**26.2**±0.41	**1.5**±0.05
17. cat	**4.0**±0.57	**4.3**±0.97	**5.2**±0.74	**11.9**±0.93	**0.6**±0.22
18. dog	**8.6**±0.79	**14.9**±1.38	**28.6**±1.13 *	**75.2**±1.06 *	**1.1**±0.03
19. pig	**1.1**±0.03	**1.1**±0.09	**1.6**±0.06	**1.3**±0.01	**0.9**±0.01
20. horse	**6.4**±0.36	**23.7**±0.67 *	**12.1**±0.10	**19.9**±1.11	**1.3**±0.03
21. cow	**7.2**±0.49	**1.6**±0.07	**19.8**±0.57	**34.1**±0.78	**1.2**±0.03
22. camel	**5.6**±0.33	**7.1**±0.48	**11.3**±0.79	**23.2**±0.95	**1.2**±0.08
23. sheep	**1.6**±0.06	**4.4**±0.25	**5.8**±0.37	**8.9**±0.51	**1.0**±0.05

Table 2.2 Inhibition of PKR by K3L orthologs represented by fold increases of luciferase activities

Fold increases caused by co-transfection of VACV K3L, VARV C3L, TATP037, CMLV M96-V032 or CMLV CMS-V032 and PKR from the indicated species were summarized in the table. Red asterisk indicate complete inhibition.

% Identity	1	2	3	4	5	6	7	8	9	10	11	12	13	14	15	16	17
1. Vaccinia virus	\	97.7	80.7	87.5	59.8	59.8	65.9	29.1	36.6	35.4	32.0	28.2	62.2	41.7	38.1	43.2	86.4
2. Cowpox virus	\	\	83.0	89.8	58.5	59.8	64.6	29.1	35.4	35.4	30.7	28.2	62.2	40.5	38.1	43.2	88.6
3. Variola virus	\	\	\	93.2	61.0	63.4	65.9	35.4	39.0	40.2	29.3	26.9	58.5	41.7	34.5	38.3	92.0
4. Taterapox virus	\	\	\	\	62.2	64.6	67.1	32.9	37.8	39.0	28.0	25.6	64.6	41.7	35.7	40.7	98.9
5. Volepox virus	\	\	\	\	\	75.6	81.7	32.1	39.0	37.8	25.7	24.0	54.9	40.2	34.1	37.0	61.0
6. Raccoonpox virus	\	\	\	\	\	\	73.2	33.3	35.4	37.8	25.7	25.3	61.0	37.8	31.7	37.0	61.0
7. Skunkpox virus	\	\	\	\	\	\	\	32.1	36.6	35.4	27.0	24.0	59.8	40.2	32.9	42.0	65.9
8. Yoka poxvirus	\	\	\	\	\	\	\	\	28.2	29.5	26.0	24.0	37.2	31.6	21.5	26.0	32.9
9. Tanapox virus	\	\	\	\	\	\	\	\	\	75.0	35.1	30.7	34.1	51.7	43.7	44.2	36.6
10. Yaba monkey tumor virus	\	\	\	\	\	\	\	\	\	\	29.7	29.3	36.6	47.1	36.8	39.5	37.8
11. Myxoma virus	\	\	\	\	\	\	\	\	\	\	\	76.0	21.6	35.1	31.1	35.6	28.0
12. Rabbit fibroma virus	\	\	\	\	\	\	\	\	\	\	\	\	22.7	27.3	29.9	33.8	25.6
13. Cotia virus	\	\	\	\	\	\	\	\	\	\	\	\	\	36.6	31.7	40.7	64.6
14. Deerpox virus	\	\	\	\	\	\	\	\	\	\	\	\	\	\	51.7	45.3	40.5
15. Sheeppox virus	\	\	\	\	\	\	\	\	\	\	\	\	\	\	\	50.0	35.7
16. Swinepox virus	\	\	\	\	\	\	\	\	\	\	\	\	\	\	\	\	40.7
17. Camelpox virus	\	\	\	\	\	\	\	\	\	\	\	\	\	\	\	\	\

Table 2.3 Sequence identities between K3L orthologs

References

1. Moss B (2011) Smallpox vaccines: targets of protective immunity. *Immunology Review* 239(1):8–26.

2. Hruby DE (1990) Vaccinia virus vectors: new strategies for producing recombinant vaccines. *Clinical Microbiology Review* 3(2):153–170.

3. Moss B (1991) Vaccinia virus: a tool for research and vaccine development. *Science* 252(5013):1662–1667.

4. McFadden G (2005) Poxvirus tropism. *Nature Reviews of Microbiology* 3(3):201–213.

5. Frey SE, Belshe RB (2004) Poxvirus zoonoses--putting pocks into context. *New England Journal of Medicine* 350(4):324–327.

6. Langland JO, Jacobs BL (2002) The role of the PKR-inhibitory genes, E3L and K3L, in determining vaccinia virus host range. *Virology* 299(1):133–141.

7. Haller SL, Peng C, McFadden G, Rothenburg S (2014) Poxviruses and the evolution of host range and virulence. *Infection, Genetics and Evolution* 21:15–40.

8. Chang HW, Uribe LH, Jacobs BL (1995) Rescue of vaccinia virus lacking the E3L gene by mutants of E3L. *Journal of Virology* 69(10):6605–6608.

9. Brandt TA, Jacobs BL (2001) Both carboxy- and amino-terminal domains of the vaccinia virus interferon resistance gene, E3L, are required for pathogenesis in a mouse model. *Journal of Virology* 75(2):850–856.

10. Dueck KJ, et al. (2015) Mutational analysis of vaccinia virus E3 protein: the biological functions do not correlate with its biochemical capacity to bind double-stranded RNA. *Journal of Virology* 89(10):5382–5394.

11. Qian W, Zhu S, Sobolev AY, Wek RC (1996) Expression of vaccinia virus K3L protein in yeast inhibits eukaryotic initiation factor-2 kinase GCN2 and the general amino acid control pathway. *Journal of Biological Chemistry* 271(22):13202–13207.

12. Carroll K, Elroy-Stein O, Moss B, Jagus R (1993) Recombinant vaccinia virus K3L gene product prevents activation of double-stranded RNA-dependent, initiation factor 2 alpha-specific protein kinase. *Journal of Biological Chemistry* 268(17):12837–12842.

13. Kawagishi-Kobayashi M, Silverman JB, Ung TL, Dever TE (1997) Regulation of the protein kinase PKR by the vaccinia virus pseudosubstrate inhibitor K3L is dependent on residues conserved between the K3L protein and the PKR substrate eIF2alpha. *Molecular Cell Biology* 17(7):4146–4158.

14. Dar AC, Sicheri F (2002) X-ray crystal structure and functional analysis of vaccinia virus K3L reveals molecular determinants for PKR subversion and substrate recognition. *Molecular Cell* 10(2):295–305.

15. Elde NC, et al. (2012) Poxviruses deploy genomic accordions to adapt rapidly against host antiviral defenses. *Cell* 150(4):831–841.

16. Rothenburg S, Seo EJ, Gibbs JS, Dever TE, Dittmar K (2009) Rapid evolution of protein kinase PKR alters sensitivity to viral inhibitors. *Nature Structural and Molecular Biology* 16(1):63–70.

17. Elde NC, Child SJ, Geballe AP, Malik HS (2009) Protein kinase R reveals an evolutionary model for defeating viral mimicry. *Nature* 457(7228):485–489.

18. Hand ES, Haller SL, Peng C, Rothenburg S, Hersperger AR (2015) Ectopic expression of vaccinia virus E3 and K3 cannot rescue ectromelia virus replication in rabbit RK13 cells. *PLoS ONE* 10(3):e0119189.

19. Zhang P, Samuel CE (2007) Protein Kinase PKR Plays a Stimulus- and Virus-Dependent Role in Apoptotic Death and Virus Multiplication in Human Cells. *Journal of Virology*.

20. Rahman MM, Liu J, Chan WM, Rothenburg S, McFadden G (2013) Myxoma virus protein M029 is a dual function immunomodulator that inhibits PKR and also conscripts RHA/DHX9 to promote expanded host tropism and viral replication. *PLoS Pathogens* 9(7):e1003465.

21. Earl PL, Cooper N, Wyatt LS, Moss B, Carroll MW (2001) *Preparation of Cell Cultures and Vaccinia Virus Stocks* (John Wiley & Sons, Inc., Hoboken, NJ, USA).

22. Crooks GE, Hon G, Chandonia J-M, Brenner SE (2004) WebLogo: a sequence logo generator. *Genome Research* 14(6):1188–1190.

23. Schneider TD, Stephens RM (1990) Sequence logos: a new way to display consensus sequences. *Nucleic Acids Research* 18(20):6097–6100.

24. Afonso CL, et al. (2002) The genome of swinepox virus. *Journal of Virology* 76(2):783–790.

25. Fan H-J, Lin H-X (2016) Recombinant Swinepox Virus for Veterinary Vaccine Development. *Methods in Molecular Biology* 1349 (Chapter 11):163–175.

26. Kawagishi-Kobayashi M, Cao C, Lu J, Ozato K, Dever TE (2000) Pseudosubstrate inhibition of protein kinase PKR by swine pox virus C8L gene product. *Virology* 276(2):424–434.

Contributions

Selection analyses for the identification of positive selective residues in rodent PKR were performed by Dr. Loubna Tazi and Sherry Haller.

Chapter 3 - Myxoma virus M156 is a specific inhibitor of rabbit PKR but contains a loss-of-function mutation in Australian virus isolates

Chen Peng[1], Sherry Haller[1], Masmudur M. Rahman[2], Grant McFadden[2] and Stefan Rothenburg[1]

1. *Division of Biology, Kansas State University, Manhattan, KS*
2. *Department of Molecular Genetics & Microbiology, University of Florida, Gainesville, FL*

Published in the *Proceedings of National Academy of Sciences USA*

2016, Vol. 113, no. 14, 3855-3860

DOI: 10.1073/pnas.1515613113

Abstract

Myxoma virus (MYXV) is a rabbit-specific poxvirus, which is highly virulent in European rabbits. The attenuation of MYXV and the increased resistance of rabbits following the release of MYXV in Australia is one of the best-documented examples of host-pathogen co-evolution. To elucidate the molecular mechanisms that contribute to the restriction of MYXV infection to rabbits and MYXV attenuation in the field, we have studied the interaction of the MYXV protein M156 with the host antiviral protein kinase R (PKR). In yeast and cell-culture transfection assays M156 only inhibited rabbit PKR but not PKR from other tested mammalian species. Infection assays with human HeLa PKR knock-down cells, which were stably transfected with human or rabbit PKR, revealed that only human but not rabbit PKR was able to restrict MYXV infection, whereas both PKRs were able to restrict replication of a vaccinia virus (VACV) strain that lacks the PKR inhibitors E3L and K3L. Inactivation of M156R led to MYXV virus attenuation in rabbit cells, which was rescued by the ectopic expression of VACV E3 and K3. We further show that a mutation in the M156 encoding gene that was identified in more than 50% of MYXV field isolates from Australia resulted in an M156 variant that lost its ability to inhibit rabbit PKR and led to virus attenuation. The species-specific inhibition of rabbit PKR by M156 and the M156 loss-of-function in Australian MYXV field isolates might thus contribute to the species-specificity of MYXV and to the attenuation in the field, respectively.

Significance

The virulence and host range of viruses is controlled by the interaction of the host innate immune system with viral molecules. This interaction is an important driver for the evolution of both the host and the virus. The attenuation of myxoma virus, a rabbit specific poxvirus, after its deliberate release to control European rabbit populations, and the increased resistance of the rabbits, is one of the best-known examples for host-virus co-evolution on the population level. We show that the myxoma virus protein M156 specifically inhibited the antiviral protein kinase R (PKR) from rabbits but not PKR from other mammals, that PKR inhibition correlated with virus replication during infection and that M156 contains a loss-of-function mutation in Australian field isolates.

Introduction

Poxviruses are large double-stranded DNA viruses that exclusively replicate in the cytoplasm of infected cells. Members of the *Poxviridae* family can productively infect a wide variety of animal hosts. Interestingly, the binding and entry of poxviruses into cells is largely independent of host species after which virus replication is initiated. The successful completion of virus replication, however, depends on the effective subversion of the host cell's innate immune responses (1). Even closely related poxviruses can exhibit drastic differences in their host ranges. Whereas some poxviruses have only one host-species, such as variola virus, the causative agent of smallpox, which is restricted to humans, others, such as cowpox and monkeypox viruses, can infect many different species and thus display very broad host ranges (2). A number of poxvirus genes have been discovered that influence the host range and cell tropism of poxviruses and have therefore been termed "host range genes" (3, 4). Although the molecular mechanisms responsible for their host range functions have not been elucidated in detail, it is clear that most poxviral host range proteins interact with components of the host immune system and that host species-specific interactions likely play a major role.

Myxoma virus (MYXV) is a poxvirus that belongs to the genus leporipoxvirus and shows a restricted host range infecting only leporids (rabbits and hares). MYXV is highly lethal to European (E.) rabbits causing case fatality rates (CFRs) of close to 100%. Since 1950, MYXV was repeatedly introduced into Australia to combat the invasive feral E. rabbit population, which has caused ecological and economical havoc. Shortly after the release of the MYXV standard laboratory strain (SLS), which caused a CFR of 99.8% in laboratory rabbits (grade 1 virulence), attenuated virus strains began to appear in the wild and started to outcompete the more virulent parental strain. The predominant strains found in the field are of grade 3 and grade 4 virulence

and exhibit a CFR in laboratory rabbits between 70-95% and 50-70%, respectively. Concomitantly, rabbits evolved increased resistance to MYXV infection. Evolution of attenuated MYXV and increased resistance of rabbits to infection were also observed after the illegal release of MYXV in Europe (reviewed in (5)). The molecular mechanisms of the attenuation of MYXV and the increased resistance of rabbits to infection are unknown. Recently, the complete genomes of 24 MYXV strains that were collected in the field in Australia were reported. Although a number of mutations were discovered, it was not immediately clear which mutations led to changes in MYXV virulence (6, 7). Two candidate genes that might contribute to changes in virulence are *M029L* and *M156R*, the MYXV orthologs of vaccinia virus (VACV) *E3L* and *K3L*, respectively. VACV *E3L* and *K3L* are virulence and host range genes, and their protein products E3 and K3 inhibit the activation and activity of PKR (8, 9). PKR is an antiviral protein that is found in most vertebrates. It is constitutively expressed at moderate levels and can be induced by type I interferons. PKR is composed of two N-terminal double-stranded RNA (dsRNA) binding domains that sense viral dsRNA, and a C-terminal kinase domain. Upon binding to dsRNA, two inactive PKR monomers dimerize and undergo autophosphorylation. Activated PKR subsequently phosphorylates the alpha subunit of eukaryotic translation initiation factor 2 (eIF2), which leads to the general suppression of protein translation and inhibition of virus replication. During vertebrate evolution PKR has evolved rapidly, likely as a consequence of positive selective pressure exerted by viral PKR antagonists. We and others previously showed that VACV K3 inhibits PKR in a species-specific manner, e.g. whereas mouse PKR was sensitive to K3 inhibition, human PKR was largely resistant (10, 11). MYXV 156 is a homolog of eIF2α and was previously tested for its ability to inhibit human PKR in a heterologous yeast assay in which it showed no inhibition of human PKR activity (12). Here we explored the

hypothesis that *M156R* evolved to inhibit rabbit PKR and that species-specific inhibition of PKR contributes to the restricted host range of MYXV to rabbits. We further tested whether variations found in MYXV field isolates affected the inhibitory potential of M156 and M029 against rabbit PKR.

Results

Predominant Expression of a Short M156 Form

M156R is located at the 3' end of the genome and partly overlaps with the inverted terminal repeat (ITR) region in the reference Lausanne (Lu) strain (13). Among all known poxvirus K3 orthologs, M156 is unique, because it contains a predicted N-terminal extension, based on an elongated ORF (open reading frame) (Fig. 3.1*A*, 3.6*A*). In MYXV strains that descended from South America, *M156R* is annotated to encode a 102-amino acid protein with a predicted molecular mass of 12 kDa (13). The M156 orthologs of the closest relatives, rabbit fibroma virus and the Californian MYXV MSW strain, lack this putative extension, but contain a putative start codon that encodes for 78- and 77-aa-long ORFs, respectively, with predicted molecular masses of 9 kDa (Fig. 3.6*A*) (14, 15). A putative start codon at the corresponding position is also found in the South American-derived MYXV strains. In the solution structure of M156, for which the long *M156R* ORF was used, the first 32 amino acids were unstructured (12). A predicted poxvirus early promoter motif is absent in the 500 bp 5' to the first start codon, but is present at nucleotide position -42 relative to the second predicted start codon (Fig. 3.6*B*). To determine the authentic ORF of *M156R*, we performed rapid amplification of cDNA ends (RACE) PCR to determine the transcriptional start sites (TSSs) using total RNA from MYXV-Lu-infected RK13 cells 4, 12 or 24 h post infection (hpi). Prominent bands were observed at about 120 bp at all time points but not in the uninfected control (Fig. 3.6*C*). PCR products were randomly cloned and sequenced. TSSs of 17 out of 18 clones started within the extended ORF, with the majority (82%) of sequences starting at positions -15 to -7 relative to the second start codon (Fig. 3.6*B* and Fig. 3.7). None of the discovered TSSs are predicted to lead to the translation of the long M156 isoform. To analyze the expression pattern of M156 and compare

its molecular mass to that of transfected M156, we performed Western blot analyses of RK13 cells infected with Lu MYXV at various time points (Fig. 3.6*D*). M156 expression was detected as early as 1 hpi and was most strongly expressed after 4-24 hpi and thus showed comparable expression to M-T7, an early expressed MYXV protein. In contrast, expression of the late protein M130 was not observed until 8 hpi. We also transfected RK13 cells with plasmids encoding the short or long M156 isoforms and analyzed their expression using anti-M156 serum. The short M156 isoform (Fig. 3.6*D*, lane 7) was detected at a comparable size as M156 in MYXV-infected cells. We were unable to detect the expression of the long M156 isoform under any conditions using our M156 antiserum. In conclusion, our data indicate that the short form of M156 is the predominant isoform in the tested cells, and we therefore used this version in subsequent experiments. To avoid confusion with *M156R* annotations of MYXV genomes, we kept the numbering of the long isoform when referring to specific amino acids.

Host-Specific PKR Inhibition by M156

Yeast-based assays have been previously used to analyze interactions of PKR and viral inhibitors (10, 11, 16-18). In one of these assays, M156 failed to inhibit human PKR, whereas its VACV ortholog K3 showed PKR inhibition (12). We hypothesized that *M156R* evolved to inhibit rabbit PKR. To test this hypothesis, we generated isogenic yeast strains that were stably transformed with empty vector (control), human PKR, or E. rabbit PKR under the control of a galactose-inducible promoter (18). These strains were subsequently transformed with plasmids encoding VACV K3, MYXV M156, or empty vector (control), which are also under the control of the galactose-inducible promoter. Under inducing conditions (galactose-containing agar plates), all transformants of the control strain expressing no PKR showed comparable growth, indicating that K3 or M156 alone had no effect on yeast growth (Fig. 3.1*B*). Induction of both human and E. rabbit PKR expression was toxic in the vector-transformed strains, whereas this toxicity was suppressed by K3 (Fig. 3.1*C*, 3.1*D*). Expression of M156 had no effect on human PKR toxicity, whereas it reduced toxicity of E. rabbit PKR, as indicated by no growth and growth, respectively (Fig. 3.1*C*, 3.1*D*). The transformants were also grown in liquid media to measure eIF2α phosphorylation levels 4 h after galactose induction by Western blot analysis. No eIF2α phosphorylation was observed in the absence of PKR (Fig. 3.1*E*). Both human and E. rabbit PKR induced eIF2α phosphorylation, which was reduced by the expression of K3 for both PKR. Expression of M156 only inhibited eIF2α phosphorylation induced by E. rabbit PKR, but not that mediated by human PKR. These results demonstrate that M156 is an inhibitor of E. rabbit PKR but not of human PKR in this yeast assay and also explain why no inhibition of human PKR was observed previously (12).

To extend the analysis of host-specific PKR inhibition by M156, we used a previously described assay in HeLa cells, in which the endogenous PKR was stably knocked down by shRNA, designated as HeLa-PKR^{kd} cells (10). To avoid the effect of RNA interference on transfected human PKR, we used knock-down resistant human PKR (PKR$^{kd\text{-}res}$) for subsequent experiments. HeLa-PKR^{kd} cells were cotransfected with E. rabbit, human, sheep, mouse, rat, Guinea pig, Syrian hamster or Chinese hamster PKR, *M156R* or a control plasmid (empty vector), and firefly luciferase. Our previous studies showed that the reduction of luciferase activity is a more sensitive indicator of PKR activity than phosphorylation of eIF2α in transient transfection assays (10). Luciferase activities were normalized to PKR-only transfected cells. Increases in luciferase activity indicate inhibition of PKR activity. Transfection of *M156R* resulted in strongly increased luciferase expression only in cells cotransfected with E. rabbit but not in cells co-transfected with the other species' PKRs, which indicates that M156 inhibited only E. rabbit PKR, whereas the other species' PKRs were resistant (Fig. 3.2*A*). This result therefore confirms and extends the results of species-specific M156 activity obtained in the yeast assays. Because MYXV contains a second PKR inhibitor encoded by *M029L*, which belongs to the poxvirus E3L family of dsRNA-binding proteins, we analyzed whether M029 also exhibits species-specific PKR inhibitory activity. HeLa-PKR^{kd} cells were cotransfected with human or E. rabbit PKR and increasing amounts of M029L or M156R. Whereas E. rabbit PKR but not human PKR was inhibited in a dose-dependent manner by M156, both PKRs showed comparable sensitivity to M029, indicating that only M156 exhibits pronounced species specificity (Fig. 3.2*B* and 3.2*C*). Myxoma virus proteins M-T5, M011, M013 and M130, used as controls, had no effect on PKR activity (Fig. 3.8).

Myxoma Virus Can Overcome the Antiviral Effects of Rabbit PKR

To characterize the antiviral effects of E. rabbit and human PKR during poxvirus infection, we established an infection assay using HeLa-PKR^{kd} cells in which we stably expressed PKR. To mimic natural PKR expression, we constructed a plasmid that contains the human PKR promoter as characterized (19), followed by the rabbit β-globin intron and a multiple cloning site, into which we cloned human PKR$^{kd\text{-}res}$ or E. rabbit PKR, followed by two FLAG tags. HeLa-PKR^{kd} cells were stably transfected with the PKR-expressing plasmids or empty vector and clones derived from single colonies were analyzed for PKR expression. For subsequent experiments, a clone (h14) that expressed transgenic human PKR (HeLa-PKR$^{kd+humanPKR}$) at levels comparable to that of control HeLa cells was chosen, as determined by Western blot using an anti-human PKR antibody (Fig. 3.9). An E. rabbit PKR-expressing clone (r15, HeLa-PKR$^{kd+E.\ rabbit\ PKR}$) was chosen that showed comparable PKR expression to that of HeLa-PKR$^{kd+humanPKR}$, using an anti-FLAG tag antibody (Fig. 3.9). HeLa control cells, as well as HeLa-PKR^{kd} and its derivatives stably transfected with vector, human, or rabbit PKR were infected with VC-R2, a VACV strain that lacks both PKR inhibitors K3 and E3, to analyze if VACV replication is suppressed when PKR is expressed. In VC-R2, the *E3L* gene is replaced with a destabilized EGFP driven by the native *E3L* promoter and its expression can be used as readout for VACV protein expression. EGFP was expressed in HeLa-PKR^{kd} and HeLa-PKR$^{kd+vector}$ cells, whereas it was strongly suppressed in HeLa control cells and HeLa-PKR^{kd} cells expressing human and E. rabbit PKR (Fig. 3.3*A*). We also determined VC-R2 replication in the infected cells by performing plaque assays on rabbit RK13 cells expressing E3 and K3, which are permissive for VC-R2. VC-R2 could only replicate in HeLa-PKR^{kd} and HeLa-PKR$^{kd+vector}$, whereas endogenous levels of PKR expression completely suppressed VC-R2

replication (Fig. 3.3*B*). These results demonstrate that transgenic expression of either human or E. rabbit PKR can compensate for the loss of PKR in HeLa cells with respect to the suppression of VACV replication. We next infected the same cell lines with MYXV that expresses EGFP under the control of a synthetic early/late poxvirus promoter (20). In HeLa control and HeLa-PKR$^{kd+humanPKR}$ cells, relatively weak EGFP expression was observed, whereas strong EGFP was observed in PKR-deficient and E. rabbit PKR-expressing cells (Fig. 3.3*A*). This observation correlated with MYXV replication in these cells, which was only suppressed in cells expressing human PKR but not E. rabbit PKR (Fig. 3.3*B*). We also monitored eIF2α phosphorylation levels in mock- and virus-infected congenic HeLa cells by Western blot analyses to assess whether the effects of transgene expression on virus replication correlated with eIF2α phosphorylation. In HeLa-PKR^{kd} and HeLa-PKR$^{kd+vector}$ cells, basal eIF2α phosphorylation levels were not increased by VC-R2 or MYXV infection (Fig. 3.3*C*). In HeLa-PKR$^{kd+humanPKR}$ and HeLa-PKR$^{kd+E. rabbit PKR}$ cells, VC-R2 infection induced strong eIF2α phosphorylation to levels comparable to that in the HeLa control cells. MYXV infection only led to increased eIF2α phosphorylation in HeLa control and HeLa-PKR$^{kd+humanPKR}$ cells, which express human PKR, but not in HeLa-PKR^{kd}, HeLa-PKR$^{kd+vector}$, and cells expressing E. rabbit PKR (Fig. 3.3*C*). Thus, the effects of PKR on virus replication correlated well with eIF2α phosphorylation levels. The combined results show that MYXV was resistant to the antiviral effects of E. rabbit PKR but sensitive to those of human PKR.

M156 Deficiency Leads to MYXV Attenuation in Rabbit Cells

We inactivated *M156R* in MYXV-M029L^{KO}, which lacks the other PKR inhibitor M029 (21), to generate MYXV-M029L^{KO}M156R^{KO}, which is devoid of both PKR inhibitors (Fig. 3.10). Deletion of *M029L* alone resulted in smaller plaque sizes and approximately 10- to 50-fold titer reduction in infected RK13 cells (21) (Fig 3.4*A* and 3.4*B*). Inactivation of *M156R* in this strain resulted in further attenuation as indicated by the reduced EGFP expression and an additional 10- to 17-fold titer reduction (Fig 3.4*A* and 3.4*B*). Viral protein synthesis was abolished in MYXV-M029L^{KO}M156R^{KO} as indicated by the absence of M-T7 and M130 expression (Fig 3.4*C*). In RK13+E3L+K3L, replication and protein synthesis of MYXV-M029L^{KO}M156R^{KO} were not impaired, indicating that the attenuation of this strain is caused by its inability to inhibit PKR. Interestingly, we consistently observed higher expression of the early proteins M156 and M-T7 in both RK13 and RK13+E3L+K3L cells infected with MYXV-M029L^{KO}, which indicates that M029 might be a negative regulator of some MYXV proteins' expression.

Loss-of-Function Mutation in M156R of Australian MYXV Isolates

Despite the availability of the full genome sequences of 24 MYXV isolates from Australia, the molecular mechanisms that underlie the attenuation of MYXV strains in the field are currently unclear. One of the identified mutations leads to a predicted leucine-to-proline amino acid substitution at position 98 (L98P) in *M156R* in 13 out of 24 isolates (7). The corresponding leucine residue in the costructure of eIF2α with human PKR (22) is shown in Fig. 3.5*A*. We introduced this mutation into M156-encoding plasmids using site-directed mutagenesis and tested its effect on E. rabbit PKR in yeast and cell culture assays. The mutation had no effect on yeast growth in a control strain, but abolished the M156-mediated rescue of yeast growth in a strain expressing rabbit PKR (Fig. 3.5*B* and 3.5*C*). In correlation with this result, M156-L98P was unable to inhibit M156-mediated inhibition of eIF2α phosphorylation in yeast grown in liquid medium (Fig. 3.5*D*). The inability of M156-L98P to inhibit PKR was also confirmed in the cell-culture-based transfection assays, in which even the highest amounts of M156-L98P had no effect on PKR activity (Fig. 3.5*E*). In transfected cells, both M156 and M156-L98P were expressed at comparable levels as determined by Western blot analysis and the loss of PKR inhibition was therefore not due to altered M156 expression (Fig. 3.5*E*). A predicted alanine-to-valine substitution at position 17 in M029, which was present in 11 out of 24 isolates (7), did not result in altered PKR inhibition (Fig. 3.11). To test the effect of M156-L98P in MYXV infection, we inserted it or wild type M156R (revertant) into MYXV-M029L^{KO}M156R^{KO} and infected RK13 cells with the viruses. M156 was able to restore EGFP expression, whereas M156-L98P could not (Fig 3.5*F*). EGFP expression correlated well with virus replication, which was restored by M156 but not by M156-L98P (Fig 3.5*G*), confirming that the latter is also a loss-of-function mutation in the context of MYXV infection. The loss of M156 function in some MYXV isolates

is thus a good candidate for a contributing factor to the virulence attenuation of MYXV in Australia.

Discussion

We have shown here that M156 of MYXV is a species-specific inhibitor of rabbit PKR, that human PKR but not rabbit PKR can restrict MYXV replication in congenic HeLa cells, and that M156 deficiency leads to virus attenuation in RK13 cells. The extent of species-specific PKR inhibition by M156 is remarkable, considering its likely mode of action as a pseudosubstrate inhibitor (23). Poxvirus K3 homologs share the common S1 fold with eIF2α, the substrate of PKR and they all likely bind to the same region of PKR. In contrast to the poxvirus K3 members, which can share as little as 20% sequence identity with each other (10), eIF2α is highly conserved, e.g., 100% sequence identity between human and rabbits in the S1 domain. The finding that PKR has been evolving rapidly can be explained by the high selective pressure exerted by pathogen-derived antagonists, such as poxviral K3 orthologs, which has caused PKR to diversify. Still, PKR faces the challenge to maintain its interaction with eIF2α, while evading inhibition by K3-family pseudosubstrate inhibitors. The best-studied PKR pseudosubstrate inhibitor is VACV K3. It was previously shown that K3 inhibited mouse PKR much better than human PKR in cell transfection assays and that hominoid PKR were more resistant to K3 inhibition than PKR from Old World and New World monkeys in yeast assays, indicating the potential for species-specific inhibition (10, 11). A limitation of studying the interaction of VACV with host proteins is that its "natural" host is unknown. Studying the interaction of MYXV proteins with innate immune proteins of a naturally infected rabbit host can therefore provide unique insights into this host-pathogen relationship. Potential species-specificity of M156 was not previously considered as an explanation for its inability to inhibit human PKR in a yeast assay (12). Our results that only rabbit PKR but not human PKR was inhibited by M156 in yeast demonstrate that this assay system is informative and that species-specific activity can

explain the earlier negative results obtained in yeast. This finding was confirmed and extended by the transfection assays, which showed that of the eight tested mammalian PKRs, only rabbit PKR was strongly inhibited by M156. Because MYXV has evolved in rabbits, it can be assumed that its gene products adapted to inhibit the immune response of its hosts. However, it is remarkable that PKR from other mammals were not considerably affected as "off-species targets" because M156 is predicted to bind to the PKR kinase domain at the same interaction surface as the PKR target eIF2α. The species-specific PKR inhibition by M156 is the first example where a species-specific interaction correlates with the host species restriction of MYXV virus.

The host range function of many poxvirus genes was described in cultured cells that originated from different species. Because it cannot be ruled out that cell-specific characteristics that are species independent contribute to the observed differences, we established a system that allows the comparison of PKR from different species in congenic HeLa cells. Infection of these cells showed that human PKR restricted MYXV infection, but that MYXV replicated as well in cells expressing rabbit PKR as in cells in which endogenous PKR expression was knocked down. Importantly, rabbit PKR was as efficient as human PKR in inhibiting the replication of a VACV strain that lacks the PKR inhibitors E3 and K3. These results demonstrate that MYXV can overcome the antiviral activities of only rabbit PKR and this correlates with the ability of M156 to inhibit rabbit PKR but not human PKR. Congenic cells expressing PKR from different species might also prove useful for studying species-specific effects of other viral inhibitors.

The coevolution of both MYXV and the feral European rabbit host after the deliberate release of MYXV into Australia and Europe constitutes one of the best-studied examples of host-virus evolution on the population level. The introduction of MYXV into Australia initially led to

a dramatic reduction of the rabbit population; however, within a few years, rabbit numbers rebounded. This could be attributed to the increased resistance of rabbits against MYXV and to the attenuation of MYXV in the field, the latter of which allowed for more efficient virus transmission (5). The molecular mechanisms behind these two phenomena are, however, poorly understood. The full genome sequencing of 24 MYXV that were isolated between 1951 and 1999 constituted an important step in understanding the molecular basis for MYXV evolution in Australia. While many mutations were present in the isolates, no common mutations were identified that could explain differences in virulence (6, 7). The L98P mutation in *M156R* was identified in 13 of these isolates. Because M156R-L98P was unable to inhibit rabbit PKR and led to MYXV attenuation in our assays (Fig. 3.5), this mutation can help explain and likely contributes to the attenuation of MYXV in Australia. The corresponding residue in eIF2α and viral homologs is highly conserved, being either a leucine in eIF2α and vIF2α, a PKR inhibitor from ranaviruses and leporipoxvirus 156R, or a valine in K3/M156 orthologs from other poxviruses (18). This residue is part of a β-sheet (β5), which also comprises residues corresponding to M156 Y95 and D97, which are 100% conserved in all eIF2α homologs and are involved in the binding of eIF2α to PKR (12, 18, 22). A proline in this β-sheet would likely disrupt the β-sheet and abolish binding to PKR. Indeed, it would be instructive to know if the rabbit PKR locus has also undergone any virus-induced selection pressures over the half century since the first field releases of MYXV.

In conclusion, the results presented here show that rabbit PKR was specifically inhibited by M156, that human PKR plays an essential role in suppressing MYXV replication in HeLa cells, and that a naturally occurring mutation in M156 abolished rabbit PKR inhibition. These phenomena might contribute to the strict host restriction of MYXV infection to only rabbits, the

prevention of productive infection in nonrabbit species (particularly humans), and the attenuation of MYXV strains currently extant in Australia. Moreover, this study shows that the choice of biologically meaningful host-virus systems is important for studying host-virus interactions. Often, studies of viral molecules or viruses are performed with molecules, cell lines or animals of nonhost species. The results of such experiments could be misleading, if the virus molecules act in a species-specific manner as shown here for M156 and rabbit PKR.

Materials and Methods

Plasmids, Yeast Strains and Cell Lines

PKR and viral genes were cloned into pSG5 for expression in mammalian cells. Generation of yeast strains, stably transformed with empty vector (J673) or human PKR (J983) under the control of a yeast GAL-CYC1 hybrid promoter, was described (18). A yeast strain stably transformed with E. rabbit PKR (O8) was generated using the same methods. VACV *K3L* and *M156R* were cloned into the vector pYX113, which contains the GAL-CYC1 hybrid promoter. HeLa-PKR^{kd} cells (24), kindly provided by Charles Samuel, were stably transfected with knock-down resistant human PKR and E. rabbit PKR under the control of the human PKR promoter (19). The generation of RK13+E3L+K3L cells was described (21). See *SI Materials and Methods* for details.

RACE PCR

E. rabbit RK13 cells were infected with MYXV-EGFP at an multiplicity of infection (MOI) of 1. Total RNA was collected with TRIzol reagent at 4, 12 and 24 h postinfection. RACE PCR was performed with the GeneRacer Core Kit (Invitrogen) according to the manufacturer's instruction. See *SI Materials and Methods* for details.

Yeast Growth and eIF2α Phosphorylation Assays

Experiments were performed as previously described (18, 25). See *SI Materials and Methods* for details.

Luciferase Assay

5×10^4 HeLa-PKR^{kd} cells were seeded in 24-well plates 1 day before transfection. For each transfection, firefly luciferase (pGL3promoter, 0.05μg, Promega), and pSG5 plasmids encoding PKR (0.2 μg), M156 or M029 (0.4 μg) were transfected using GenJet-HeLa (Signagen). For titration experiments, amounts of transfected plasmids are indicated in the figures. For controls, empty pSG5 vector was transfected using the same amount. Each transfection was conducted in triplicate. After 48 hours, cell lysates were harvested using mammalian lysis buffer (Goldbio) and luciferase activity was determined using luciferase detection reagents (Promega) in a luminometer (Berthold).

Construction of Recombinant Viruses

The construction of VC-R2 and MYXV-EGFP were described previously (20, 26) and the construction of *M156R* mutant viruses is illustrated in Fig. S5 and described in *SI materials and methods*.

Infection Assays

HeLa-control, HeLa-PKR^{kd}, HeLa-PKR$^{kd+vector}$, HeLa-PKR$^{kd+hPKR}$ and HeLa-PKR$^{kd+E.rabbit\ PKR}$ cells were seeded into six-well plates and confluent monolayers ($1x10^6$ cells) were mock infected with PBS or infected with VC-R2 and MYXV-EGFP at an MOI of 0.1 and 1, respectively. RK13 cells were infected with MYXV-EGFP or MYXV-EGFP-derived recombinant viruses at an MOI of 5. Fluorescent pictures were taken with an inverted fluorescent microscope (Leica) and viruses were collected at 0, 24, 48 and 72 hpi for titration in RK13 cells that stably express E3 and K3. See *SI Materials and Methods* for details.

Western blot analyses

Protein lysates from RK13 cells that were infected with MYXV-EGFP (MOI = 10) were blotted on PVDF membranes and incubated with anti-M156 (27), and after stripping, re-probed with anti-serum against M-T7 (28), M130 (29) and anti-β-actin. For eIF2α phosphorylation assays, PKR-expressing cells were infected with VC-R2 or MYXV-EGFP at an MOI of 5. Total protein lysates were collected 8 hpi and eIF2α was detected with phospho-specific eIF2α and total eIF2α. See *SI Materials and Methods* for details.

Acknowledgments

We thank Thomas E. Dever for helpful discussions. This work was supported, in part, by Grant R01 AI114851 (to S.R.) from the National Institute of Allergy and Infectious Diseases, National Institutes of Health and grants from Johnson Cancer Research Center (to C.P., S.L.H. and S.R.).

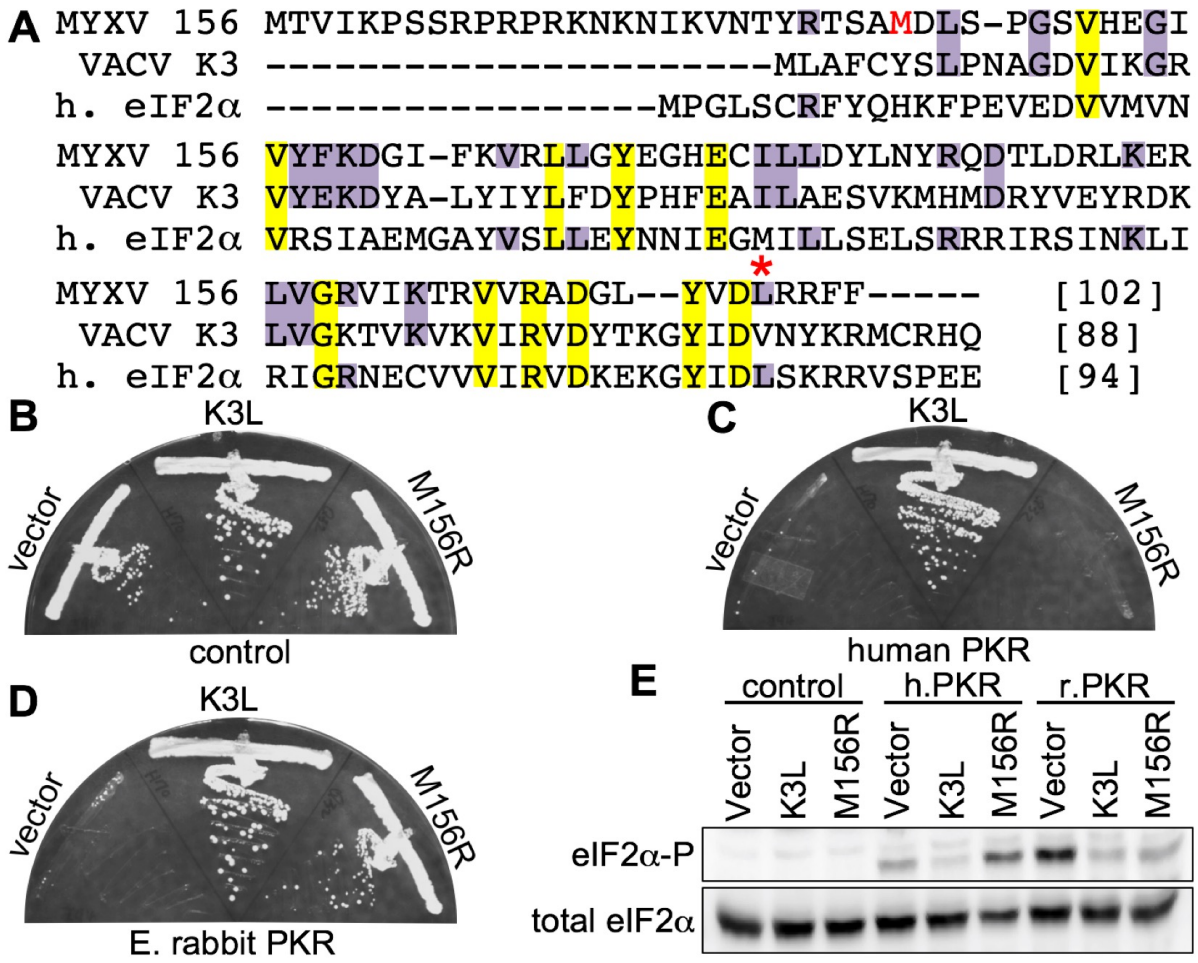

Figure 3.1 M156 inhibits rabbit but not human PKR in yeast

(*A*) Multiple sequence alignment of MYXV-Lu M156, VACV K3, and human (h) eIF2α. Conserved residues are highlighted in yellow (100% conservation) or purple (identical with M156). The methionine encoded by the putative start codon of the predominant M156 isoform is shown in red. An asterisk indicates L98 in MYXV-Lu M156. Plasmids encoding VACV K3, MYXV M156 or empty vector under the control of a yeast GAL-CYC1 hybrid promoter were transformed into isogenic yeast strains, which have either empty vector (control) (*B*), human

PKR (*C*), or E. rabbit PKR (*D*) stably integrated at the LEU2 locus under the control of the GAL-CYC1 promoter. Transformants were colony purified and grown under inducing conditions at 30 ˚C for 4 d. Results shown are representative of 4 independent transformants for each plasmid. (*E*) Transformants described above were grown in liquid SC-Gal medium for 4 hours to induce expression. Whole cell protein extracts were obtained from equal numbers of cells and subjected to Western blot analyses. The blots were probed with phospho-specific antibodies against Ser51 eIF2α (eIF2α-P), then stripped and probed with polyclonal antiserum against total eIF2α.

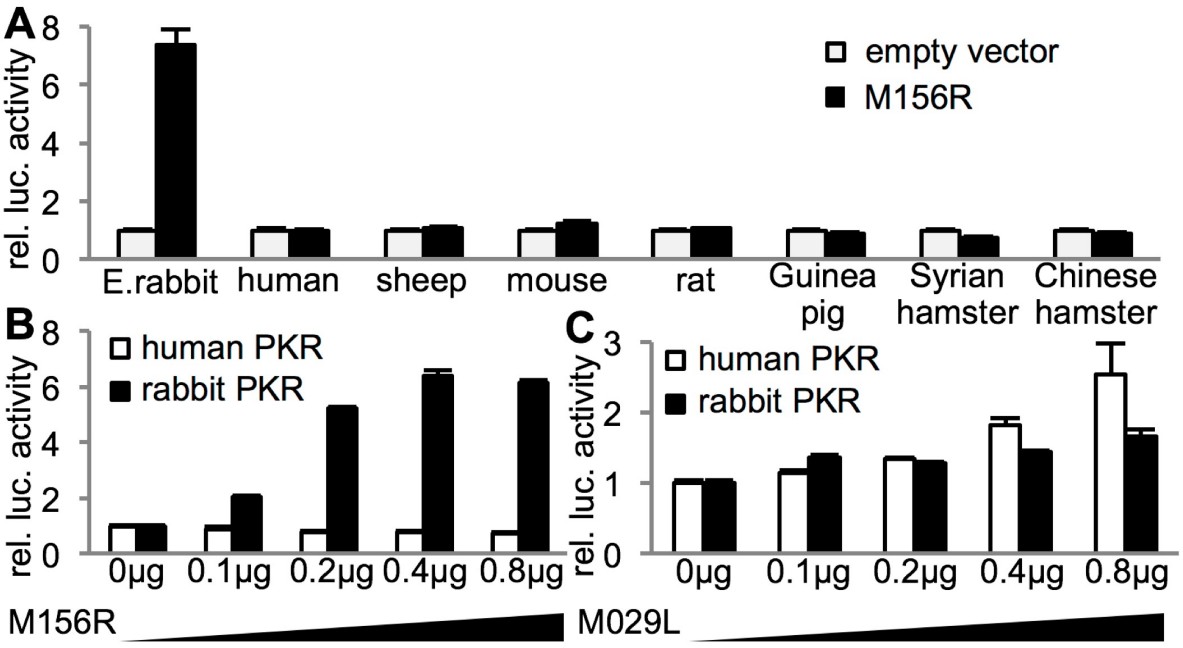

Figure 3.2 Species-specific inhibition of rabbit PKR by M156

(*A*) Human HeLa-PKR^{kd} cells were transfected with expression vectors for luciferase (0.05 µg), MYXV *M156R* (0.4 µg) and PKR (0.2 µg) from the indicated mammalian species. Luciferase light units were normalized to PKR-only transfected cells to obtain relative luciferase activities. Constant amounts (0.1 µg) of human PKR or E. rabbit PKR were cotransfected with increasing amounts of *M156R* (*B*) or *M029L* (*C*) and relative luciferase activities are shown. Experiments were performed in triplicate and the results are representative of three independent experiments. Error bars indicate SD.

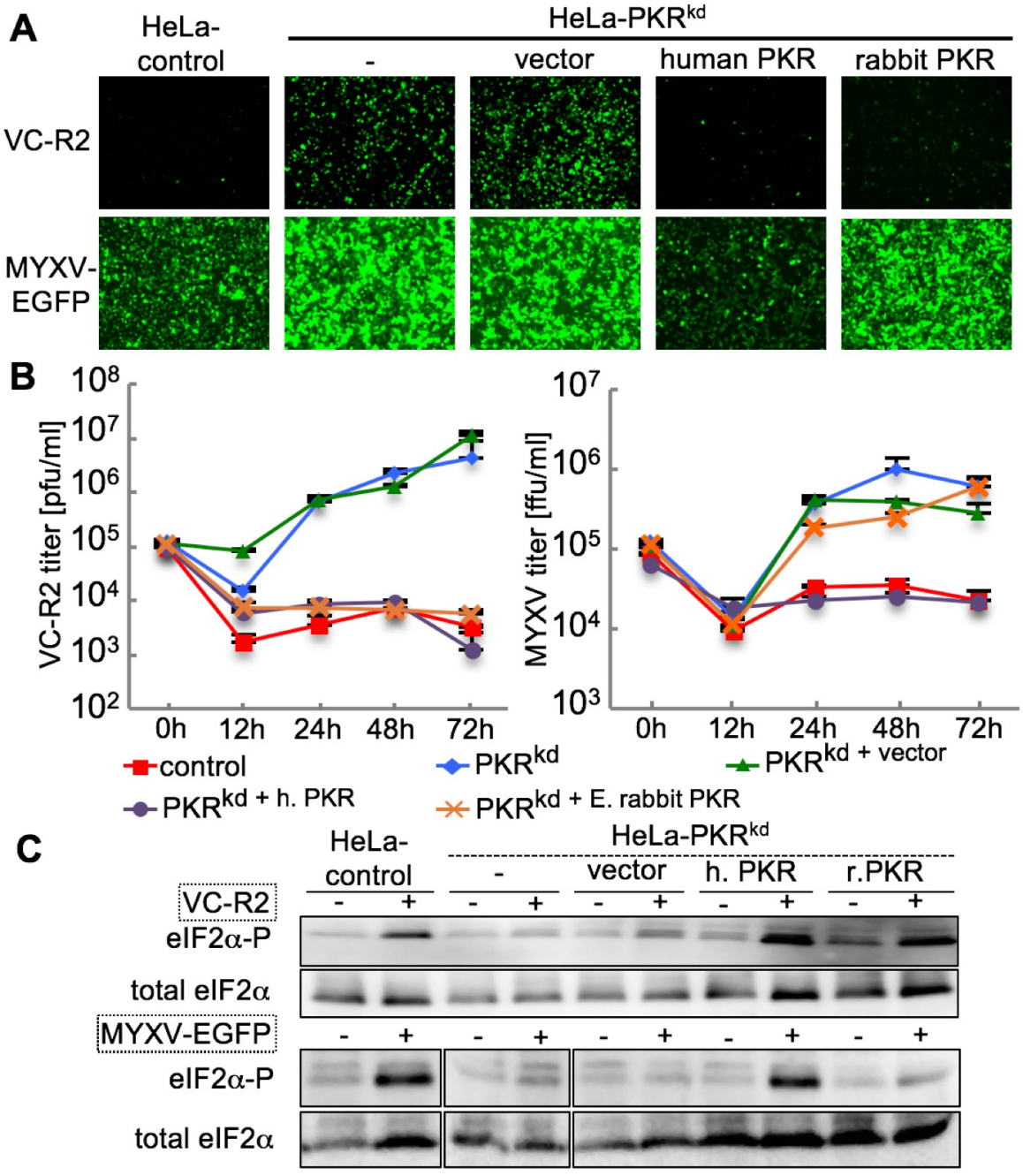

Figure 3.3 Human PKR but not rabbit PKR suppresses MYXV replication

(*A*) Control and congenic HeLa-PKR^{kd} HeLa cell lines that were stably transfected with

vector, human PKR, or E. rabbit PKR were infected with VC-R2 [VACVΔE3L(EGFP-d2)/ΔK3L] or MYXV-EGFP at MOI of 0.1 or 1, respectively. Representative images taken 48 hpi at 100x magnification are shown. EGFP levels in the two viruses cannot be compared directly, because in VC-R2 a destabilized EGFPd2 is driven by the natural E3L promoter, whereas in MYXV unmodified EGFP is driven by a synthetic early-late poxvirus promoter. (*B*) Indicated HeLa cell lines were infected with VC-R2 or MYXV-EGFP at an MOI of 0.1 or 1, respectively. Viruses were collected at 0, 12, 24, 48 and 72 hpi and titered on RK13 cells, which stably express VACV E3 and K3. (*C*) Total protein lysates were collected from mock (-), VC-R2 or MYXV-EGFP-infected HeLa cells at 8 hpi to measure phosphorylated and total eIF2α by Western blot analyses. Lysates shown were run on the same gel in a different order and lanes were reordered for clarity (Fig. 3.12 shows original).

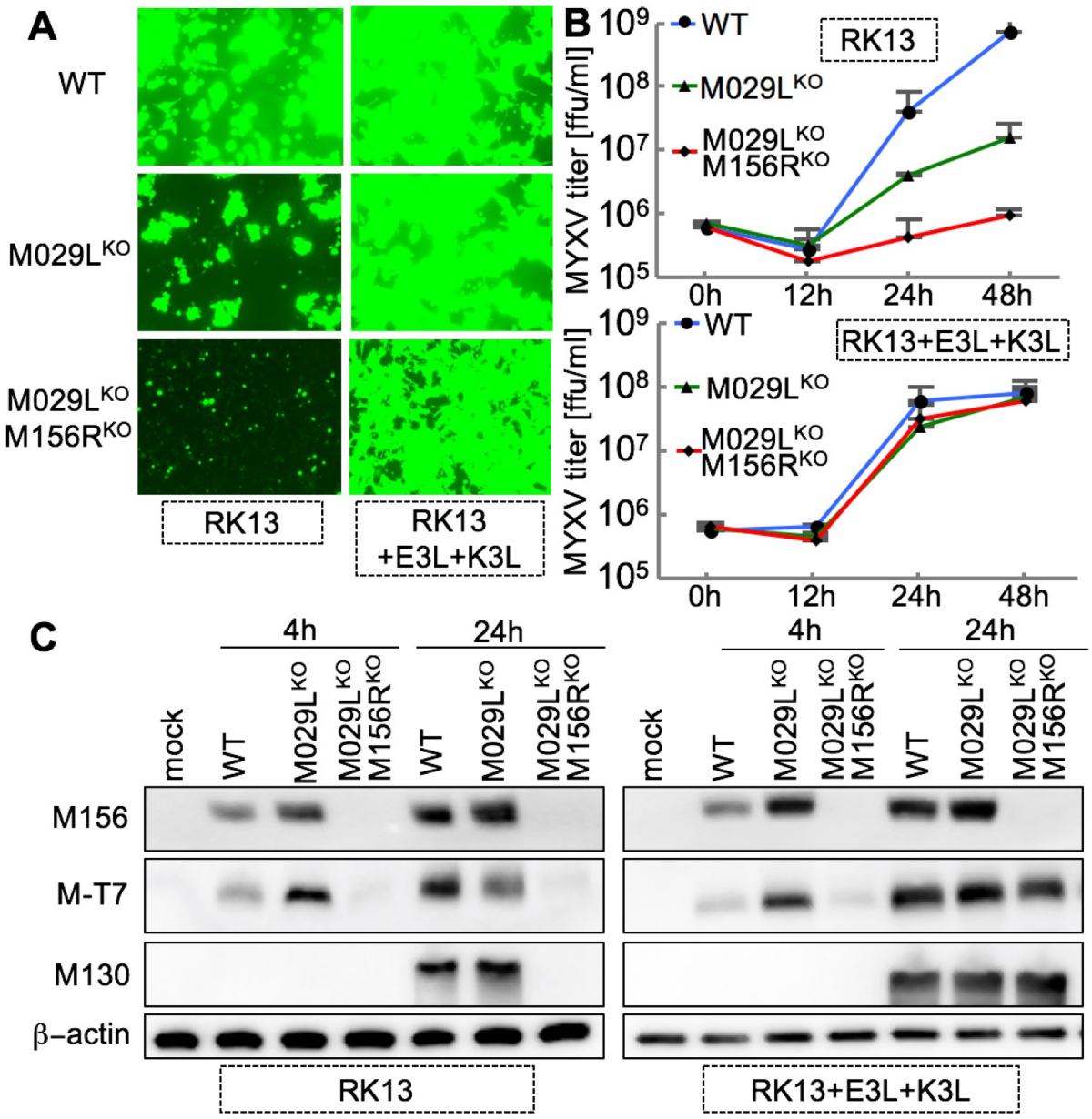

Figure 3.4 Deletion of M156R further attenuates MYXV that lacks M029L

RK13 cells (RK13-WT) and RK13 cells stably expressing E3 and K3 (RK13+E3L+K3L) were infected with MYXV-EGFP (WT), MYXV-M029L^{KO} or MYXV-M029L^{KO}M156R^{KO} at a MOI of 5. (*A*) Fluorescent images were taken at 48 hpi at 100x magnification. (*B*) Viruses were

collected at 0, 12, 24 and 48 hpi and titered on RK13+E3L+K3L cells. Error bars indicate SD (n=2). (*C*) Total protein lysates were collected at 4 and 24 hpi to monitor expression of MYXV early (M156 and M-T7) and late (M130) proteins. β-actin was included as loading control.

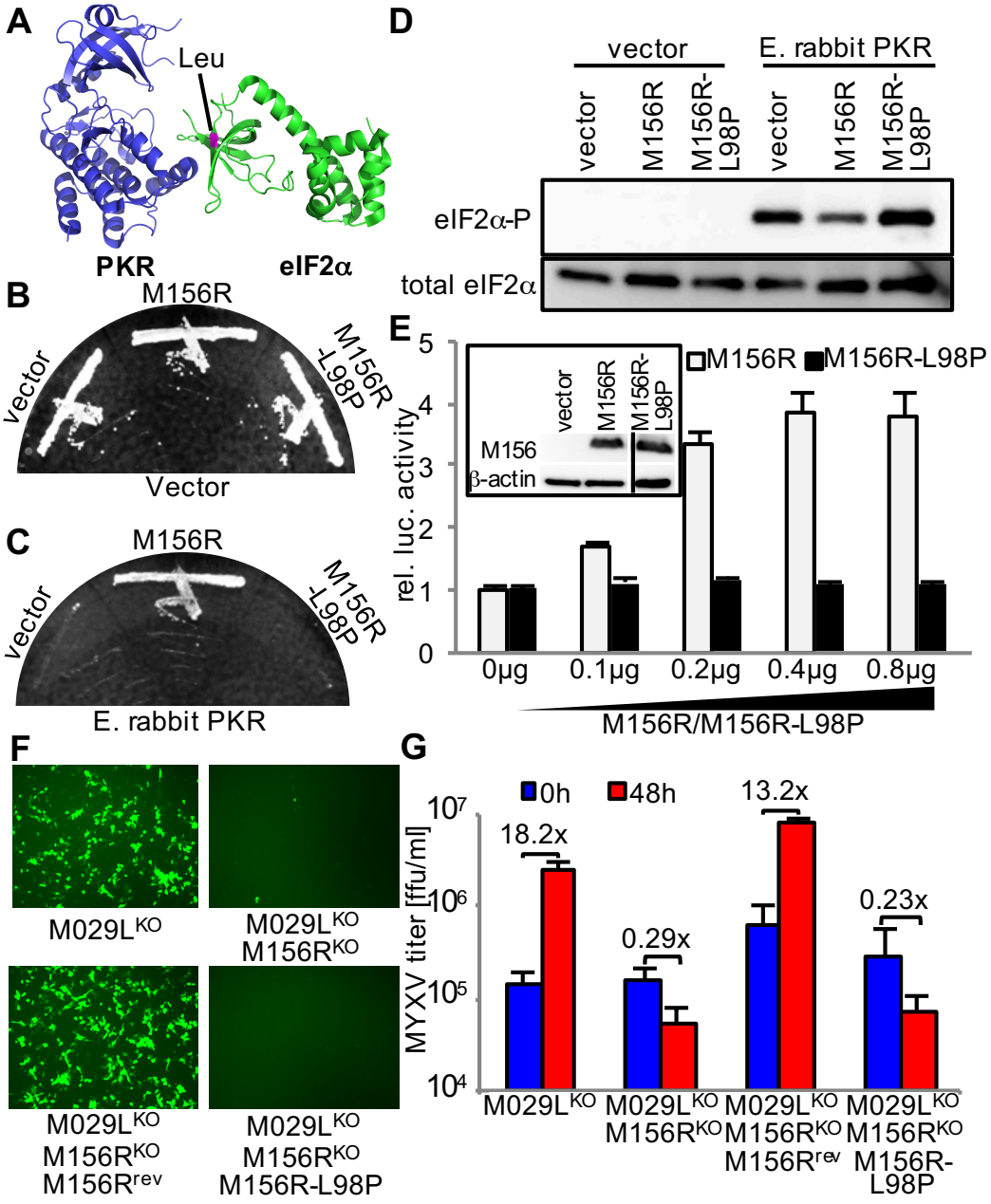
A
Leu
PKR
eIF2α
B
M156R
vector
M156R -L98P
Vector
C
M156R
vector
M156R -L98P
E. rabbit PKR
D
vector
E. rabbit PKR
vector
M156R
M156R-L98P
vector
M156R
M156R-L98P
eIF2α-P
total eIF2α
E
M156R
M156R-L98P
rel. luc. activity
M156
β-actin
0μg
0.1μg
0.2μg
0.4μg
0.8μg
M156R/M156R-L98P
F
M029L^KO
M029L^KO M156R^KO
M029L^KO M156R^KO M156R^rev
M029L^KO M156R^KO M156R-L98P
G
0h
48h
MYXV titer [ffu/ml]
18.2x
0.29x
13.2x
0.23x
M029L^KO
M029L^KO M156R^KO
M029L^KO M156R^KO M156R^rev
M029L^KO M156R^KO M156R-L98P

Figure 3.5 A naturally occurring M156R mutant lost its ability to inhibit PKR

(*A*) Crystal structure of the PKR-eIF2α complex. The residue highlighted in pink in the structure of eIF2α corresponds to Leu-98 in M156. Plasmids encoding empty vector, M156, or M156-L98P under the control of a yeast GAL-CYC1 hybrid promoter were transformed into isogenic vector (*B*) or E. rabbit PKR (*C*) containing yeast strains. Colony-purified transformants were grown under inducing conditions at 30 ºC for 4 d. (*D*) Transformants were grown in liquid SC-Gal medium for 4 h to induce expression. Lysates were subjected to Western blot analysis for phosphorylated and total eIF2α. (*E*) HeLa-PKR^{kd} cells were transfected with expression vectors for luciferase (0.05 μg), E. rabbit PKR (0.1 μg) and increasing amounts of *M156R* or *M156R-L98P*. After 48 h, luciferase activities were determined and normalized to control transfections lacking PKR inhibitors to obtain relative luciferase activities. (*Inset*) HeLa-PKR^{kd} cells were transiently transfected with 3 μg of vector, *M156R* or *M156R-L98P* plasmids. Total protein lysates were collected 48 hours after transfection to monitor M156 and β−actin expression. All samples were run on the same gel and lanes were spliced together (line) for clarity. (*F* and *G*) RK13 cells were infected with MYXV-M029L^{KO}, MYXV-M029L^{KO}M156R^{KO}, MYXV-M029L^{KO}M156R^{KO}M156R$^{revertant(rev)}$ and MYXV-M029L^{KO}M156R^{KO}M156R-L98P (MOI of 5). Fluorescent images were taken at 24 hpi (*F*) and virus titers were measured 0 and 48 hpi (*G*).

Supporting Information

SI Materials and Methods

Plasmids, Yeast strains and Cell Lines

PKR and viral genes were cloned into the pSG5 vector (Stratagene) for transient expression in mammalian cells. European rabbit (*Oryctolagus cuniculus*) PKR was cloned from spleen total RNA from a New Zealand white rabbit. The obtained PKR (accession number: KT272867) differed from NP_001075682 at 8 amino acid positions but was identical to ENSOCUT00000007225 (Ensmbl database). Sheep (*Ovis aries*) PKR (KT272868) was cloned from MDOK cells (ATCC CRL-1633). Three identical cDNA were obtained that differ from the predicted sheep PKR (XM_004007300.1) at six synonymous nucleotide positions. Rat (*Rattus norvegicus*) PKR was cloned from rat-1 cells and is identical to XM_008764426.1. Syrian hamster (*Mesocricetus auratus*) PKR was cloned from BHK-21 cells (ATCC CCL-10) and is identical to NM_001281945.1. Chinese hamster (*Cricetulus griseus*) PKR (KT272869) was cloned from CHO cells. Guinea pig (*Cavia porcellus*) PKR (KT272870) was cloned from 104C1 cells (ATCC CRL-1405) and is identical to the predicted Genbank sequence XM_003472904.2. Cloning of knock-down resistant human PKR and mouse PKR was described (1). VACV *K3L*, *M029L* and *M156R* short and long forms were cloned into pSG5. The M156R-L98P mutation was generated by site-directed mutagenesis PCR using the PfuUltra High-Fidelity DNA polymerase (Invitrogen). PCR was performed using the pSG5-M156R-short construct as the template with primers containing the leucine-to-proline mutation (C<u>T</u>G to C<u>C</u>G) flanked by 15

nucleotides identical to the template up- and downstream of the mutation. All ORFs were sequenced to confirm correct sequences.

Generation of yeast strains stably transformed with empty vector (J673) or human PKR (J983) under the control of a yeast GAL-CYC1 hybrid promoter was described (18). A yeast strain stably transformed with E. rabbit PKR (O8) was generated using the same methods. VACV *K3L* and *M156R* were cloned into the vector pYX113 (R&D systems), which contains the GAL-CYC1 hybrid promoter and the selectable marker URA3. HeLa-PKR^{kd} cells and control HeLa cells were kindly provided by Charles Samuel (24). RK13 cells were kindly provided by Bernard Moss. To generate HeLa-PKR^{kd} cells that express PKR, a plasmid was constructed that contains the human PKR promoter as described (19) (nucleotide positions -412 to + 97 relative to the transcriptional start site) followed by the intron of the rabbit β-globin gene from pSG5 and a multiple cloning site followed by a sequence encoding two FLAG tags and inserted into the pEGFP-N1 (Clontech) in place of the CMV promoter/enhancer, the multiple cloning site and the EGFP open reading frame. Knock-down resistant human PKR and E. rabbit PKR were cloned into this vector with the FLAG tags at their C-termini. HeLa-PKR^{kd} cells were transfected using GenJet-HeLa (SignaGen Laboratories) according to the manufacturer's instructions. Cells were trypsinized 48 h after transfection and cultured in the presence of 1μg/ml Geneticin (Invitrogen) for 14 days. To select clones, cells were seeded on 96-well plates at the density of 0.3 and 1 cell/well until single colonies appeared. Clones were then amplified and proteins were isolated to detect the expression of transfected PKR with an anti-FLAG tag antibody (ABM) and the absence of endogenous human PKR with the monoclonal anti-human PKR antibody 71/10. A human PKR reconstituted clone (HeLa-hs14) that showed comparable PKR expression level as the endogenous human PKR in HeLa control cells was selected and

amplified. A E. rabbit PKR expressing clone that showed PKR expression levels comparable to that of human PKR in HeLa-hs14, as determined with the anti-FLAG tag antibody, was used for subsequent experiments. For transfections, plasmids were prepared using NucleoBond Xtra Midi Endotoxin Free (Macherey-Nagel).

5' RACE PCR

E. rabbit RK13 cells were infected with MYXV-EGFP at a MOI of 1. Total RNA was collected with TRIzol reagent (Invitrogen) at 4, 12 and 24 hours postinfection. RACE PCR was performed with the GeneRacer Core Kit (Invitrogen) according to the manufacturer's instruction. Briefly, two rounds of PCR were conducted to amplify the 5' end of M156R cDNA using 5' adaptor primers provided in the kit and M156R-specific reverse primers. The second-round PCR products were cloned into the TOPO-TA vector (Invitrogen) and 6 colonies from each time point were randomly chosen for sequencing.

Yeast Growth and eIF2α Phosphorylation Assays

Yeast transformation was performed using the Lithium Acetate/PEG method. J673, J983 and O8 strains were transformed with empty vector pYX113, K3 or M156 expressing plasmids. For each transformation, four independent clones were picked and colony-purified on SD plates. Purified colonies were then streaked on either glucose (non-inducing conditions) or galactose containing medium [synthetic complete medium containing 2% (wt/vol) galactose and all amino acids without uracil, inducing conditions], and grown for 4 d at 30 ˚C. For Western blot analyses of yeast proteins, all transformants were grown to saturation in SD medium overnight. The start culture was then diluted 1:40 in SD medium on the second day and grown to OD600 = 0.6 and subsequently shifted to SC-Gal medium to induce expression. After 4 h, ODs of the cultures were obtained and cultures were diluted accordingly in water to reach the same ODs. Equal

amounts of cells for each sample were lysed using the trichloroacetic acid (TCA) method. Samples were mixed with loading buffer with reducing agent and neutralized with 1M Tris-base. Proteins were fractionated on 10% (vol/vol) SDS-PAGE gels and then transferred to PVDF membranes (Millipore). Membranes were incubated with anti-phospho-S51 eIF2α (Bio-Source International) and then stripped and re-probed with anti-total eIF2α antibodies (25). Enhanced chemiluminescence was detected with a Kodak image system.

Luciferase Assay

5 x 10^4 HeLa-PKR^{kd} cells were seeded in 24-well plates 1 d before transfection. For each transfection firefly luciferase (pGL3promoter, 0.05 μg, Promega), and pSG5 plasmids encoding PKR (0.3 μg), M156, M156-L98P or M029 (0.4 μg) were transfected using GenJet-HeLa. For titration experiments, amounts of transfected plasmids are indicated in the figures. For controls, empty pSG5 vector was transfected using the same amount. Each transfection was conducted in triplicate. After 48 hours, cell lysates were harvested using mammalian lysis buffer (Goldbio) and luciferase activity was determined using luciferase detection reagents (Promega) in a luminometer (Berthold). Each experiment was performed at least three times and representative experiments are shown in the results. Error bars represent the standard deviations of three independent transfections.

Infection Assays and Western blot Analyses

RK13 cells were infected with mock (PBS) or MYXV-EGFP (Lu strain) at an MOI of 10. Proteins were collected at the indicated time points using an Nonidet P-40 lysis buffer (50mM Tris, 150mM NaCl, 1% Nonidet P-40, and proteinase inhibitor cocktail, Roche). Protein concentrations were determined by the Bradford assay (BioRad). Protein samples were separated

on 10% (vol/vol) SDS-PAGE gels and transferred to PVDF membranes (GE Healthcare) using a methanol-based wet transfer apparatus (BioRad). Membranes were blocked with 5% (wt/vol) non-fat milk or 5% BSA when detecting eIF2α-P in TBST buffer (20mM Tris, 150mM NaCl and 0.1% Tween-20 pH7.6) for 3 hours at 4°C and then incubated overnight with anti-serum raised against M156 (27) at 4˚C with rocking, and then stripped and re-probed with anti-serum against M-T7 (28), M130 (29), and an antibody against β-actin (Sigma-Aldrich). After washing, membranes were incubated with goat-anti-rabbit or goat-anti-mouse secondary antibodies (1:30,000) in TBST containing 5% (wt/vol) non-fat milk for 1 h at room temperature with agitation followed by TBST washing 4 times for 20 minutes each. Proteins were detected with Proto-Glo ECL (National Diagnostics) and images were taken with a Kodak image system.

HeLa-control, HeLa-PKR^{kd}, HeLa-PKR$^{kd+vector}$, HeLa-PKR$^{kd+hPKR}$, and HeLa-PKR$^{kd+E.rabbit\ PKR}$ cells were seeded into six-well plates and confluent monolayers (1x10^6 cells) were mock infected with PBS or infected with VC-R2 and MYXV-EGFP at an MOI of 0.1 and 1, respectively. Fluorescent pictures were taken with an inverted fluorescent microscope (Leica) at 48 hpi and viruses were collected at 0, 24, 48 and 72 hpi and were titered in RK13 cells that stably express E3 and K3 (21). For eIF2α phosphorylation assays, the previously described PKR-expressing cells were infected with VC-R2 and MYXV-EGFP at an MOI of 5. Total protein lysates were collected at 8 hpi with 1% SDS in PBS and fractionated on 10% (vol/vol) SDS-PAGE gels. Western blot analyses were performed as described above. Primary antibodies detecting S51 phospho-eIF2α (Bio-Source International) and total eIF2α (Santa Cruz) were diluted 1:10,000 and 1:1000, respectively, in TBST.

Construction of Recombinant Viruses

The generation of VC-R2, a vaccinia virus Copenhagen strain that lacks *E3L* and *K3L* ($VACV^{\Delta K3L/\Delta E3L}$) and carries a destabilized EGFP gene in the *E3L* locus, and MYXV-EGFP in which a synthetic vaccinia virus early/late promoter-driven EGFP cassette was inserted into the intergenic region in the M135-136 locus, were described previously (20, 26). The strategy to generate recombinant myxoma viruses is illustrated in Fig. S5. To create a *M156R* deficient virus, a recombinant plasmid was first constructed in which a poxvirus synthetic early/late promoter-driven mRFP is flanked by sequences 5' and 3' of the M156R locus, which contain partial sequences of *M154L* (5'), *M008.1L* (3') and intergenic sequences (both 5' and 3'). MYXV-$M029L^{KO}M156R^{KO}$ was generated by infecting RK13+E3L+K3L cells with MYXV-EGFP-$M029L^{KO}$ (Lu), followed by transfection of the recombinant plasmid. Multiple rounds of foci purification were performed with the same cell line using mRFP as selection marker. The recombinant locus was then PCR-amplified from the viral clone and sequenced to confirm successful recombination. To generate MYXV-$M029L^{KO}M156R^{KO}M156R^{rev}$ and MYXV-$M029L^{KO}M156R^{KO}$M156R-L98P recombinant viruses, RK13+E3L+K3L cells were infected with MYXV-$M029L^{KO}M156R^{KO}$ followed by transfection of recombinant plasmids in which the original M156 or the M156-L98P coding sequences were flanked by 5' and 3' arms described above. Multiple rounds of foci-purification were performed in RK13+E3L+K3L cells based on the absence of mRFP expression. In all recombinant MYXV, the *M156R* locus as well as the region comprising the partially duplicated *M156R* copy in the 5' region was PCR-amplified and sequenced to confirm successful integration and exclude unwanted mutations.

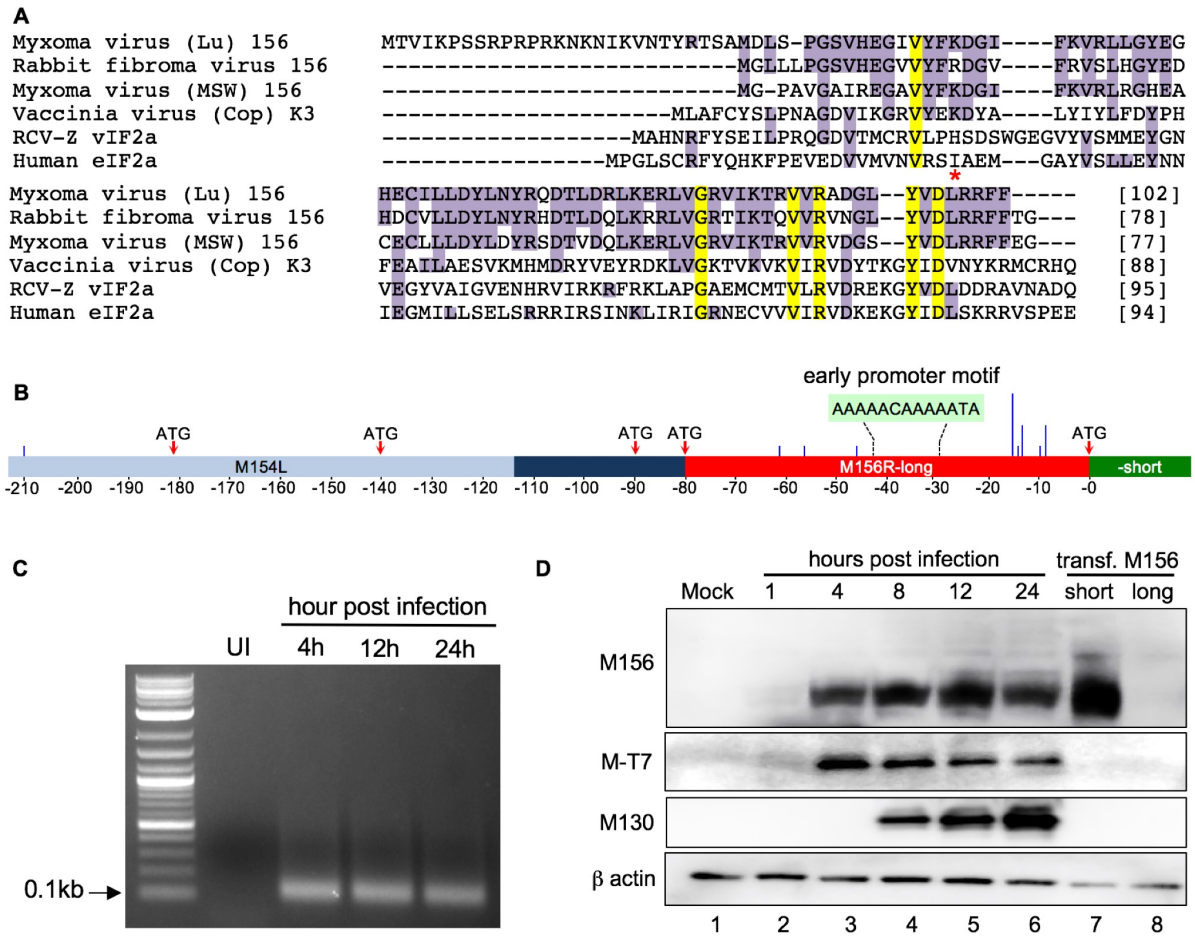
A
Myxoma virus (Lu) 156 MTVIKPSSRPRPRKNKNIKVNTYRTSAMDLS-PGSVHEGIVYFKDGI----FKVRLLGYEG
Rabbit fibroma virus 156 ----------MGLLLPGSVHEGVVYFRDGV----FRVSLHGYED
Myxoma virus (MSW) 156 ----------MG-PAVGAIREGAVYFKDGI----FKVRLRGHEA
Vaccinia virus (Cop) K3 ----------MLAFCYSLPNAGDVIKGRVYEKDYA----LYIYLFDYPH
RCV-Z vIF2a ----------MAHNRFYSEILPRQGDVTMCRVLPHSDSWGEGVYVSMMEYGN
Human eIF2a ----------MPGLSCRFYQHKFPEVEDVVMVNVRSIAEM---GAYVSLLEYNN
Myxoma virus (Lu) 156 HECILLDYLNYRQDTLDRLKERLVGRVIKTRVVRADGL--YVDLRRFF----- [102]
Rabbit fibroma virus 156 HDCVLLDYLNYRHDTLDQLKRRLVGRTIKTQVVRVNGL--YVDLRRFFTG--- [78]
Myxoma virus (MSW) 156 CECLLLDYLDYRSDTVDQLKERLVGRVIKTRVVRVDGS--YVDLRRFFEG--- [77]
Vaccinia virus (Cop) K3 FEAILAESVKMHMDRYVEYRDKLVGKTVKVKVIRVDYTKGYIDVNYKRMCRHQ [88]
RCV-Z vIF2a VEGYVAIGVENHRVIRKRFRKLAPGAEMCMTVLRVDREKGYVDLDDRAVNADQ [95]
Human eIF2a IEGMILLSELSRRRIRSINKLIRIGRNECVVVIRVDKEKGYIDLSKRRVSPEE [94]
B
early promoter motif
AAAAACAAAAATA
ATG
ATG
ATG ATG
ATG
M154L
M156R-long
-short
-210 -200 -190 -180 -170 -160 -150 -140 -130 -120 -110 -100 -90 -80 -70 -60 -50 -40 -30 -20 -10 -0
C
hour post infection
UI 4h 12h 24h
0.1kb
D
hours post infection
transf. M156
Mock 1 4 8 12 24 short long
M156
M-T7
M130
β actin
1 2 3 4 5 6 7 8

Figure 3.6 (S1) Identification of the major M156 transcription start sites (TSSs)

(*A*) Multiple sequence alignment of human eIF2α and viral eIF2α homologs from MYXV-Lu, rabbit fibroma virus, MYXV-MSW, VACV and Rana catesbeiana virus Z. Conserved residues are highlighted in yellow (100% conservation) or purple (identical with MYXV-Lu). An asterisk indicates L98 in MYXV-Lu M156. (*B*) Illustration of the observed TSSs for *M156R*. The genomic composition of the 5' end of *M156R* locus is indicated with red arrows denoting the presence of ATG codons. Numbers indicate relative nucleotide positions with respect to the identified start codon. Blue bars represent observed TSSs at any of the 3 time points. The height of each bar is proportional to the number of times each particular site TSS was observed. A predicted poxvirus early promoter motif is highlighted in the light green box. (*C*) 5'-RACE PCR was performed with RNA collected from MYXV-infected RK13 cells at 4, 12 and 24 hpi. Total PCR products were cloned and sequenced. (*D*) M156 is an early protein. RK13 cells were left uninfected (mock, lane 1) or infected with MYXV with an MOI of 10. Total protein was collected at indicated time points (lane 2-6). Short and long forms of *M156R* were transiently transfected and total protein was collected 24 hours later. All protein samples were separated on SDS-PAGE and subjected to Western blotting analyses. The membrane was first probed with an anti-M156 antibody, then consecutively stripped and probed for M-T7 (early gene), M130 (late gene), and β-actin (loading control).

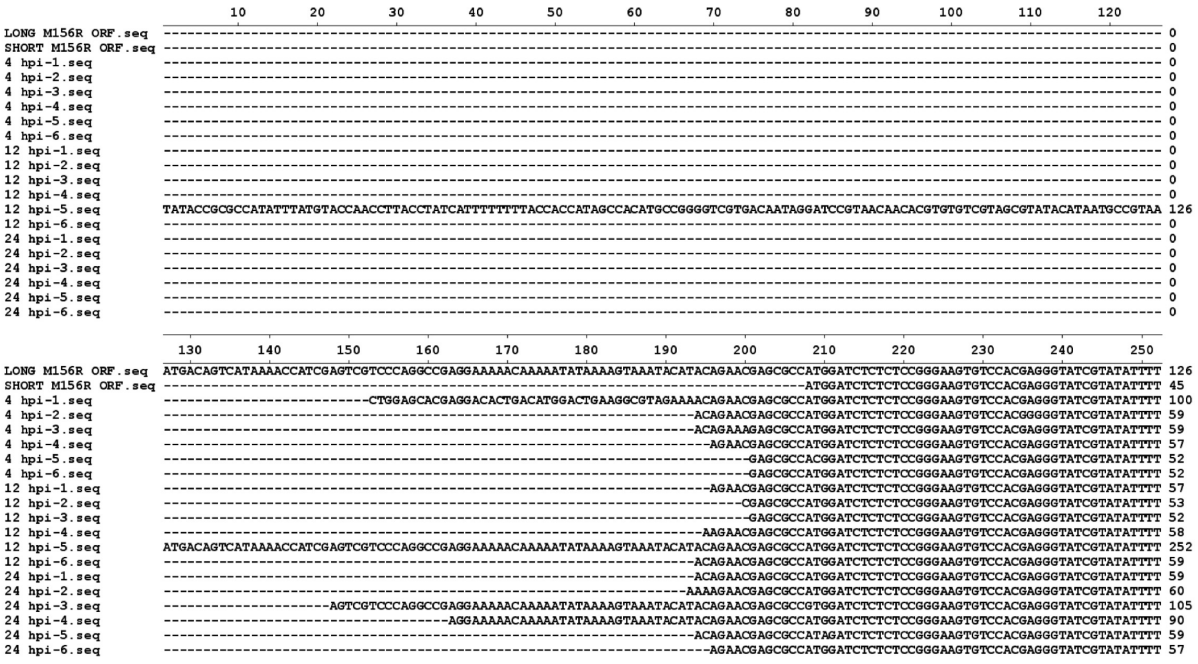

Figure 3.7 (S2) Sequence alignment of the 5' RACE PCR products

European rabbit RK13 cells were infected with MYXV-Lu and the total RNA was collected at indicated time points. The 5' RACE PCRs were performed and the PCR products were cloned and sequenced. The 5' ends of the predicted long (126 bp) and short (45 bp) forms of *M156R* were aligned with sequences of the 5' RACE PCR clones by the program MegAlign (DNASTAR).

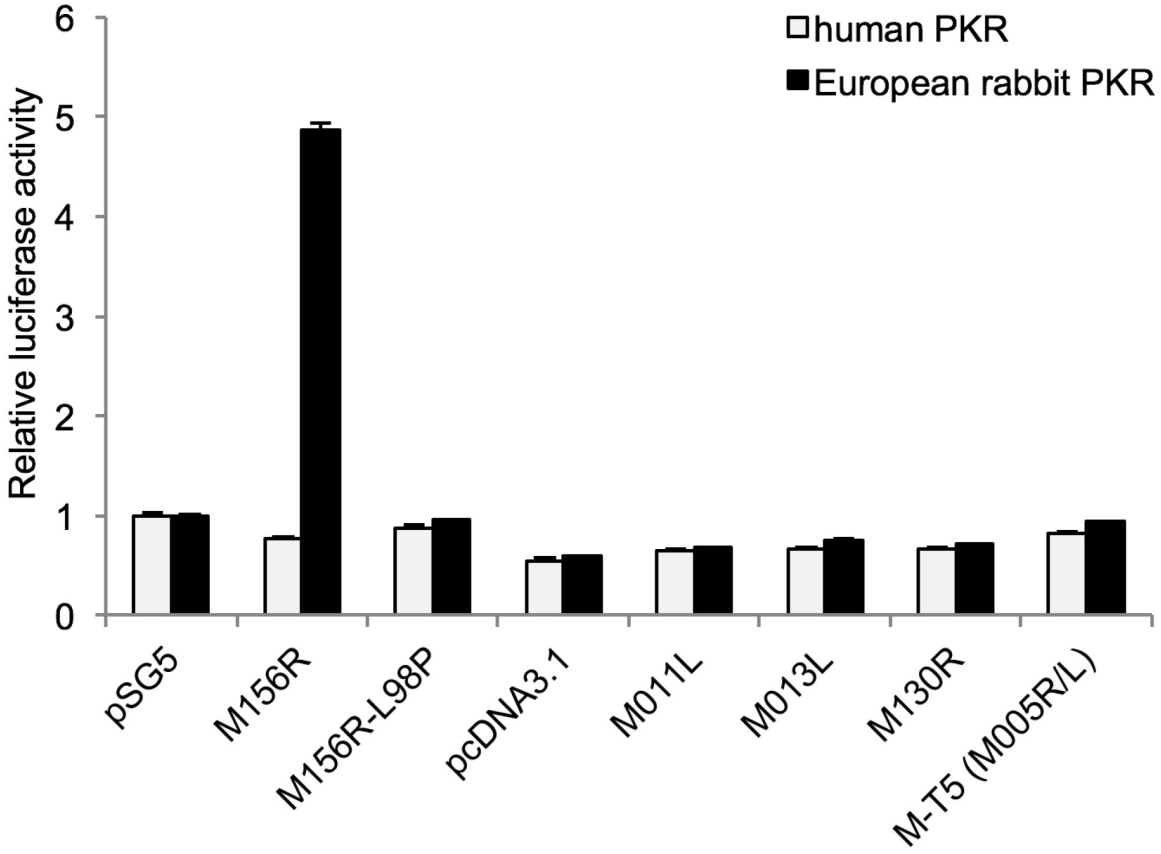

Figure 3.8 (S3) M156 but not M011, M013, M130 or MT-5 inhibits E. rabbit PKR

Human HeLa-PKR^{kd} cells were transfected with expression vectors for luciferase (0.05 μg), human, or E. rabbit PKR (0.2 μg) and myxoma virus M156, M156-L98P, M011, M013, M130 or MT-5 (0.4 μg each). pSG5 and pcDNA3.1 serve as empty vector controls. Luciferase light units were normalized to cells transfected only with PKR and pSG5 to obtain relative luciferase activities. Error bars indicate SD.

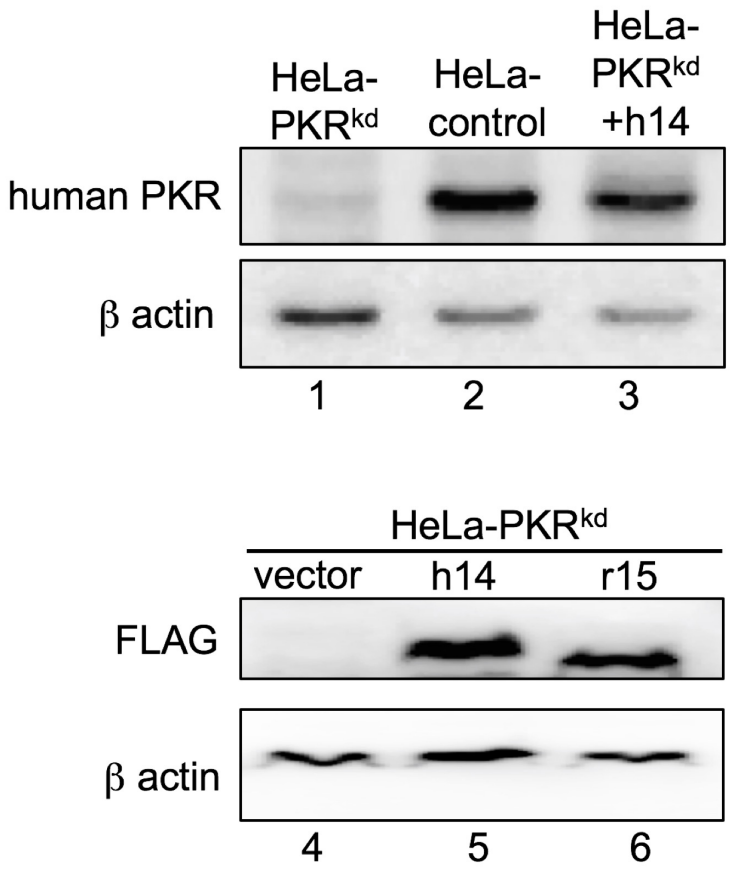

Figure 3.9 (S4) PKR expression in HeLa cells and derived cell lines

HeLa-PKRkd cells were stably transfected with vector, human (h) or E. rabbit (r) PKR under the control of the human PKR promoter. The human PKR-expressing clone h14 (lane 3) showed PKR expression comparable to that in HeLa control cells (lane 2) using an anti-human PKR antibody. Untransfected HeLa-PKR^{kd} cells are shown in lanes 1 and 4. Clone h14 was used to identify rabbit PKR-expressing clone r15, which showed comparable expression levels using an anti-FLAG tag antibody (lanes 5 and 6). After stripping, membranes were re-probed with anti-β-actin antibodies.

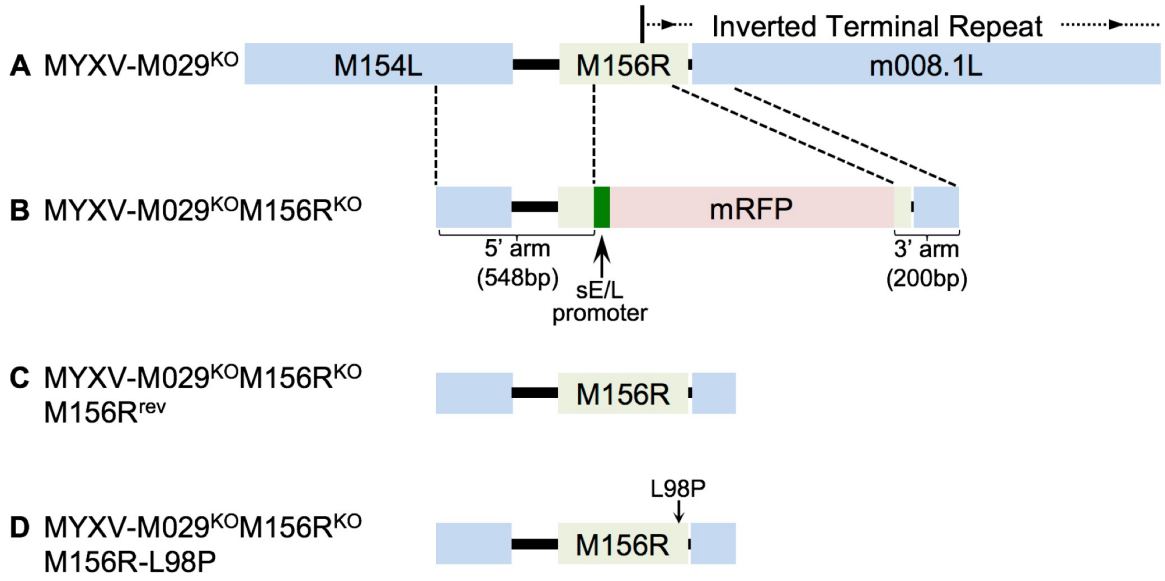

Figure 3.10 (S5) Construction of recombinant myxoma virus strains

The M156 coding sequence was partially replaced by a DNA cassette containing a monomeric red fluorescent protein (mRFP) encoding gene. The genomic region surrounding the M156R locus is shown in *A*. The region duplicated in the inverted terminal repeat is indicated. (*B*) The recombination plasmid to delete *M156R* contains a part of the *M154L* gene, the intergenic region between *M154L* and *M156R*, part of the *M156R* sequence, a poxvirus synthetic early/late (sE/L) promoter followed by the mRFP gene, followed by a part of the *M156R* sequence, the intergenic region between *M156R* and *M008.1L* and a part of *M008.1L*. To generate revertant *M156R*- (MYXV-M029L^{KO}/M156R^{KO}M156R^{rev}) and *M156R-L98P*- (MYXV-M029L^{KO}/M156R^{KO}M156R-L98P) containing strains, the constructs shown in *C* and *D*, respectively, were used.

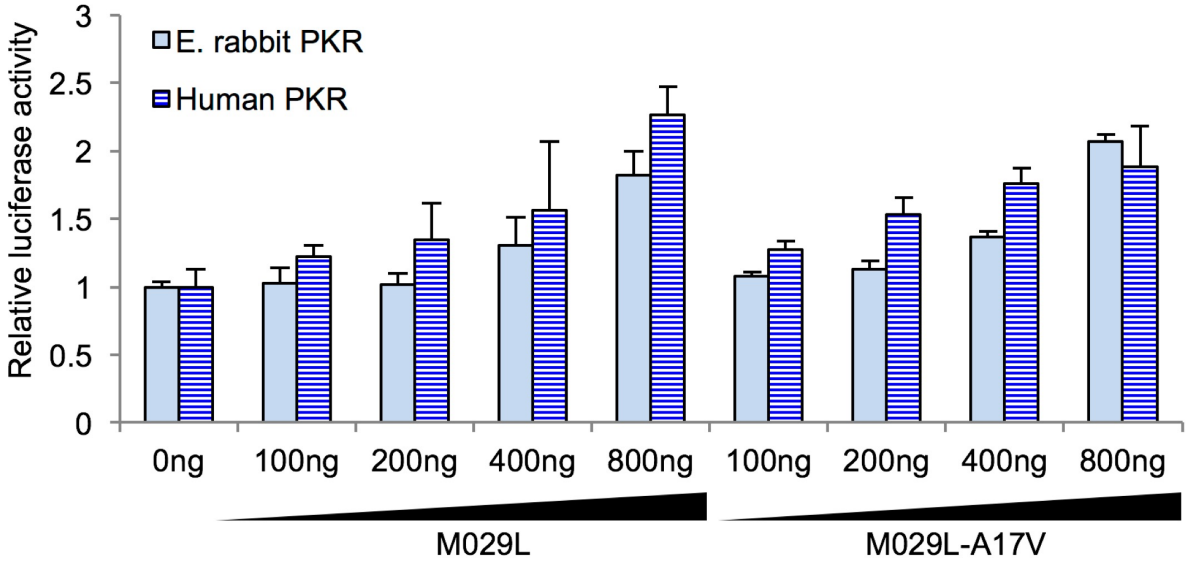

Figure 3.11 (S6) M029-A17V does not show altered PKR inhibition

Constant amounts of human or E. rabbit PKR (0.1 μg) and firefly luciferase (0.05 μg) were cotransfected with increasing amounts of *M029L* or *M029L-A17V*. Relative luciferase activities are shown. Experiments were performed in triplicate and the results are representative of three independent experiments. Error bars indicate SD.

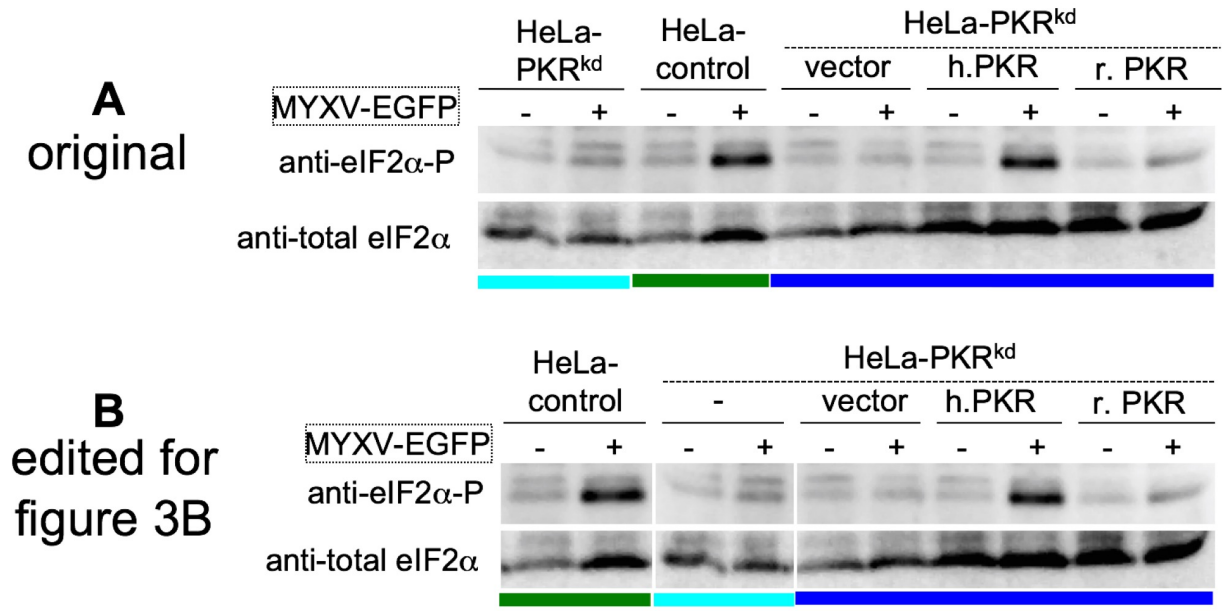

Figure 3.12 (S7) Original Western blot modified for Fig. 3B

(*A*) Original Western blots for phosphorylated and total eIF2α in total protein lysates collected from mock (-) or MYXV-EGFP (+) infected HeLa cells at 8 hpi. For clarity, the lanes that show eIF2α from HeLa-PKR^{kd} (light blue bar) and HeLa control cells (green bar) were switched to generate the figure shown in *B* and Fig. 3*B*.

References

1. Seet BT*, et al.* (2003) Poxviruses and immune evasion. *Annual Review of Immunology* 21:377-423.

2. Haller SL, Peng C, McFadden G, & Rothenburg S (2014) Poxviruses and the evolution of host range and virulence. *Infection, Genetics and Evolution* 21:15-40.

3. Werden SJ, Rahman MM, & McFadden G (2008) Poxvirus host range genes. *Advances in Virus Research* 71:135-171.

4. Bratke KA, McLysaght A, & Rothenburg S (2013) A survey of host range genes in poxvirus genomes. *Infection, Genetics and Evolution* 14:406-425.

5. Kerr PJ (2012) Myxomatosis in Australia and Europe: a model for emerging infectious diseases. *Antiviral Research* 93(3):387-415.

6. Kerr PJ*, et al.* (2012) Evolutionary history and attenuation of myxoma virus on two continents. *PLoS Pathogens* 8(10):e1002950.

7. Kerr PJ*, et al.* (2013) Genome scale evolution of myxoma virus reveals host-pathogen adaptation and rapid geographic spread. *Journal of Virology* 87(23):12900-12915.

8. Davies MV, Chang HW, Jacobs BL, & Kaufman RJ (1993) The E3L and K3L vaccinia virus gene products stimulate translation through inhibition of the double-stranded RNA-dependent protein kinase by different mechanisms. *Journal of Virology* 67(3):1688-1692.

9. Langland JO & Jacobs BL (2002) The role of the PKR-inhibitory genes, E3L and K3L, in determining vaccinia virus host range. *Virology* 299(1):133-141.

10. Rothenburg S, Seo EJ, Gibbs JS, Dever TE, & Dittmar K (2009) Rapid evolution of protein kinase PKR alters sensitivity to viral inhibitors. *Nature Structural and Molecular Biology* 16(1):63-70.

11. Elde NC, Child SJ, Geballe AP, & Malik HS (2009) Protein kinase R reveals an evolutionary model for defeating viral mimicry. *Nature* 457(7228):485-489.

12. Ramelot TA*, et al.* (2002) Myxoma virus immunomodulatory protein M156R is a structural mimic of eukaryotic translation initiation factor eIF2alpha. *Journal of Molecular Biology* 322(5):943-954.

13. Cameron C*, et al.* (1999) The complete DNA sequence of myxoma virus. *Virology* 264(2):298-318.

14. Willer DO, McFadden G, & Evans DH (1999) The complete genome sequence of shope (rabbit) fibroma virus. *Virology* 264(2):319-343.

15. Kerr PJ*, et al.* (2013) Comparative analysis of the complete genome sequence of the California MSW strain of myxoma virus reveals potential host adaptations. *Journal of Virology* 87(22):12080-12089.

16. Kawagishi-Kobayashi M, Silverman JB, Ung TL, & Dever TE (1997) Regulation of the protein kinase PKR by the vaccinia virus pseudosubstrate inhibitor K3L is dependent on residues conserved between the K3L protein and the PKR substrate eIF2alpha. *Molecular and Cellular Biology* 17(7):4146-4158.

17. Kawagishi-Kobayashi M, Cao C, Lu J, Ozato K, & Dever TE (2000) Pseudosubstrate inhibition of protein kinase PKR by swine pox virus C8L gene product. *Virology* 276(2):424-434.

18. Rothenburg S, Chinchar VG, & Dever TE (2011) Characterization of a ranavirus inhibitor of the antiviral protein kinase PKR. *BMC Microbiol* 11:56.

19. Kuhen KL & Samuel CE (1997) Isolation of the interferon-inducible RNA-dependent protein kinase Pkr promoter and identification of a novel DNA element within the 5'-flanking region of human and mouse Pkr genes. *Virology* 227(1):119-130.

20. Johnston JB*, et al.* (2003) Role of the serine-threonine kinase PAK-1 in myxoma virus replication. *Journal of Virology* 77(10):5877-5888.

21. Rahman MM, Liu J, Chan WM, Rothenburg S, & McFadden G (2013) Myxoma virus protein M029 is a dual function immunomodulator that inhibits PKR and also conscripts RHA/DHX9 to promote expanded host tropism and viral replication. *PLoS Pathogens* 9(7):e1003465.

22. Dar AC, Dever TE, & Sicheri F (2005) Higher-order substrate recognition of eIF2alpha by the RNA-dependent protein kinase PKR. *Cell* 122(6):887-900.

23. Dar AC & Sicheri F (2002) X-ray crystal structure and functional analysis of vaccinia virus K3L reveals molecular determinants for PKR subversion and substrate recognition. *Molecular Cell* 10(2):295-305.

24. Zhang P & Samuel CE (2007) Protein kinase PKR plays a stimulus- and virus-dependent role in apoptotic death and virus multiplication in human cells. *Journal of Virology* 81(15):8192-8200.

25. Dever TE*, et al.* (1992) Phosphorylation of initiation factor 2 alpha by protein kinase GCN2 mediates gene-specific translational control of GCN4 in yeast. *Cell* 68(3):585-596.

26. Brennan G, Kitzman JO, Rothenburg S, Shendure J, & Geballe AP (2014) Adaptive gene amplification as an intermediate step in the expansion of virus host range. *PLoS Pathogens* 10(3):e1004002.

27. Liu J*, et al.* (2012) Myxoma virus M064 is a novel member of the poxvirus C7L superfamily of host range factors that controls the kinetics of myxomatosis in European rabbits. *Journal of Virology* 86(9):5371-5375.

28. Mossman K*, et al.* (1996) Myxoma virus M-T7, a secreted homolog of the interferon-gamma receptor, is a critical virulence factor for the development of myxomatosis in European rabbits. *Virology* 215(1):17-30.

29. Barrett JW*, et al.* (2009) Myxoma virus M130R is a novel virulence factor required for lethal myxomatosis in rabbits. *Virus Research* 144(1-2):258-265.

Chapter 4 - Host species-specific inhibition of rabbit PKR by leporipoxvirus pseudosubstrate inhibitors

Abstract

The introduction of myxoma virus (MYXV) into European rabbits in Australia has provided us with one of the best documented examples to explore how a virus pathogen evolves to adapt to a new host species. Therefore, for years, the studies that characterize MYXV proteins and their interactions with the host immune systems have been using non-rabbit cell lines or cell lines directly derived from European rabbits (*Oryctolagus cuniculus*). However, the interactions between MYXV and its natural hosts American *Sylvilagus* rabbits have been largely ignored. *Oryctolagus* and *Sylvilagus* rabbits shared their last ancestor about 10 million years ago (30). Interestingly, infections of MYXV in *Sylvilagus* rabbits are completely non-lethal in adult animals, in contrast to the extremely high fatality rate caused by MYXV in European rabbits. The reason why a virus displays such a dramatic difference in virulence in two intermediately related species likely lies in how the immune responses of these two rabbit species differ during MYXV infection. In order to address a potential molecular explanation for the observed difference in virulence, we have compared the interactions of the host antiviral protein kinase R (PKR) from European rabbits and brush rabbits (*Sylvilagus bachmani*) with the MYXV PKR inhibitor M156R and its ortholog from rabbit fibroma virus R156R, a closely related leporipoxvirus. The transfection-based luciferase assay revealed that brush rabbit PKR is more sensitive to M156R inhibition than European rabbit PKR, that European rabbit PKR is completely resistant to R156R inhibition whereas brush rabbit PKR is highly sensitive. Additionally, NF-κB reporter assays indicate that this differential PKR sensitivity may contribute to variable expression of NF-κB-regulated pro-inflammatory cytokines, which may result in the high virulence of MYXV in European rabbits, but not in brush rabbits. We also identified the residues in European rabbit and brush rabbit PKR that are responsible for their sensitivity to

M156R and R156R inhibition. Our results indicate that PKR from European rabbits and brush rabbits exhibit distinctive sensitivities to MYXV M156R due to their different compositions at the helix αG region, and these differences may contribute to the difference of MYXV virulence observed in two different rabbit species.

Introduction

The biological control of European rabbits in Australia with MYXV is one of the best-documented examples for virus adaptation and evolution of virulence after a virus "jumps" into a new host species. The fast attenuation of MYXV and the concomitant selection of genetically somewhat resistant rabbits provides us with a classical demonstration of natural selection in both the virus and the host. MYXV belongs to the genus leporipoxvirus, which also includes rabbit fibroma virus, squirrel fibroma virus and hare fibroma virus (1). Leporipoxvirus members often display very narrow host range, infecting only leporids or squirrels (reviewed in (2) and (3)). In their natural hosts, leporipoxviruses usually cause benign and localized skin fibromas that are non-lethal (reviewed in (4)). For example, in the natural hosts of MYXV, the American tapeti or brush rabbits (*Sylvilagus* rabbits), the virus causes innocuous cutaneous fibromas that are usually restricted to the site of inoculation. The infection typically persists for several weeks but does not kill the host unless in very young rabbits (1). In contrast, in European rabbits (*Oryctolagus cuniculus*), MYXV causes a lethal systemic infection termed myxomatosis with a case fatality rate of close to 100% in naïve rabbits (5). This dramatic virulence difference of the same virus displayed in two intermediately related species provides a great model to explore the determinants for poxvirus virulence at the molecular level.

In nature, MYXV is predominantly passively transmitted by biting arthropods, in which the virus does not replicate. Therefore, successful transmission is dependent on the titer of virus propagated in the virus-induced fibromas (6). Highly attenuated virus strains fail to replicate to a high titer before being cleared by the host's immune system, while highly virulent strains often kill the host before efficient dissemination of the virus occurs, which prevents virus transmission to the next host (7). Hence in Australia, MYXV strains with moderate virulence often quickly

predominate the field after each release of the highly virulent strains, suggesting that MYXV evolved to attenuate in European rabbits to achieve optimal transmission.

There are two geographically distinct clades of MYXV. The South American MYXV clade includes strains that naturally infect American tapeti rabbits (*Sylvilagus brasiliensis*) localized in the South America. On the other hand, the Californian MYXV clade includes those that are (including the MSW strain and the MSD strain) found in North America, which naturally infect brush rabbits (*Sylvilagus bachmani*). The Californian MYXV strains are more virulent than the SLS and the Lausanne strains in European rabbits, exhibited by the ability of the virus to kill the rabbits before clinical symptoms of myxomatosis appear (8-10).

Rabbit fibroma virus (RFV, also known as Shope fibroma virus) is another member of the genus leporipoxvirus, which naturally infects Eastern cottontails (*Sylvilagus floridanus*) that are widely distributed throughout the USA (8, 11). In its natural host, RFV causes cutaneous fibroma that are restricted to the site of inoculation and the infection can last for months before being cleared completely by the host's immune system (12). Recovered rabbits are protected from reinfection (12). Interestingly, in contrast to the drastic virulence difference displayed by MYXV between its natural *Sylvilagus* rabbit hosts and European rabbits, RFV causes very similar, benign and transient tumors in Eastern cottontails and European rabbits without inducing any generalized infection like myxomatosis (reviewed in (13)). In fact, due to the heterologous protection provided by RFV for myxomatosis in European rabbits, the virus was used extensively as a vaccine strain in farmed and wild European rabbits in France before attenuated MYXV strains were introduced for vaccination (reviewed in (14)).

The genomes of Lu MYXV, MSW MYXV and RFV have been fully sequenced and published (10, 12, 15). The MSW MYXV is more closely related to Lu MYXV than to RFV, but

has an expanded genome size compared to the Lu strain (164kb compared to 161kb of MYXV-Lu), mainly due to the extension of the inverted terminal repeat region. This region contains mostly host range and virulence genes and is more variable than the central region of the genome. Truncated genes are also identified in MSW MYXV compared to those of Lu MYXV. This includes two genes: M008.1L/R and M152R, which are known to be major virulence factors previously characterized in European rabbits (16-18). The RFV genome, on the other hand, is smaller than both MYXV strains with only 159 kb. Compared to MYXV-Lu, a cluster of genes close to the end of the RFV genome are missing or are truncated in the RFV genome, such as M000.5L/R, M008.1L/R and M152R (19).

Both MSW MYXV and RFV contain a K3L/M156R ortholog, which are putative PKR inhibitors. Compared to MYXV-Lu M156R characterized in the previous chapter, both MSW M156R and RFV R156R lack the extended N-terminus, displaying 53% and 77% sequence identity at the protein level with the Lu M156R, respectively (16-18). Moreover, both MSW M156R and RFV R156R are duplicated in the inverted repeat region while the MYXV-Lu contains only one complete copy of this gene in its genome. However, it is worth noting that the 3' end of the M156R coding sequence is partly duplicated (109 bp) in the 5' ITR region in the MYXV-Lu (15). It is unclear, however, whether or not the copy number of M156R and R156R influences the virus virulence or host range.

This chapter aims to expand the analysis of PKR's interactions with pseudosubstrate inhibitors to other leporipoxviruses including RFV and MSW MYXV. We thoroughly explored the sensitivities of PKR from European rabbit and brush rabbit to selected leporipoxvirus K3L/M156R orthologs. In addition, we unveiled a potential connection between the activity of

PKR and NF-κB-regulated protein expression, which may contribute to the pathogenesis of myxomatosis in European rabbits.

Materials and Methods

Plasmids and cell lines

Cloning of European rabbit PKR and MYXV M156R was described in the previous chapter (Chapter 3). Brush rabbit PKR was cloned from total RNA collected from muscle and connective tissues of the paws of brush rabbits, which were kindly provided by the Riparin Brush Rabbit Recovery project. RFV R156R, MSW MYXV M156R were cloned into the pSG5 vector for expression in mammalian cells. The NF-κB reporter plasmid contains a firefly luciferase gene driven by six NF-κB binding sites followed by a minimal beta-globin promoter (28). The renilla luciferase vector was driven by an SV40 promoter. The PKR^{kd} HeLa cell line was generated by stably transfecting HeLa cells with shRNA and was kindly provided by Charles E. Samuel (Chapter 3). The European rabbit and brush rabbit triple-mutant PKR containing the swapped helix αG region were generated by site-directed mutagenesis PCR using the PfuUltra High-Fidelity DNA polymerase (Invitrogen). PCR was performed using pSG5-European rabbit PKR and pSG5-brush rabbit PKR as the templates with primers containing the designed mutations flanked by 15 nucleotides identical to the template up- and downstream of the mutation. All open reading frames were sequenced to confirm correct sequences.

HeLa-PKR^{kd} cells were cultured in DMEM medium supplemented with 5% FBS and 50μg/ml of gentamycin and were maintained at 37˚C with 5% CO_2.

Generation of hyperactive M156R

The hyperactive M156R was identified by transforming a European rabbit PKR expressing yeast strain with M156R-containg plasmids that were randomly mutagenized with a low-fidelity polymerase. The mutagenesis generated a library of approximately 85,000 clones

with a calculated mutation rate of 57%. 4,000 transformants containing the mutagenized M156R were picked and analyzed by transforming them into the yeast strain that has chromosomally integrated European rabbit PKR driven by a galactose-inducible promoter described in the previous chapter (Chapter 3). The transformants that showed better growth were selected through replica printing under inducing conditions. Plasmids from 50 yeast colonies were transformed into *E.coli* and sequenced after plasmid preparations. Mutants confirmed by sequencing were further re-transformed into yeast for confirmation of better PKR inhibition. Additionally, the mutations were introduced into pSG5-M156R to perform luciferase assays.

Luciferase assay and NF-kB activity assay

5 x10^4 HeLa-PKR^{kd} cells were seeded in 24-well plates one day before transfection. For each transfection firefly luciferase (pGL3promoter, 50 ng, Promega) and pSG5 plasmids encoding European rabbit or brush rabbit PKR (200 ng), M156R, R156R, MSW M156R, M156R-K48Q (400 ng) were transfected using GenJet-HeLa (SignaGen). For controls, empty pSG5 vector was transfected using the same amount. Each transfection was conducted in triplicate. For NF-κB activity assays, the plasmids encoding NF-κB-luc (50ng) and SV40-luc were co-transfected with the above mentioned PKR plasmids, M156 and a renilla luciferase driven by the TK promoter as internal controls. After 48 hours, cell lysates were harvested using mammalian lysis buffer (Goldbio) and luciferase activity was determined using luciferase detection reagents (Promega) in a luminometer (Berthold). Each experiment was performed at least three times independently and representative results are shown. Error bars represent the standard deviations of three replicate transfections.

Western blot analyses

Proteins were collected at the indicated time points using an NP-40 lysis buffer (50mM Tris, 150mM NaCl, 1% NP-40 and proteinase inhibitor cocktail, Roche). Protein concentrations were determined by the Bradford assay (BioRad). Protein samples were separated on 10% SDS-PAGE gels and transferred to PVDF membranes (GE Healthcare) using a methanol-based wet transfer apparatus (BioRad). Membranes were blocked with 5% non-fat milk in TBST buffer (20mM Tris, 150mM NaCl and 0.1% Tween-20 pH7.6) for 3 hours at 4°C and then incubated overnight with monoclonal anti-FLAG antibody at 4˚C with rocking, and then stripped and re-probed with antibody for β-actin (Sigma-Aldrich). After washing, membranes were incubated with goat-anti-rabbit or goat-anti-mouse secondary antibodies (1:30,000) in TBST containing 5% non-fat milk for 1 hour at room temperature with agitation followed by TBST washing 4 times for 20 minutes each. Proteins were detected with Proto-Glo ECL (National Diagnostics) and images were taken with a Kodak image system.

Results

M156R inhibits PKR from the natural host of MYXV with higher efficiency

Our previous results showed that MYXV M156R specifically inhibited European rabbit PKR but not PKR from non-rabbit mammals (Chapter 3). Considering that the natural hosts of MYXV are *Sylvilagus* rabbits, including the American tapeti and brush rabbits, we investigated if MYXV M156R shows differential inhibition of PKR from different rabbit species. We cloned and sequenced PKR from muscular tissues of three brush rabbits (*Sylvilagus bachmani riparius*). A sequence alignment revealed that European rabbit and brush rabbit PKR display 93% sequence identity at the protein level (Fig. 4.1). Discrepancies between the two PKRs are found throughout the protein sequence including the dsRNA binding domains, linker region and the kinase domain (Fig. 4.1). We next analyzed the PKR inhibitory activity of M156R on both brush rabbit and European rabbit PKR in the previously described cell culture-based luciferase assay. Human HeLa cells, in which endogenous PKR expression was stably knocked-down by shRNA, designated as HeLa-PKR^{kd} cells, were co-transfected with firefly luciferase, European or brush rabbit PKR and M156R or an empty vector as control. Luciferase activities were monitored 48 hours after transfection and normalized to that in PKR-only transfected cells (control) for better comparison. Consistent with the previous observation, co-transfection of Lu-M156R resulted in an increase of luciferase activity compared to European rabbit PKR-only transfected cells, indicating European rabbit PKR is sensitive to Lu-M156R inhibition (Fig. 4.2). Interestingly, we observed that co-transfection of brush rabbit PKR and Lu-M156R led to a statistically significant increase of luciferase activity compared to that caused by the co-transfection of European rabbit PKR and Lu-M156R (Fig. 4.2). This result showed that PKR from brush rabbit was more sensitive to M156R inhibition than European rabbit PKR. To investigate whether this difference

is specific to the inhibition by Lu-M156R, we also examined the sensitivity of both PKR to K3L, the M156R ortholog from VACV, whose natural host is unknown, but is known to be able to infect many different species including rabbits. K3L was able to inhibit PKR-mediated luciferase reduction in both European and brush rabbit PKR-transfected cells to comparable levels, suggesting both PKR are sensitive to K3L (Fig. 4.3). This result indicates that the difference in PKR sensitivity that we observed was specific to Lu-M156R. We also tested if the difference in PKR sensitivity was due to different levels of PKR expression between the two species by Western blot analyses and found that in HeLa-PKR^{kd} cells, Flag-tagged European rabbit PKR and brush rabbit PKR were expressed at comparable levels (Fig. 4.4).

To further confirm the differential sensitivity of PKR to M156R inhibition between European rabbit and brush rabbit PKR, we utilized a dual luciferase assay in which the firefly luciferase expression was driven by a full-length mouse ATF4 (Activating Transcription Factor 4) mRNA leader sequence (designated ATF4-luc fusion), while the renilla luciferase expression is controlled by a non-inducible TK promoter (20). In eukaryotic cells, translational up-regulation of ATF4 is induced as a result of eIF2α phosphorylation during ER (endoplasmic reticulum) stress. Therefore, in this assay, the firefly luciferase activity can be used to indirectly quantify eIF2α phosphorylation (20). Using this assay, we compared the ATF4-luc fusion expression when European rabbit PKR or brush rabbit PKR were co-transfected with K3L or Lu-M156R. As shown in Fig. 4.5, co-transfection of both K3L and Lu-M156R reduced ATF4-luciferase expression compared to PKR only-transfected cells, indicating alleviated eIF2α phosphorylation when PKR was co-transfected with viral inhibitors. Co-transfection of K3L diminished ATF4-luciferase expression in European rabbit or brush rabbit PKR-transfected cells to comparable levels, suggesting the two PKRs are comparably sensitive to K3L inhibition. In contrast, co-

transfection of M156R resulted in approximately 70% reduction of luciferase activity in European rabbit PKR-transfected cells, but led to an approximately 98% reduction of luciferase activity reduction in brush rabbit PKR-transfected cells. This indicates that MYXV M156R can relieve brush rabbit PKR-mediated eIF2α phosphorylation more efficiently than that mediated by European rabbit PKR. This result confirmed our previous observation in the single-luciferase assay that brush rabbit PKR was more sensitive to M156R inhibition than European rabbit PKR.

We also examined PKR inhibition by MYXV-MSW M156R (MSW-M156R) and found comparable inhibition of European PKR as mediated by MYXV-Lu M156R (Lu-M156R) (Fig. 4.6). Both Lu-M156R and MSW-M156R showed comparable capability in restoring PKR-mediated translational suppression in both European rabbit and brush rabbit PKR-transfected cells (Fig. 4.6). This results showed European rabbit PKR, as well as brush rabbit PKR, were inhibited by Lu-M156R and MSW-M156R comparably. Therefore, we kept using the Lu-M156R, designated M156R, in the next tests.

All these results confirmed that MYXV M156R inhibited PKR from the natural host of the virus with higher efficiency.

RFV R156R inhibits brush rabbit but not E. rabbit PKR

To further explore the species-specific PKR inhibition by leporipoxvirus pseudosubstrate inhibitors, we cloned and examined the PKR inhibitory ability of the RFV K3L/M156R orthologs, R156R, with European and brush rabbit PKR in the luciferase assay. Both R156R and M156R co-transfection with brush rabbit PKR resulted in increased luciferase activities, suggesting that brush rabbit PKR was inhibited by both M156R and R156R (Fig. 4.7). Surprisingly, the luciferase reduction mediated by European rabbit PKR was not alleviated by co-transfection of R156R, but only by co-transfection of M156R as observed previously (Fig. 4.7). In addition, the two K3L orthologs, M156R and R156R, were expressed at comparable levels in HeLa-PKR^{kd} cells as shown by Western blot analyses (Fig. 4.8), suggesting the observed difference between M156R and R156R was not due to different levels of protein expression. This indicates that RFV R156R inhibited only brush rabbit PKR but not European rabbit PKR.

The helix αG region is responsible for the differential sensitivity of rabbit PKR to M156R and R156R inhibition

We have discovered that European rabbit and brush rabbit PKR display differential sensitivities to leporipoxvirus pseudosubstrate inhibitors M156R and R156R. We next asked which amino acids of the two PKR molecules were responsible for these differences. Previous results from our lab suggested that single amino acid mutations of residues A488 and E451, which reside in the helix αG region on human and mouse PKR, respectively, altered their sensitivities to vaccinia virus (VACV) K3L inhibition (21). We thus sought to examine if the helix αG regions, which directly contact with eIF2α, as seen in the co-crystal structure of eIF2a with human PKR (29), of European rabbit PKR (amino acid residues 483-496) and brush rabbit PKR (amino acid residues 482-495) contribute to their sensitivities. Four residues are different between European and brush rabbit PKR in the helix αG region (Fig. 4.9 A). We swapped these four residues between European rabbit and brush rabbit PKR either as a group or individually and tested the mutants' sensitivities to M156R and R156R. The mutated European and brush rabbit PKR with completely swapped helix αG regions were as competent as their wild type counterparts in translational reduction of luciferase (Fig. 4.9 B), suggesting their ability to phosphorylate eIF2α was not jeopardized by the mutations. Importantly, compared to the wild-type European rabbit PKR, we observed that the mutant with the brush rabbit PKR helix αG region behaved comparably as brush rabbit PKR in terms of PKR sensitivity to M156R and R156R (Fig. 4.9 B). The brush rabbit PKR mutant containing helix αG residues from the European rabbit PKR, on the other hand, showed reduced sensitivity to M156R and was largely resistant to R156R inhibition (Fig. 4.9 B). These results suggest that the helix αG region of both rabbit PKR contribute to the observed differences in PKR sensitivity to M156R and R156R.

To determine if specific amino acid residues are important for these differences, we next swapped amino acids V485, A488, A492 and R496 in European rabbit PKR and their corresponding residues in brush rabbit PKR individually and examined their sensitivities to M156R and R156R. As summarized in Fig. 4.10, none of the single residue exchanges could completely replicate the phenotypic exchange observed with quadruple mutations of all four residues, but mutations of residues 485, 488 or 492 in European rabbit PKR and the corresponding residues in brush rabbit PKR partly altered their sensitivities. In contrast, mutations R496S in European rabbit PKR and S495R in brush rabbit PKR showed no phenotypic change compared to the wild type PKRs, indicating this residue may not be involved in the direct interaction of PKR with M156R or R156R (Fig. 4.10). We next performed triple amino acid mutations that exchanged residues 485/484, 488/487 and 492/491 between the two PKRs, and discovered that the swapping of these three residues could completely replicate the phenotypic exchange observed with quadruple mutations of both PKRs (Fig. 4.11 and 4.12).

In conclusion, our findings suggest that the helix αG region, especially the residues A485, V488 and A492 in European rabbit PKR and their corresponding residues in brush rabbit PKR, are mainly responsible for the differential sensitivity of rabbit PKR to inhibition by leporipoxvirus pseudosubstrate inhibitors.

Intermediate PKR inhibition induces strong NF-κB activity

NF-κB is a central regulator of both innate and adaptive immune responses against viral pathogens (reviewed in (22)). Overreaction of NF-κB regulated immune responses may lead to pathogenic effects due to aberrant accumulation of pro-inflammatory cytokines resulting in local and systemic inflammation (23). Acute inflammation is often observed in dermis, lymph nodes or skin lesions in myxoma-infected European rabbits (24). Therefore, the NF-κB-induced pro-inflammatory cytokines may contribute to the pathogenesis of myxomatosis in European rabbits. We examined the hypothesis that varied levels of PKR activation can influence NF-κB activity in transfected HeLa cells. To test this hypothesis, we used an NF-κB activity reporter, designated NF-κB-luc, in which a firefly luciferase coding cassette is driven by multiple NF-κB binding motifs. The firefly luciferase activity can thus be used as a proxy for NF-κB activity. We co-transfected HeLa-PKR^{kd} cells with plasmids encoding European or brush rabbit PKR, NF-κB-luc and M156R as well as a plasmid encoding for a TK promoter-driven renilla luciferase as internal controls. The internally controlled luciferase activities (firefly luciferase light units /renilla luciferase light units) were normalized to that of PKR-only transfected cells to obtain relative luciferase activity as shown in our results. We first observed that the co-transfection of M156R and European rabbit PKR resulted in an approximately 4.5-fold increase of luciferase activity compared to that of European rabbit PKR-only transfected cells (Fig. 4.13 A). In contrast, co-transfection of M156R with brush rabbit PKR failed to increase, but instead led to a slight decrease in luciferase activity (Fig. 4.13 A), indicating that NF-κB activity was not induced when brush rabbit PKR was fully inhibited by M156R, but only when PKR was moderately inhibited, demonstrated by the inhibition of European rabbit PKR by M156R. We next performed a control experiment where a similar dual-luciferase transfection was conducted in

which the NF-κB-luc was replaced by an SV40 promoter-driven firefly luciferase (SV40-luc). The luciferase activity restored by M156R co-transfection was slightly higher in brush rabbit PKR-transfected cells than European rabbit PKR-transfected cells but the difference was not statistically significant ($P>0.05$) (Fig. 4.13 B), indicating the difference we observed in the NF-κB reporter assay could be attributed to different levels of NF-κB activity. Overall, these results indicate that NF-κB activity in cells can be influenced by the extent of PKR inhibition by M156R, and that intermediate PKR inhibition stimulates higher level of NF-kB activation than that when PKR is not inhibited or completely inhibited.

We next tested if mutations on the helix αG region of European and brush rabbit PKR, which exchanged PKR sensitivities to M156R inhibition, could also alter NF-κB activity in transfected HeLa cells. For an easier comparison, we set the internally controlled firefly luciferase activity (as a readout of NF-κB activity) from cells co-transfected with European rabbit PKR and M156R as 100%. Similar to what we observed previously, co-transfection of M156R with brush rabbit PKR, caused reduced NF-kB activity compared to that with European rabbit PKR (~70% reduction) (Fig. 4.14). However, the mutation of European rabbit PKR with the helix αG region from brush rabbit PKR led to reduced NF-κB activity comparable to levels observed when brush rabbit PKR was co-transfected with M156R. Moreover, the NF-κB activity induced by co-transfection of the brush rabbit PKR mutant and M156R was augmented greatly when the helix αG from European rabbit PKR was introduced (Fig. 4.14). These observations confirm that the cellular NF-κB activity level rises only when PKR is moderately inhibited but not when completely inhibited by M156R.

We have concluded that M156R did not evolve to most efficiently to inhibit European rabbit PKR, causing an intermediate level of inhibition, which resulted in high NF-κB activation. Because of this we surmised that mutants of M156R might be identified who show stronger inhibition of European rabbit PKR. To identify such gain-of-function mutants, we screened a library of randomly mutated M156R for increased PKR inhibitory capabilities. We engineered a yeast strain that possesses chromosomally integrated European rabbit PKR (J986) and randomly mutagenized M156R by PCR with a low-fidelity polymerase. The J986 strain was then transformed with the mutagenized library and 4,000 clones were picked and analyzed in a yeast growth assay. Plasmids were isolated from clones that showed better growth than the wild type M156R transformant, amplified and re-transformed into the J986 strain for confirmation. Candidates were also subjected to the luciferase assay described in the previous section for confirmation, because this is more sensitive than the yeast growth assay, for confirmation. Four mutations (K48Q, E55V, N66D and Q69L) were identified that all exhibited more efficient PKR inhibition than the wild type M156R. Among them, M156R-K48Q significantly increased its inhibition of European rabbit PKR in the luciferase assay, but interestingly, this mutation did not influence the inhibition of brush rabbit PKR (Fig. 4.15 A). We also verified that the increased PKR inhibitory ability of M156R-K48Q was not due to over-expression of the protein by Western blot analysis (Fig. 4.15 B). These results show that M156R could be optimized to better inhibit European rabbit PKR and identified residue K48 as being important for its interaction with PKR.

We next examined if increased PKR inhibition by M156R-K48Q could alter the NF-κB activation mediated by PKR and found that co-transfection of European rabbit PKR with M156R-K48Q resulted in a 70% reduction of NF-κB activity compared to that in cells co-

transfected with European rabbit PKR and the wild type M156R (Fig. 4.16). This result confirms our hypothesis that the degree of PKR inhibition by M156R is directly correlated with NF-κB activation mediated by PKR.

All these results indicate that intermediate inhibition of European rabbit PKR by M156R led to higher NF-κB activity in transfected HeLa cells than the strong inhibition of brush rabbit PKR by M156R. This difference may constitute a molecular mechanism which explains the virulence difference of MYXV observed in European and brush rabbits.

Discussion

MYXV is a rabbit-specific pathogen that naturally infects *Sylvilagus* rabbit species. We previously showed that the MYXV PKR pseudosubstrate inhibitor M156R selectively inhibited only rabbit PKR, but not PKR from other mammalian species, which constitutes a molecular explanation for the restriction of MYXV infection to rabbits. The previous study was performed with PKR derived from European rabbits (*Oryctolagus cuniculus*), the most commonly used species for rabbit models in laboratories. European rabbits are intermediately related to American *Sylvilagus* rabbits, but they are not natural host of MYXV and have never naturally encountered MYXV in its evolutionary history before the very deliberate release of the virus in Australia and Europe in the 1950s. In research focused on virus-host interactions between MYXV and rabbits, European rabbits, but not brush rabbits are often used. In fact, the majority of research in the area of host-pathogen interactions with MYXV has been performed with New Zealand White rabbits, which is an European rabbit strain, with European rabbit-derived cells lines or cell lines derived from non-rabbit species.

Like all poxviruses, MYXV possesses a large arsenal of immunomodulatory genes, that evolved to specifically antagonize one or multiple pathways in the hosts' antiviral immune systems to facilitate viral replication (25). The immunomodulatory genes from MYXV all evolved in its natural host *Sylvilagus* rabbits, including tapeti rabbits and brush rabbits. The differential PKR sensitivity to M156R inhibition between European rabbit and brush rabbit demonstrated here, indicates that the host-virus interactions can be very distinct even between closely related species such as European rabbits and brush rabbits. Ideally, studies of host-virus interactions should be conducted in biologically relevant species, otherwise, the conclusions could be misleading or incomplete.

An even more dramatic example of species-specific PKR inhibition was revealed by the selective inhibition of brush rabbit PKR by the RFV K3L orthologs, R156R. RFV naturally infects Eastern cottontails (*Sylvilagus floridanus*), which are closely related to the brush rabbits (*Sylvilagus bachmani*). Unlike MYXV, which also evolved in *Sylvilagus* rabbits, RFV displays low virulence in European rabbits and provides heterologous protection in European rabbits for MYXV infection. R156R shows 77% sequence identity with M156R at the protein level, and could inhibit brush rabbit PKR as efficiently as M156R at various concentrations. However, R156R completely failed to inhibit European rabbit PKR. The inability of R156R to inhibit European rabbit PKR could contribute to the lower virulence of RFV in European rabbits compared to that of MYXV.

The helix αG region on PKR constitutes the principal binding sites for eIF2α, making it also the likely target of poxvirus K3L orthologs, which compete with eIF2α for PKR binding. A selection analysis covering PKR from twelve different rodent and rabbit species revealed that three out of the four residue positions that differ between European and brush rabbit PKR are also under strong positive selective pressure in rodent species (Sherry Haller, personal communication). Our experiments with PKR mutants demonstrate that the swapping of the three residues (V485, A488 and A492 in European rabbit PKR and the corresponding residues in brush rabbit PKR) can exchange their sensitivities to M156R and R156R, without compromising their catalytic activity. This suggests that the selective pressure placed on the helix αG region was partly due to interactions with viral pseudosubstrate inhibitors. Mutations that exchange the residue 496 and its corresponding residue on brush rabbit PKR, which is not under positive selective pressure, did not change PKR sensitivity to M156R or R156R.

PKR contributes to many different aspects of antiviral immune responses in vertebrates. In addition to its roles as both a virus sensor and an antiviral effector, PKR is also shown to contribute to the activation of NF-κB, a transcription factor that orchestrates pro-inflammatory responses in response to virus infection. It has been shown that catalytically active PKR is required for NF-κB induction during poxvirus infection (26). Under normal condition, NF-κB is sequestered in the cytoplasm by a family of NF-κB inhibitors called IκB. During virus infection, the expression of IκB and NF-κB are both inhibited due to PKR-mediated translational suppression. However, IκB degrades more rapidly than NF-κB due to its shorter half-life. As a result, free NF-κB can translocate to the nucleus and becomes active. Activation of NF-κB leads to induction of cytokines such as interleukin-1, interleukin-6 and tumor necrosis factor-α, which are collectively named pro-inflammatory cytokines, which promote inflammation (reviewed in (23)). Severe inflammatory responses, such as swellings of the ears, eyelids, scrotums and genital areas, are signature symptoms of myxomatosis in European rabbits (27). We thus speculate that the balance between PKR activation and inhibition may contribute to the pathogenesis of myxomatosis by regulating NF-κB activity. A possible explanation for the correlation between PKR activity and NF-κB activation is summarized in Fig. 4.17. When PKR is completely inhibited by viral inhibitors (scenario A), the NF-κB pathway is not activated because the continuous production of IκB is not prohibited. When PKR is not being inhibited, or PKR is completely resistant to viral inhibition (scenario B), the NF-κB pathway is readily activated, resulting in transcriptional upregulation of pro-inflammatory cytokines. However, due to the strong global translational suppression mediated by PKR, translation of the cytokine transcripts (or firefly luciferase assay in our assay) are prevented. When PKR is moderately inhibited (scenario C), the intermediate activity levels of PKR trigger activation of the NF-κB

pathway, which induces the transcription of pro-inflammatory cytokines. Meanwhile, the transcripts are able to be translated due to incomplete shut down of translation by the partially inhibited PKR. These scenarios correlate with the differential NF-κB activity we observed in our experimental settings and might contribute to the dramatic difference in pathology of MYXV infection in different rabbit species. However, it is worth noting that further experiments are required to directly monitor the levels of NF-κB-induced transcripts under all three scenarios and to perform infection experiments in rabbits to corroborate our hypothesis.

We discovered that NF-κB-regulated luciferase expression is tightly associated with the degree of PKR activity, and demonstrate that intermediate inhibition of European rabbit PKR could result in the elevated expression of NF-κB-inducible proteins compared to when PKR is completely inhibited such as with brush rabbit PKR by M156R. One possible explanation is that MYXV M156R evolved to optimally inhibit brush rabbit PKR, and by chance making it a less efficient inhibitor of European rabbit PKR.

Overall, our results suggest that viral immunomodulatory proteins that evolved in one host species may display different levels of immunomodulation in another host species, as exemplified by the inability of RFV R156R to inhibit European rabbit PKR, or the reduced inhibition of European rabbit PKR by MYXV M156R. However, such differences might have been overlooked in the past, because most MYXV immunomodulatory proteins are characterized in European rabbits, European rabbit-derived cells lines or even cells from non-rabbit mammals. We demonstrated here that it is important to study virus host range and virulence factors in biologically relevant species.

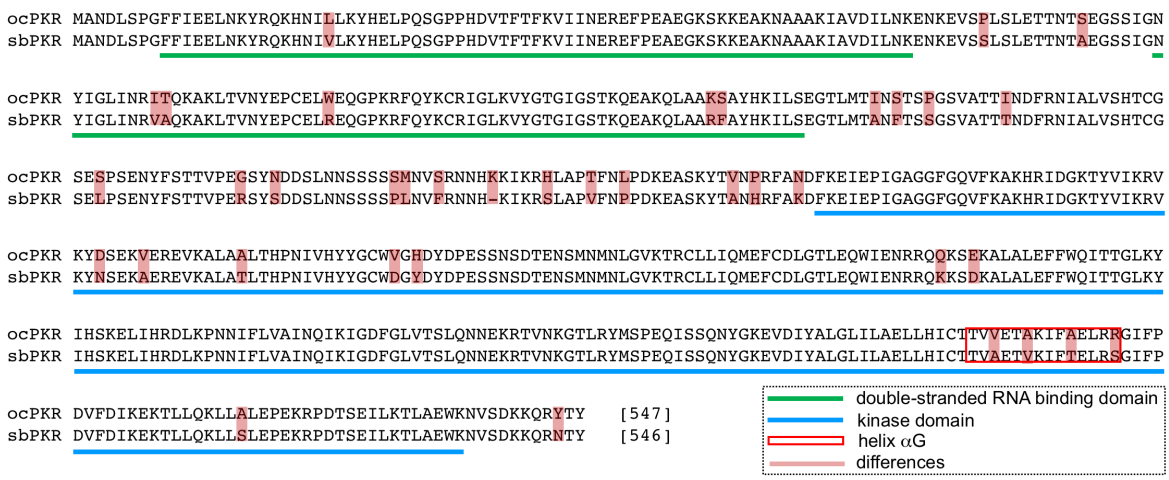

Figure 4.1 Comparison of PKR from different rabbit species

Sequences alignment was performed using the program MUSCLE (url: http://www.ebi.ac.uk/Tools/msa/muscle). Abbreviations: oc: *Oryctolagus cuniculus*, European rabbit; sb: *Sylvilagus bachmani*, brush rabbit.

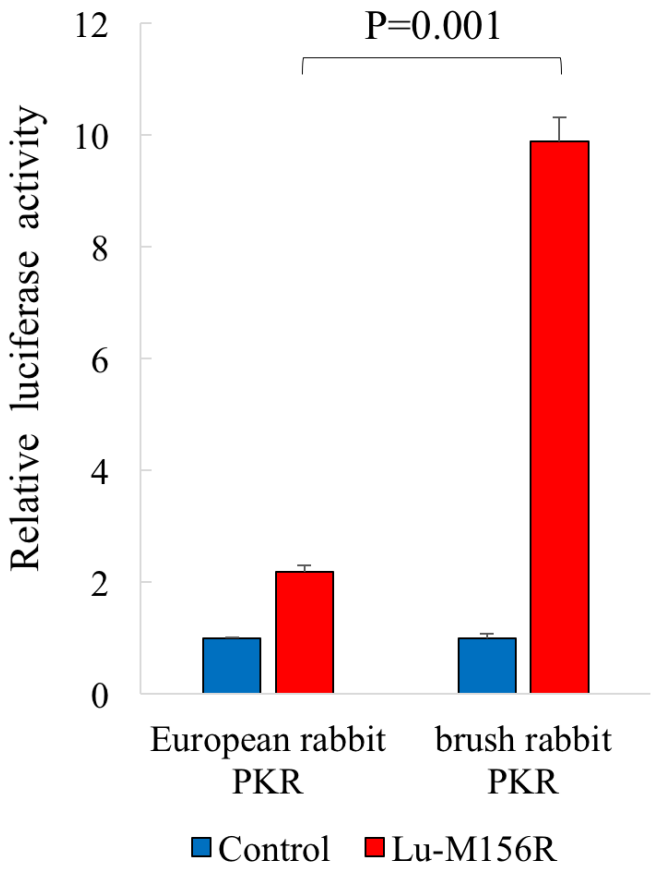

Figure 4.2 Inhibition of rabbit PKR by MYXV M156R

Human HeLa-PKR^{kd} cells were transfected with expression vectors for luciferase (0.05μg), MYXV Lu-M156R (0.4μg) and PKR (0.2μg) from the indicated species. Luciferase light units were normalized to PKR-only transfected cells to obtain relative luciferase activities. Experiments were performed in triplicate and the results are representative of three independent experiments. Error bars indicate standard deviations. P values were calculated by the Student's T-test.

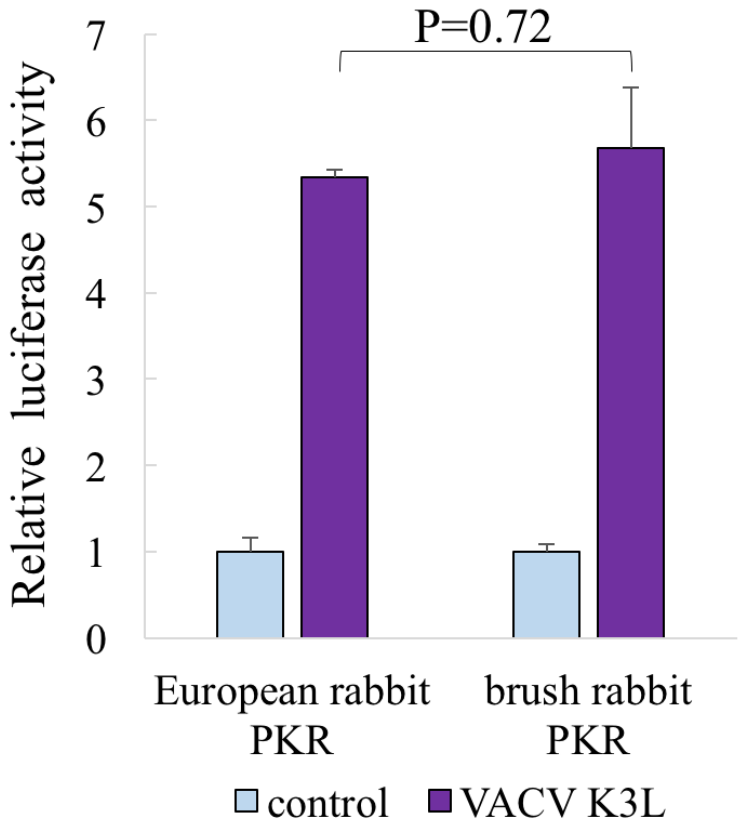

Figure 4.3 Inhibition of rabbit PKR by VACV K3L

Human HeLa-PKR^{kd} cells were transfected with expression vectors for luciferase (0.05μg), VACV K3L (0.4μg) and PKR (0.2μg) from the indicated species. Luciferase light units were normalized to PKR-only transfected cells to obtain relative luciferase activities. Experiments were performed in triplicate and the results are representative of three independent experiments. Error bars indicate standard deviations. P values were calculated by the Student's T-test.

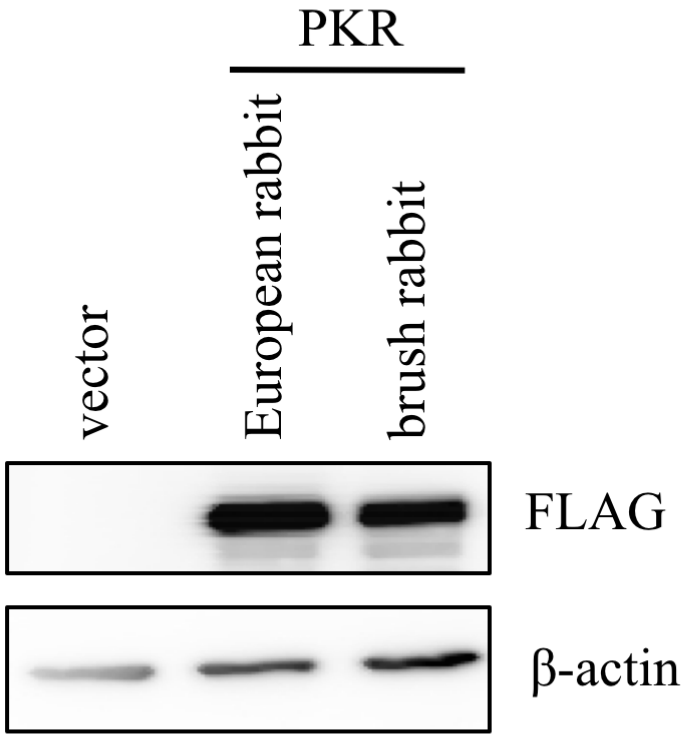

Figure 4.4 Expression of rabbit PKR in HeLa cells

HeLa-PKR^{kd} cells were transfected with 3μg of vector, FLAG-tagged European rabbit PKR or brush rabbit PKR plasmids. Total protein was collected 48 hours after transfection with 1%-SDS. All protein samples were separated by SDS-PAGE and subjected to Western blotting analyses. The membrane was first probed with an anti-FLAG antibody, then consecutively stripped and re-probed for β-actin (loading control).

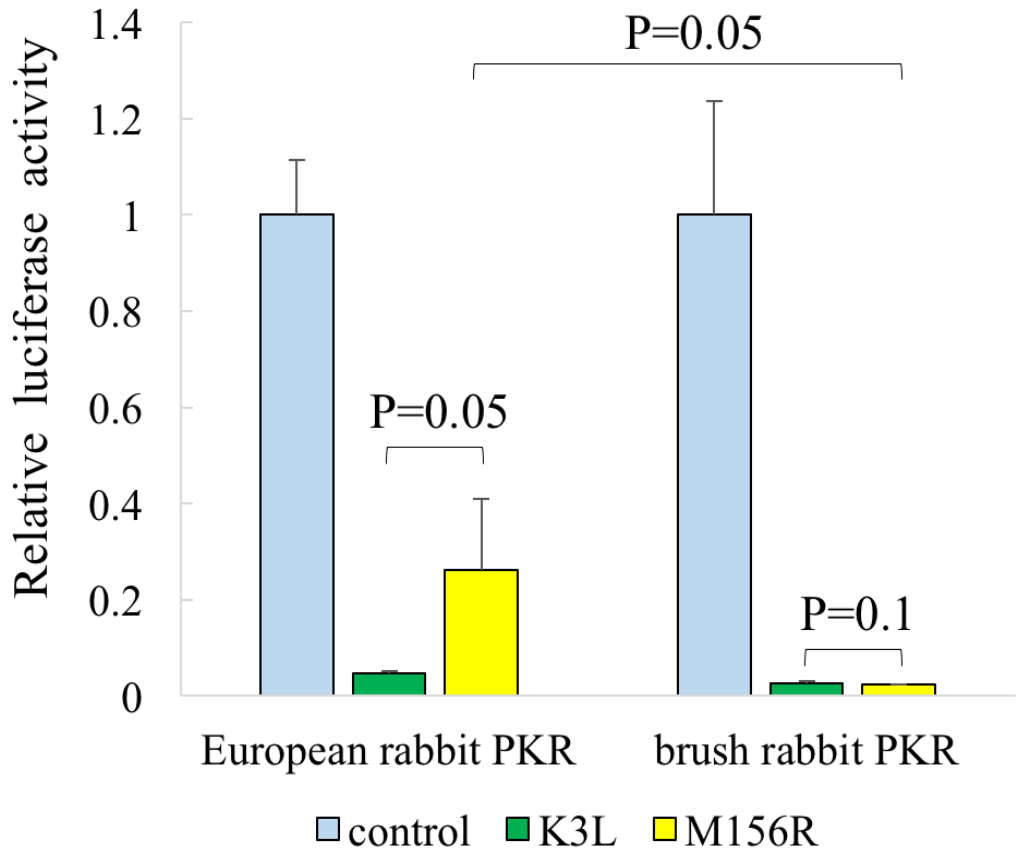

Figure 4.5 Quantification of eIF2α phosphorylation in PKR-transfected HeLa cells

HeLa-PKR^{kd} cells were transfected with expression vectors for ATF4-firefly luciferase (0.05µg) which contains the mouse ATF4 mRNA-5'UTR sequence (20), TK-renilla luciferase (0.05µg) driven by the TK promoter, VACV K3L (0.4µg), MYXV M156R (0.4µg), European rabbit PKR (0.2µg) or brush rabbit PKR (0.2µg). Luciferase activities were measured after 48 hours and was internally controlled by normalizing light units produced by firefly luciferase to that produced by renilla luciferase. Values obtained were then further normalized to PKR-only transfected cells to calculate relative luciferase activity. Error bars indicate standard deviation. P values were calculated by the Student's T-test.

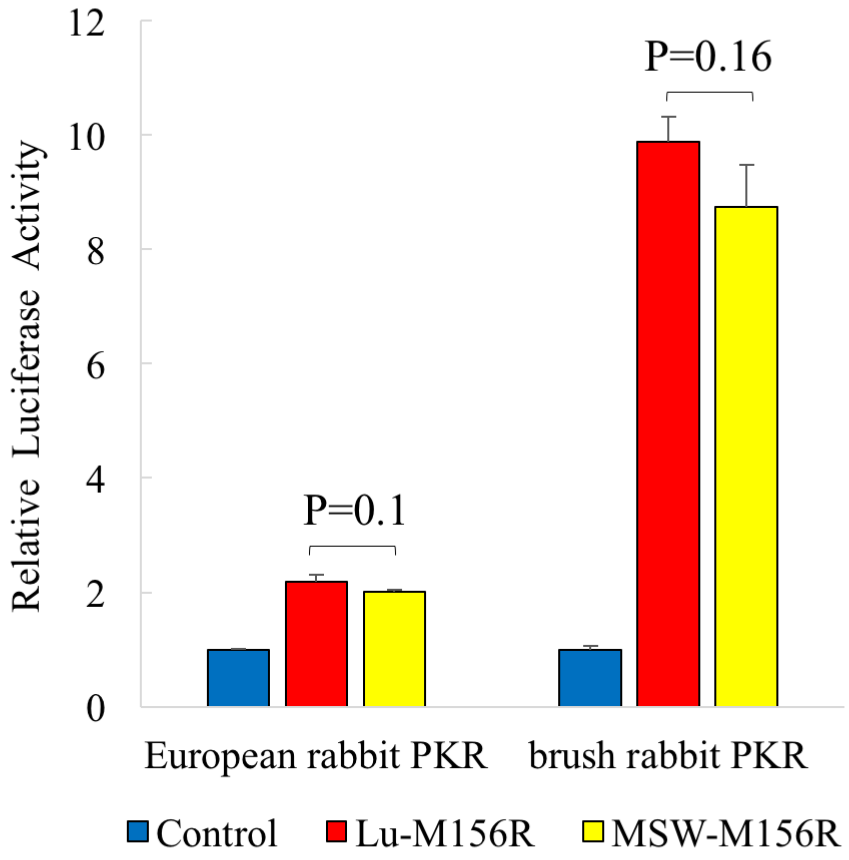

Figure 4.6 Inhibition of rabbit PKR by M156R from two different MYXV strains

Human HeLa-PKR^{kd} cells were transfected with expression vectors for firefly luciferase (0.05μg), MYXV Lu-M156R (0.4μg) or MSW-M156R and PKR (0.2μg) from the indicated species. Luciferase light units were normalized to PKR-only transfected cells to obtain relative luciferase activities. Experiments were performed in triplicate and the results are representative of three independent experiments. Error bars indicate standard deviations. P values were calculated by the Student's T-test.

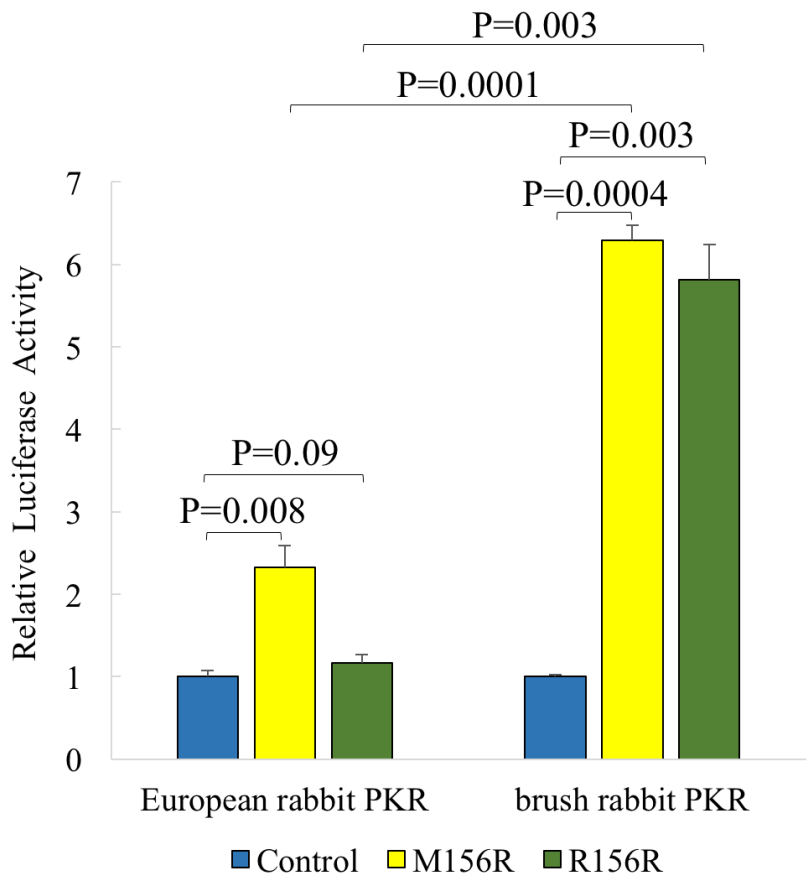

Figure 4.7 Inhibition of rabbit PKR by M156R and R156R

Human HeLa-PKR^{kd} cells were transfected with expression vectors for firefly luciferase (0.05µg), Lu-MYXV M156R or RFV R156R (0.4µg) as well as PKR (0.2µg) from the indicated species. Luciferase light units were normalized to PKR-only transfected cells to obtain relative luciferase activities. Experiments were performed in triplicate and the results are representative of three independent experiments. Error bars indicate standard deviations and P values were calculated by the Student's T-test.

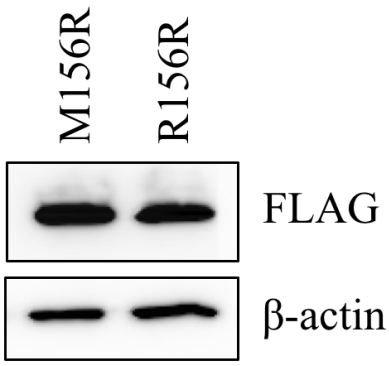

Figure 4.8 Expression of M156R and R156R in HeLa cells

HeLa-PKR^{kd} cells were transfected with 3μg of M156R or R156R encoding plasmids. Total proteins was collected 48 hours after transfection with 1%-SDS. All protein samples were separated on SDS-PAGE and subjected to Western blotting analyses. The membrane was first probed with an anti-FLAG antibody, then consecutively stripped and probed for β-actin (loading control).

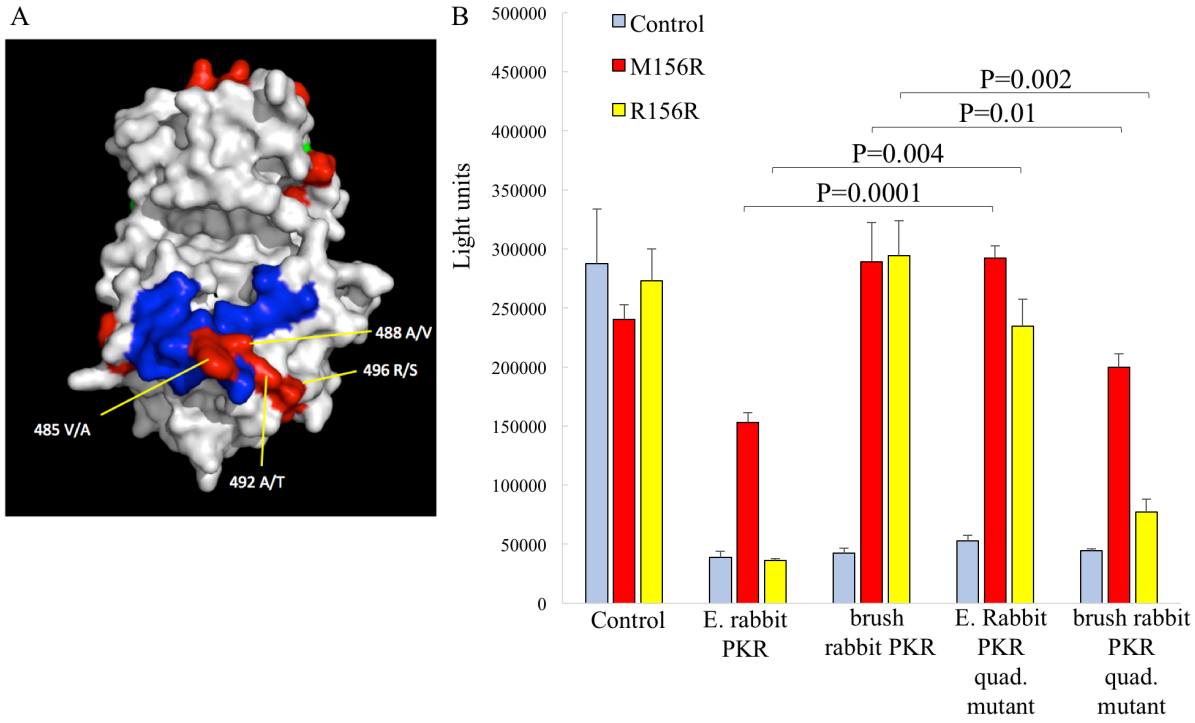

Figure 4.9 Quadruple mutation in the helix αG region altered PKR sensitivity to MYXV M156R and R156R

(A) The kinase domain of human PKR. The corresponding residues in European and brush rabbit PKRs are labeled according to European rabbit PKR. Blue: residues directly contact eIF2α. Red: residues that are different between European rabbit and brush rabbit PKR. The four residues that differ between European and brush rabbit PKR in the helix αG region are labeled with yellow lines. (B)Human HeLa-PKR^{kd} cells were transfected with expression vectors for firefly luciferase (0.05μg), MYXV M156R or RFV R156R (0.4μg), and PKR or PKR mutants (0.2μg) from the indicated species. Experiments were performed in triplicate and the results are representative of three independent experiments. Error bars indicate standard deviations.

Residue(s) exchanged	-		485		488		492		496		485 488 492		485 488 492 496	
on PKR	**E.**	**b.**	**E.**	**b.**	**E.**	**b.**	**E.**	**b.**	**E.**	**b.**	**E.**	**b.**	**E.**	**b.**
Sensitivity to M156	++	++ ++	++ +	++ +	++ +	++ ++	++ +	++ +	++	++ ++	++ ++	++ +	++ ++	++ +
Sensitivity to R156	-	++ ++	+	++ +	+	++ ++	-	++ ++	-	++ ++	++ ++	-	++ ++	-

-: resistant to M156 or R156

++++: sensitive to M1565 or R156.

The degree of sensitivity is indicated by the number of "+" with "++++" being the most sensitive and "+" being the least sensitive. Different numbers of "+" are coded with different colors.

Figure 4.10 Effects of the single mutations in the helix αG region on PKR sensitivity to M156R and R156R

Single amino-acid mutations in the helix αG region of European or brush rabbit PKR were tested in the luciferase assay described previously and the results are summarized here. Amino acid residues are numbered according to their positions in European rabbit PKR.

Abbreviations: E=European rabbit, b=brush rabbit.

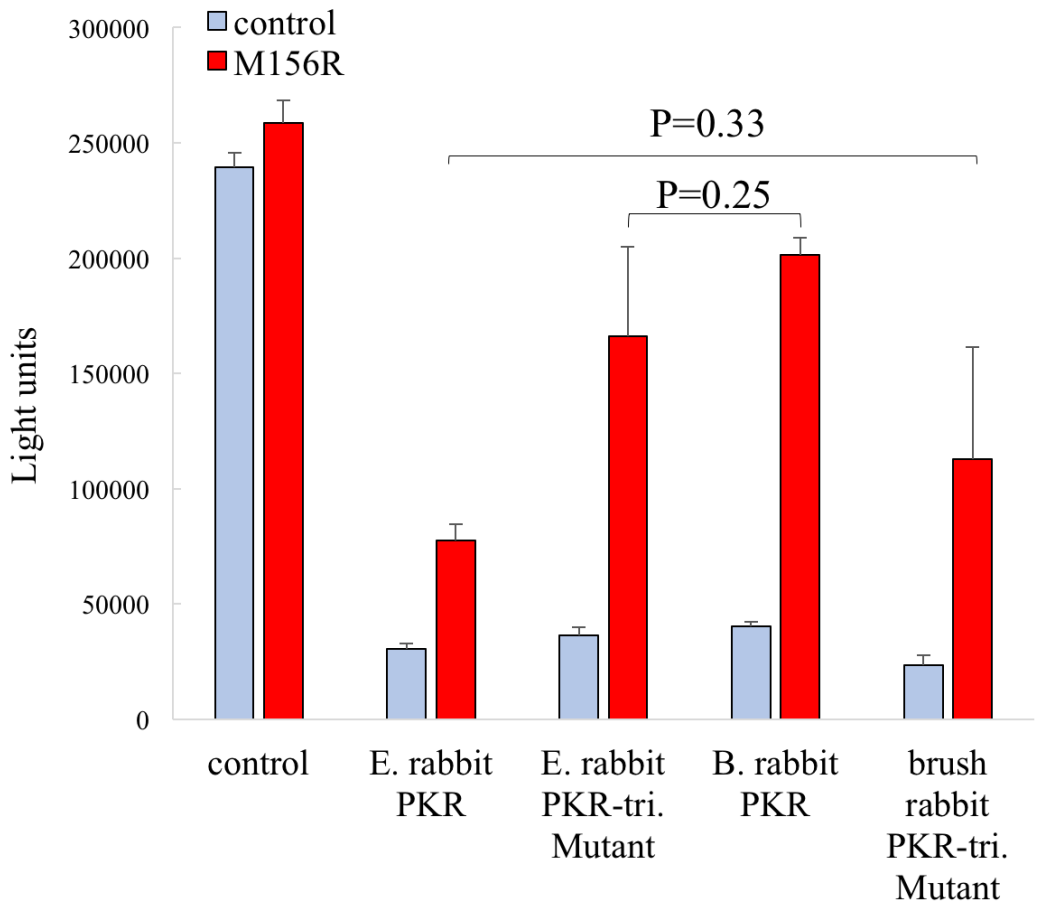

Figure 4.11 Triple mutations in the helix αG region altered PKR sensitivity to M156R inhibition

Human HeLa-PKR^{kd} cells were transfected with expression vectors for firefly luciferase (0.05μg), MYXV M156R as well as PKR and PKR mutants (0.2μg) from the indicated species. Luciferase light units were normalized to PKR-only transfected cells to obtain relative luciferase activities. Experiments were performed in triplicate and the results are representative of three independent experiments. Error bars indicate standard deviations.

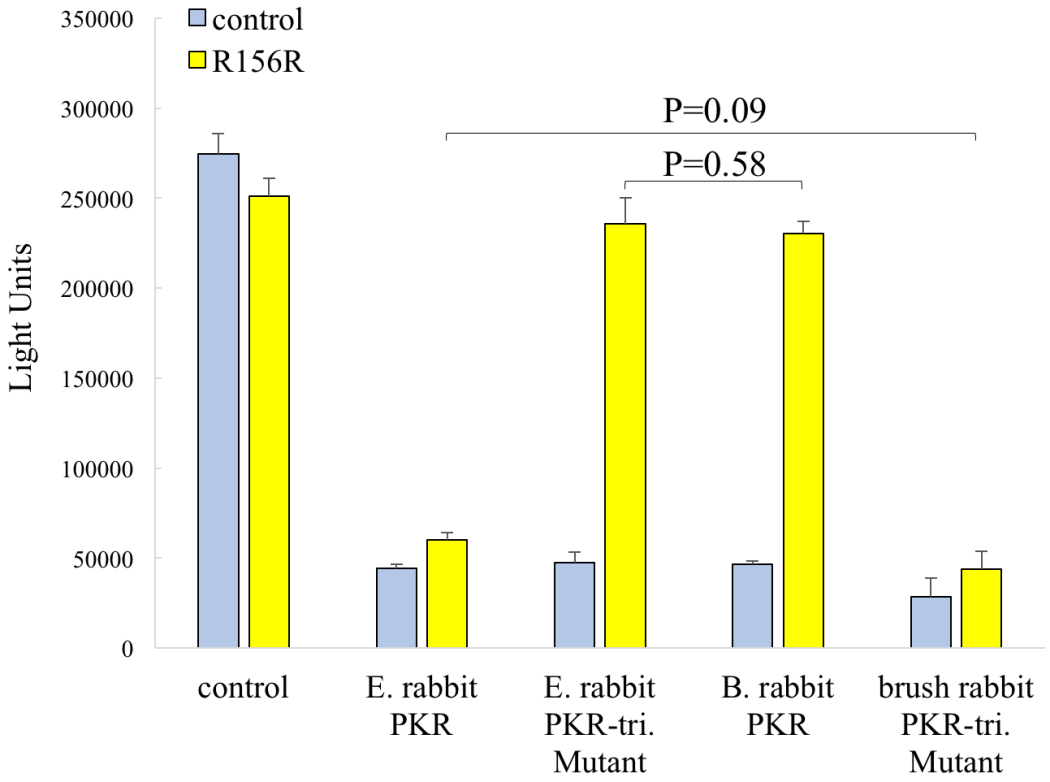

Figure 4.12 Triple mutations in the helix αG region altered PKR sensitivity to R156R inhibition

Human HeLa-PKR^{kd} cells were transfected with expression vectors for firefly luciferase (0.05μg), RFV R156R as well as PKR and PKR mutants (0.2μg) from the indicated species. Luciferase light units were normalized to PKR-only transfected cells to obtain relative luciferase activities. Experiments were performed in triplicate and the results are representative of three independent experiments. Error bars indicate standard deviations.

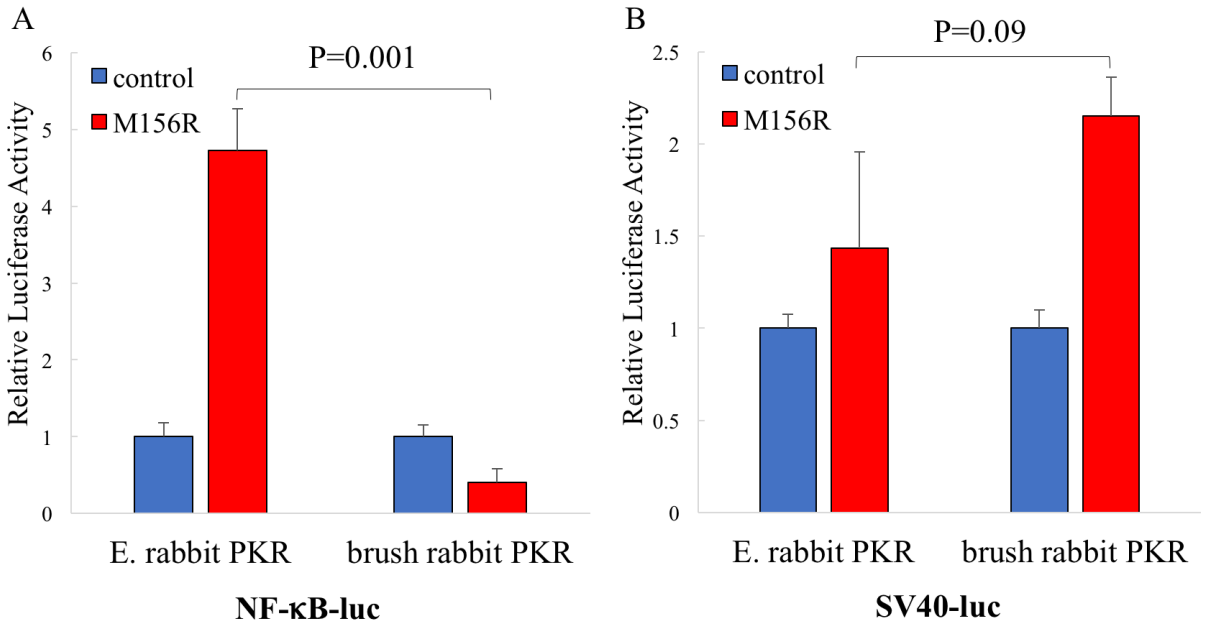

Figure 4.13 Moderate inhibition of PKR resulted in NF-κB activation

HeLa-PKR^{kd} cells were transfected with TK-renilla luciferase (0.05µg), NF-κB-luc (0.05µg) (A) or SV40-luc (0.05µg) (B), MYXV M156R (0.4µg) and PKR (0.2µg) plasmids from indicated rabbit species. Light units for firefly and renilla luciferase were measured with the Dual-glo detection kit (Promega) 48 hours after transfection. Results from the firefly luciferase were normalized to renilla luciferase results in the same well to obtain internally controlled luciferase activity. The values were further normalized to PKR-only transfected cells to obtain relative luciferase activities. Error bars indicate standard deviation. P values were calculated by the Student's T-test.

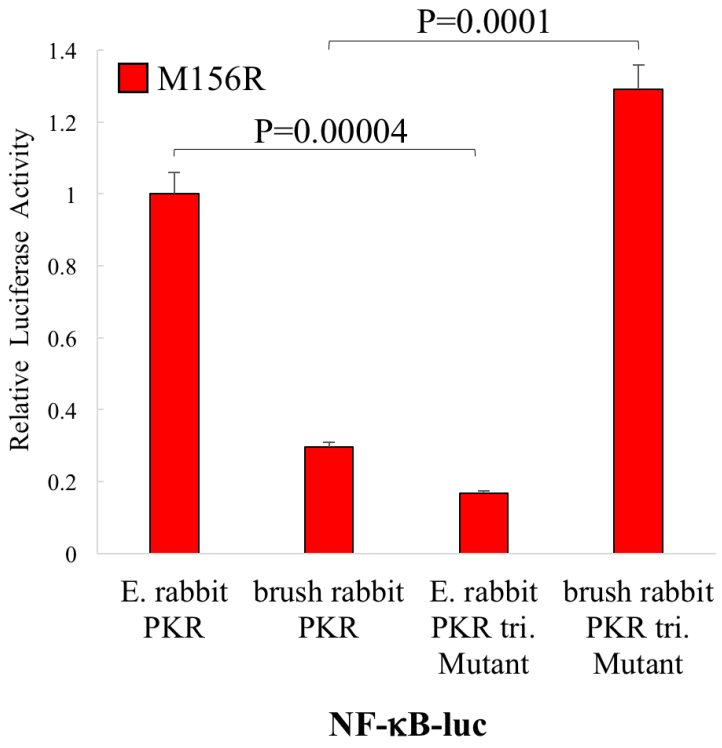

Figure 4.14 Intermediate PKR sensitivity to M156R resulted in NF-κB activation

HeLa-PKRkd cells were transfected with TK-renilla luciferase (0.05μg), NF-κB-luc (0.05μg), MYXV M156R (0.4μg) as well as European rabbit PKR, brush rabbit PKR and their mutants indicated in the figure (0.2μg). Light units for firefly and renilla luciferase were measured with the Dual-glo detection kit (Promega) 48 hours after transfection. Results from the firefly luciferase were normalized to results from the renilla luciferase in the same well to obtain internally controlled luciferase activity. The values were further normalized to PKR-only transfected cells to obtain relative luciferase activities. Error bars indicate standard deviation. P values were calculated by the Student's T-test.

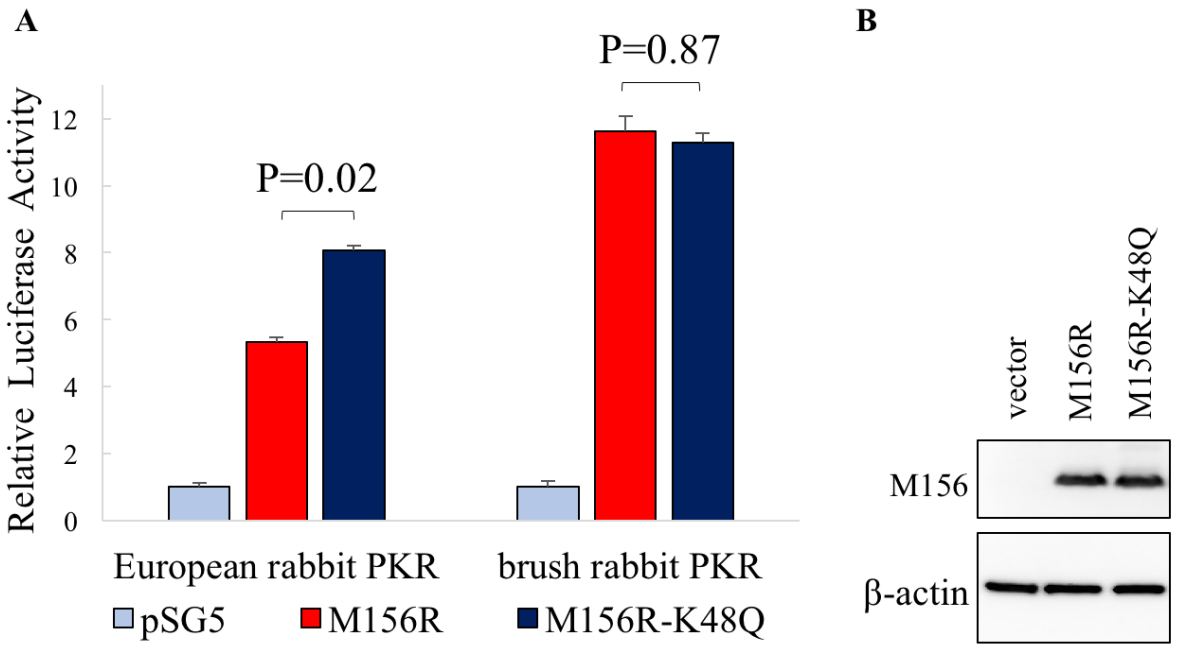

Figure 4.15 M156R-K48Q is a hyperactive inhibitor of European rabbit PKR

(A) Human HeLa-PKR^{kd} cells were transfected with expression vectors for firefly luciferase (0.05µg), MYXV M156R or M156R-K48Q (0.4µg) as well as PKR (0.2µg) from the indicated species. Luciferase light units were normalized to PKR-only transfected cells to obtain relative luciferase activities. Experiments were performed in triplicate and the results are representative of three independent experiments. Error bars indicate standard deviations. P values were calculated with the Student's T-test. (B) HeLa-PKR^{kd} cells were transfected with 3µg of vector, M156R or M156R-K48Q plasmids. Total protein was collected 48 hours after transfection and separated by SDS-PAGE for Western blotting analysis. The membrane was first probed with anti-M156 antiserum and then stripped and reprobed with anti-β-actin antibody (loading control)

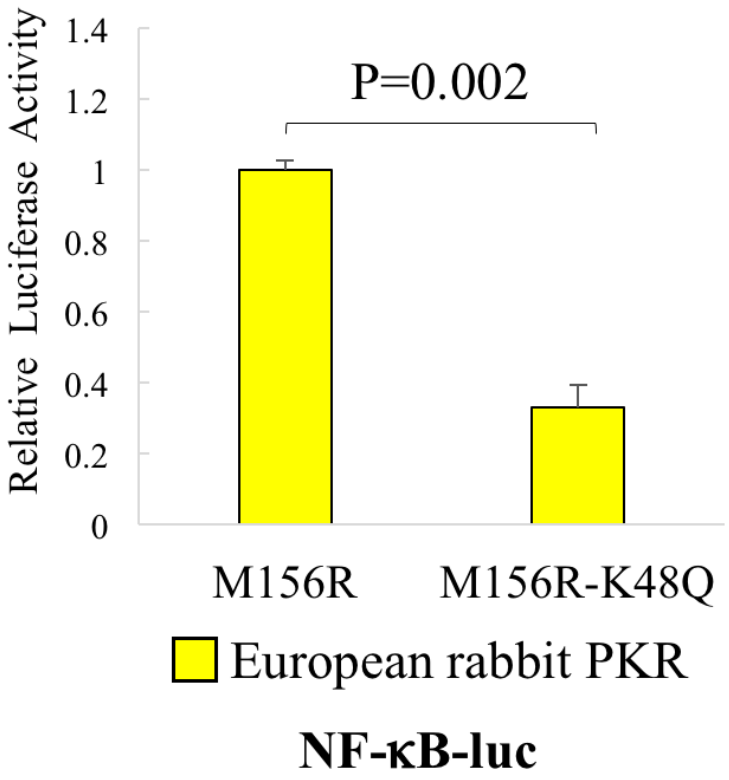

Figure 4.16 Enhanced inhibition of European rabbit PKR resulted in reduced

HeLa-PKR^{kd} cells were transfected with TK-renilla luciferase (0.05µg), NF-κB-luc (0.05µg), MYXV M156R or M156R-K48Q (0.4µg) as well as European rabbit PKR (0.2µg). Light units for firefly and renilla luciferase were measured with the Dual-glo detection kit (Promega) 48 hours after transfection. Results from the firefly luciferase were normalized to renilla luciferase results in the same well to obtain internally controlled luciferase activity. The values were further normalized to PKR-only transfected cells to obtain relative luciferase activities. Error bars indicate standard deviation. P values were calculated by the Student's T-test.

Situations	PKR inhibition	NF-κB activation	Pro-Inflammatory cytokine transcription	Pro-Inflammatory cytokine translation
A	Complete inhibition	-	-	-
B	No inhibition	+++	+++	-
C	Intermediate inhibition	++	++	+

Figure 4.17 Hypothetical correlation between PKR activity and the expression of NF-κB-regulated pro-inflammatory cytokines

References

1. Kerr PJ, Liu J, Cattadori I, Ghedin E, Read AF (2015) Myxoma Virus and the Leporipoxviruses: An Evolutionary Paradigm. *Viruses* 7(3): 1020-1061.

2. Barrett JW, McFadden G (2007) Genus Leporipoxvirus. *Poxviruses*, Birkhäuser *Advances in Infectious Diseases*. pp 183–201.

3. Stanford MM, Werden SJ, McFadden G (2007) Myxoma virus in the European rabbit: interactions between the virus and its susceptible host. *Veterinary Research* 38(2):299–318.

4. Haller SL, Peng C, McFadden G, Rothenburg S (2014) Poxviruses and the evolution of host range and virulence. *Infection, Genetics and Evolution* 21:15–40.

5. Fenner F, Ratcliffe FN (1965) Myxomatosis. *Myxomatosis*.

6. Fenner F, Fantini B (1999) Biological control of vertebrate pests: the history of myxomatosis, an experiment in evolution. CABI Publishing.

7. Kerr PJ, Merchant JC, Silvers L, Hood GM, Robinson AJ (2003) Monitoring the spread of myxoma virus in rabbit (*Oryctolagus cuniculus*) populations on the southern tablelands of New South Wales, Australia. II. Selection of a strain of virus for release. *Journal of Hygiene* 130(01):123–133.

8. Silvers L, et al. (2006) Virulence and pathogenesis of the MSW and MSD strains of Californian myxoma virus in European rabbits with genetic resistance to myxomatosis compared to rabbits with no genetic resistance. *Virology* 348(1):72–83.

9. Labudovic A, Perkins H, van Leeuwen B, Kerr P (2004) Sequence mapping of the Californian MSW strain of Myxoma virus. *Archive of Virology* 149(3):553–570.

10. Kerr PJ, et al. (2013) Comparative analysis of the complete genome sequence of the California MSW strain of myxoma virus reveals potential host adaptations. *Journal of Virology* 87(22):12080–12089.

11. McFadden G (1988) Poxviruses of Rabbits. *Virus Diseases in Laboratory and Captive Animals* pp 37–62.

12. Willer DO, McFadden G, Evans DH (1999) The complete genome sequence of shope (rabbit) fibroma virus. *Virology* 264(2):319–343.

13. Kerr PJ, Donnelly TM (2013) Viral Infections of Rabbits. *Veterinary Clinics of North America: Exotic Animal Practice* 16(2):437–468.

14. Spiesschaert B, McFadden G, Hermans K, Nauwynck H, Van de Walle GR (2011) The current status and future directions of myxoma virus, a master in immune evasion. *Vet Res* 42(1):76.

15. Cameron C, et al. (1999) The complete DNA sequence of myxoma virus. *Virology* 264(2):298–318.

16. Macen JL, Upton C, Nation N, McFadden G (1993) SERP1, a Serine Proteinase Inhibitor Encoded by Myxoma Virus, Is a Secreted Glycoprotein That Interferes with Inflammation. *Virology* 195(2):348–363.

17. Upton C, Macen JL, Wishart DS, McFadden G (1990) Myxoma virus and malignant rabbit fibroma virus encode a serpin-like protein important for virus virulence. *Virology* 179(2):618–631.

18. Guerin J-L, et al. (2001) Characterization and functional analysis of Serp3: a novel myxoma virus-encoded serpin involved in virulence. *Journal of General Virology* 82(6):1407–1417.

19. Cameron C, Hota-Mitchell S, Chen L, Barrett J, Cao JX (1999) The Complete DNA Sequence of Myxoma Virus. *Virology*.

20. Vattem KM, Wek RC (2004) Reinitiation involving upstream ORFs regulates ATF4 mRNA translation in mammalian cells. *Proceedings of the National Academy of Sciences of USA* 101(31):11269–11274.

21. Rothenburg S, Seo EJ, Gibbs JS, Dever TE, Dittmar K (2009) Rapid evolution of protein kinase PKR alters sensitivity to viral inhibitors. *Nature Structural and Molecular Biology* 16(1):63–70.

22. Siebenlist U, Franzoso G, Brown K (2003) Structure, Regulation and Function of NF-kappaB. *Annual review of cell biology 10.1 (1994): 405-455.*

23. Tak PP, Firestein GS (2001) NF-κB: a key role in inflammatory diseases. *Journal of Clinical Investigation* 107(1):7–11.

24. Fenner F, Woodroofe GM (1953) The pathogenesis of infectious myxomatosis; the mechanism of infection and the immunological response in the European rabbit (*Oryctolagus cuniculus*). *British Journal of Experimental Pathology* 34(4):400–411.

25. Johnston JB, McFadden G (2003) Poxvirus immunomodulatory strategies: current perspectives. *Journal of Virology* 77(11):6093–6100.

26. Gil J, Rullas J, García MA, Alcami J, Esteban M (2001) The catalytic activity of dsRNA-dependent protein kinase, PKR, is required for NF-kB activation. *Oncogene* 20.3: 385-394.

27. Kerr PJ (2012) Myxomatosis in Australia and Europe: a model for emerging infectious diseases. *Antiviral Research* 93(3):387–415.

28. Krüll M, et al. (1999) Signal transduction pathways activated in endothelial cells following infection with Chlamydia pneumoniae. *Journal of Immunology* 162(8):4834–4841.

29. Dar AC, Dever TE and Sicheri F (2005) Higher-order substrate recognition of eIF2alpha by the RNA-dependent protein kinase PKR. *Cell* 122(6):887–900.

30. Matthee CA, van Vuuren BJ, Bell D, Robinson TJ (2004) A molecular supermatrix of the rabbits and hares (Leporidae) allows for the identification of five intercontinental exchanges during the Miocene. *Systemic Biology* 53(3):433–447.

Chapter 5 - Conclusion

The research presented in this dissertation reveals that inhibition of the host antiviral protein kinase R (PKR) by poxvirus pseudosubstrate inhibitors is species-specific. Furthermore, we noticed that myxoma virus and swinepox virus K3L orthologs inhibit PKR from the natural hosts of the viruses with highest efficiency, which may explain why infections of these two viruses are restricted to only certain host species. We also observed that PKR from even very closely related species, such as European rabbit and brush rabbit, show differential sensitivities to myxoma virus M156 inhibition, and most importantly, we unveil a possible mechanism by which moderate PKR activity triggers robust induction of NF-κB-regulated protein expression, which may contribute to the pathogenesis of myxomatosis. Overall, our findings suggest that the species-specific interactions between PKR and its viral antagonists is a critical factor that influences poxvirus replication and host range.

Through a combination of molecular, biological and biochemical approaches, we demonstrated that myxoma virus M156R specifically inhibited only rabbit PKR, but not human PKR and PKR from other mammalian species tested. We also showed that M156R-L98P, a mutant that arose from a single nucleotide mutation in M156R found in more than 50% field isolates lost its PKR inhibitory ability. This finding reveals a possible mechanism for the attenuation of the myxoma virus in Australia after its repeated release.

We next thoroughly examined the differences between European rabbit and its close relative, the brush rabbit, in terms of PKR sensitivity to M156R inhibition and find that brush rabbit PKR was better inhibited by M156R than European rabbit PKR. This difference in PKR sensitivity is intriguing, considering the dramatically distinctive evolutionary history of myxoma virus in these two rabbit species. Whereas myxoma virus has been evolving in American *Sylvilagus* rabbits, European rabbit population in the wild have never naturally encountered the

virus before the 1950's. The difference we observed in PKR sensitivity between European rabbit and brush rabbit to M156R inhibition suggests that myxoma virus M156R evolved to inhibit PKR from its natural host with highest efficiency. Generally, in the co-evolution of any virus-host pair, it is acknowledged that the effects of evolution on the fitness of the virus and the host act in opposite directions: the evolutionary advantages gained by the virus are bad for the host and vice versa. However, the data described in this dissertation demonstrate that even though the long-term adaptation of myxoma virus to its natural host *Sylvilagus* rabbit resulted in the optimization of M156R to completely inhibit this species' PKR, this "advantage" obtained through evolution for the virus does not necessarily lead to increased virulence that directly reduces the host fitness. In contrast, we show in our NF-κB reporter assays that the stronger inhibition of brush rabbit PKR by M156R surprisingly led to the reduced activity of a pro-inflammatory transcription factor NF-κB, in contrast to the higher NF-κB resulting from the moderate inhibition of European rabbit PKR. This difference correlates with the virulence difference of myxoma virus in these two rabbit species. Therefore, we propose that stronger inhibition of PKR, as the result of extensive virus-host co-evolution, does not lead to higher virulence, but instead decreases its virulence, which increases the fitness of both the host and the virus. However, whether NF-κB activity directly contributes to the pathogenesis of myxomatosis still requires further investigation.

By combining a selection analysis and molecular biology techniques, we successfully pin-pointed the residues on rabbit PKRs that are responsible for their differential sensitivity to pseudosubstrate inhibitors from myxoma and rabbit fibroma viruses. We discovered that mutations of residues that differ between European rabbit PKR and brush rabbit PKR, which are also under strong positive selective pressure, altered PKR sensitivities to M156R and R156R.

This indicates that the selective pressure exerted by viral antagonists on PKR is a major driving force for the rapid evolution of this antiviral protein. While PKR is constantly evolving to evade viral inhibition, viral inhibitors are also evolving quickly to re-establish effective PKR inhibition to allow virus replication. The ongoing arms-race between the host and the virus drives the fast evolution of both PKR and its viral antagonists.

Emerging and re-emerging infectious diseases including Ebola, SARS, influenza and monkeypox remain a major threat to human health because the host range of each virus and the likelihood of cross-species transmission is unpredictable based on current knowledge. Through the study of interactions between vaccinia virus K3L and PKR from multiple species, we learned that PKR from different species are inhibited differentially by a given viral antagonist, and that these differences play a role in determining virus replication and suppression of the host's immune response during infection. Information like these is valuable because it might help us to better predict the virulence and host range of newly emerging and re-emerging viral pathogens.